

# **SANDIA REPORT**

SAND2011-3119

Unlimited Release

Printed May 2011

## **Proton Exchange Membrane Fuel Cells for Electrical Power Generation On-Board Commercial Airplanes**

Joseph W. Pratt, Leonard E. Klebanoff, Karina Munoz-Ramos, Abbas A. Akhil, Dita B. Curgus, and Benjamin L. Schenkman

Prepared by  
Sandia National Laboratories  
Albuquerque, New Mexico 87185 and Livermore, California 94550

Sandia National Laboratories is a multi-program laboratory managed and operated by Sandia Corporation, a wholly owned subsidiary of Lockheed Martin Corporation, for the U.S. Department of Energy's National Nuclear Security Administration under contract DE-AC04-94AL85000.

Approved for public release; further dissemination unlimited.

Issued by Sandia National Laboratories, operated for the United States Department of Energy by Sandia Corporation.

**NOTICE:** This report was prepared as an account of work sponsored by an agency of the United States Government. Neither the United States Government, nor any agency thereof, nor any of their employees, nor any of their contractors, subcontractors, or their employees, make any warranty, express or implied, or assume any legal liability or responsibility for the accuracy, completeness, or usefulness of any information, apparatus, product, or process disclosed, or represent that its use would not infringe privately owned rights. Reference herein to any specific commercial product, process, or service by trade name, trademark, manufacturer, or otherwise, does not necessarily constitute or imply its endorsement, recommendation, or favoring by the United States Government, any agency thereof, or any of their contractors or subcontractors. The views and opinions expressed herein do not necessarily state or reflect those of the United States Government, any agency thereof, or any of their contractors.

Printed in the United States of America. This report has been reproduced directly from the best available copy.

Available to DOE and DOE contractors from

U.S. Department of Energy  
Office of Scientific and Technical Information  
P.O. Box 62  
Oak Ridge, TN 37831

Telephone: (865) 576-8401  
Facsimile: (865) 576-5728  
E-Mail: [reports@adonis.osti.gov](mailto:reports@adonis.osti.gov)  
Online ordering: <http://www.osti.gov/bridge>

Available to the public from

U.S. Department of Commerce  
National Technical Information Service  
5285 Port Royal Rd.  
Springfield, VA 22161

Telephone: (800) 553-6847  
Facsimile: (703) 605-6900  
E-Mail: [orders@ntis.fedworld.gov](mailto:orders@ntis.fedworld.gov)  
Online order: <http://www.ntis.gov/help/ordermethods.asp?loc=7-4-0#online>



# Proton Exchange Membrane Fuel Cells for Electrical Power Generation On-Board Commercial Airplanes

Joseph W. Pratt<sup>1</sup>, Leonard E. Klebanoff<sup>2</sup>, Karina Munoz-Ramos<sup>3</sup>, Abbas A. Akhil<sup>4</sup>, Dita B. Curgus<sup>1</sup>, and Benjamin L. Schenkman<sup>4</sup>

<sup>1</sup>Thermal/Fluid Science and Engineering (8365)  
Sandia National Laboratories  
P.O. Box 969  
Livermore, California, MS-9409

<sup>2</sup>Hydrogen and Combustion Technologies (8367)

<sup>3</sup>Energy Systems Analysis (6111)

<sup>4</sup>Energy Infrastructure & Distributed Energy Resources (6113)

## Abstract

Deployed on a commercial airplane, proton exchange membrane fuel cells may offer emissions reductions, thermal efficiency gains, and enable locating the power near the point of use. This work seeks to understand whether on-board fuel cell systems are technically feasible, and, if so, if they offer a performance advantage for the airplane as a whole.

Through hardware analysis and thermodynamic and electrical simulation, we found that while adding a fuel cell system using today's technology for the PEM fuel cell and hydrogen storage is technically feasible, it will not likely give the airplane a performance benefit. However, when we re-did the analysis using DOE-target technology for the PEM fuel cell and hydrogen storage, we found that the fuel cell system would provide a performance benefit to the airplane (i.e., it can save the airplane some fuel), depending on the way it is configured.

## **Acknowledgements**

The authors of this study had a great deal of enthusiastic support from both within and outside of Sandia National Laboratories.

Dr. Joe Breit of The Boeing Company directly or indirectly provided most of the information about airplane electrical systems and issues in current airplane design that might be able to leverage the capabilities of a fuel cell. In the rare cases he could not answer our frequent questions, he referred us to others at Boeing who were just as happy to help: Andy Bayliss for issues concerning airplane performance, Trevor Laib for information on the existing environmental control systems, and Farhad Nozari and Casey Roberts for more electrical system details.

Ryan Sookhoo of Hydrogenics was gracious in his support of our project, offering details on their PEM fuel cell technology to assist us in making reasonable estimates for the current state of the art as well as predictions of what may be possible for future aviation-designed fuel cell systems. His insight into the European world of aviation fuel cells was also useful to help put this study into perspective.

Dr. Andy Lutz of Sandia (now at the University of Pacific) provided his extensive knowledge on the Simulink thermodynamic models that were used in this study.

Of course, this project would not have taken place without the support of the Department of Energy's Fuel Cell Technologies Program, Pete Devlin and Nancy Garland in the Market Transportation group in particular. The encouragement and suggestions we received from them was invaluable.

## Summary

Fuel cells have become increasingly important as alternative sources of power, offering the potential for drastic reduction in emissions in particulate matter (PM), nitrogen oxides (NO<sub>x</sub>), and CO<sub>2</sub>. In addition, they offer exceptionally quiet operation, highly efficient use of the fuel energy, and a high energy storage density compared to batteries. For a number of years, the manufacturers of commercial aircraft, most notably Boeing and Airbus, have realized that fuel cells may offer advantages for commercial aircraft operation. Apart from emissions reductions and thermal efficiency referenced above, they can constitute distributed power systems, enabling locating the power near the point of use and also reducing the power draw from the engines.

The real question is if fuel cells offer operational advantages over traditional power in systems that are used routinely in flight, for example galley power, in flight entertainment, and to provide additional power to the aircraft electrical grid when “peaker” power is needed. This interest in the use of fuel cells is timely, as the electrical needs on-board are going up considerably, with systems that were formerly hydraulic in operation are converted to electric operation [1]. For the new Boeing 787, the aircraft-wide electrical generation capacity is 1.5 MW – almost an order of magnitude larger than previous designs. This study, then, is an initial investigation of the use of proton exchange membrane (PEM) fuel cells on-board commercial aircraft. We seek to understand how to physically deploy a fuel cell on an aircraft, understand the impact on system volume, weight, and to understand the impact on jet fuel consumption, both in relation to fuel currently devoted to electricity generation, and the overall fuel needed by the airplane to fly a given mission.

To accomplish this analysis, two basic airplane designs were considered: one airplane without a fuel cell (the base airplane), and one airplane designed to perform the same mission as the first airplane, only carrying a fuel cell and associated hardware to fulfill a specific electrical need. The difference in the performance of these two airplanes is made quantitative by calculating the fuel required to fly the mission in the two cases, which requires understanding the influence of weight and drag. Calculating the required fuel also allows us to assess fuel use as it directly relates to power generation on the airplane. The key point here is that we assess not only the benefit of the fuel cell on generating electricity, but also the penalty the fuel cell system has on the airplane’s performance due to its added weight and possibly drag. Combining these two is necessary to determine the overall effect of the fuel cell system.

We performed the analysis by designing and examining several system options using realistic assumptions about performance and size of the various components. After assessment of the available state of the art in commercially-available PEM fuel cells, the Hydrogenics HyPM 12 PEM fuel cell was chosen as a unit representative of the industry. For hydrogen storage, several options were considered: 350 bar compressed gas, 700 bar compressed gas, metal hydrides, and liquid. 350 bar compressed gas was selected for use in the analysis due to its combination of high specific energy and current availability. Other equipment such as heat exchangers, blowers, and pumps were all selected based on commercially available units with the specifications appropriate for the system. For the electrical components, a ±270 Volt DC distribution system provided the lowest system weight, although the

increase in weight due to a 230 Volt AC system was less than 50 kg (110 lb). Both of these options provide the advantage of direct interface with the existing electrical system on the 787.

After consideration of factors such as safety, available space, maintenance, and wiring and tubing/piping lengths, we chose to locate the fuel cell system in the airplane's fairing area (where the wings join the fuselage), although locating the system in the tail cone would not change the results by much. Locating the fuel cell system next to the load it serves could save up to 150 kg (331 lb) of mass and provide some redundancy benefits, but this was avoided because of the concern with occupying space that is currently used for other purposes.

The amount and method of recovering the heat rejected from the fuel cell (waste heat recovery) was found to be a critical factor in determining the performance benefit of the fuel cell system. To this end, eleven different waste heat recovery options were examined thermodynamically. We found that a system that uses the heat from the fuel cell to pre-heat the jet fuel carried by the airplane will provide the largest overall performance benefit. This method of heat recovery is already used in commercial airplanes within the engine compartment, where the lubrication oil is cooled by jet fuel, and it is more ubiquitous in military aircraft where the fuel is used to cool many of the airplane's systems.

We considered the integration of the fuel cell system with the airplane's electrical system, for it is necessary to ensure that the addition of the fuel cell system does not disrupt the electrical system or cause instabilities. Through dynamic simulation we found that the fuel cell system performed satisfactorily whether connected to the airplane's system or as a stand-alone system. In fact, our results indicate that the integration of the fuel cell system with the existing electrical system may provide a faster response to load changes.

In the end, we found that while adding a fuel cell system using today's technology for the PEM fuel cell and hydrogen storage is technically feasible, it will not give the airplane a performance benefit no matter which configuration was chosen (although there may be other benefits that make it worthwhile from the airplane manufacturer's or airline's point of view). However, when we re-did the analysis using DOE-target technology for the PEM fuel cell and hydrogen storage, we found that the fuel cell system would provide a performance benefit to the airplane (i.e., it can save the airplane some fuel), depending on the way it is configured. This analysis also showed that the DOE-target technology fuel cell system could generate electricity using over 30% less fuel than the current airplane, even considering the penalties due to the fuel cell system's weight and drag. If a fleet of 1,000 airplanes were equipped with such systems, it could save over 20,000 metric tons of CO<sub>2</sub> annually.

# Contents

Acknowledgements.....	3
Summary .....	4
Figures.....	9
Tables.....	16
Nomenclature .....	17
1 Introduction .....	19
1.1 Content of the Report.....	20
1.2 Analysis Approach.....	22
1.2.1 Base Airplane and Mission.....	22
2 Airplane Systems and Concepts.....	25
2.1 Environmental Control System .....	25
2.1.1 Pressurization.....	25
2.1.2 Clean Air Supply .....	25
2.1.3 Temperature Control .....	26
2.2 Power Electronics Cooling System.....	26
2.3 Galley System.....	26
2.4 Water System.....	27
2.5 In-flight Entertainment System.....	28
2.6 Electrical Power Generation and Distribution System.....	28
2.7 Airplane Performance .....	30
2.7.1 Base Airplane, Base Mission .....	30
2.7.2 Effect of Weight and Drag Changes .....	31
3 Fuel Cell System Hardware and Concepts .....	37
3.1 Fuel Cells .....	37
3.1.1 PEM Fuel Cell: Background .....	38
3.1.2 PEM Fuel Cell: Specifics for the Study.....	39
3.2 Hydrogen Storage .....	40
3.2.1 Metal Hydride .....	41
3.2.2 Liquid.....	42
3.2.3 Compressed Gas.....	44
3.3 Heat Exchangers, Blowers, and Water Pumps.....	45

3.4	Electrical Load and Components.....	46
3.5	Piping and Tubing.....	48
3.6	Fuel Cell Waste Heat Recovery Options.....	48
3.6.1	On-board Uses of Waste Heat .....	49
3.7	Location Options for On-board Fuel Cell Systems .....	50
3.7.1	Available Space on the Airplane .....	50
3.7.2	Safety of the Installed Systems .....	52
3.7.3	Tubing, Ducting, and Wiring.....	52
3.7.4	Waste Heat Recovery.....	52
3.7.5	Rejection of Waste Streams from the Fuel Cell .....	53
4	Thermodynamic Analysis Method .....	55
4.1	Fuel Cell Module .....	55
4.1.1	PEM fuel cell.....	55
4.1.2	Fuel flow controller .....	57
4.1.3	Air flow controller .....	57
4.1.4	Cooling water block.....	58
4.2	Hydrogen storage vessel.....	59
4.3	Heat exchangers.....	59
4.4	Furnace .....	59
4.5	Efficiency calculator .....	59
4.6	Compressor/blower .....	60
4.7	Pump.....	60
5	Electrical System Analysis Method .....	61
5.1	Approach.....	61
5.2	Major Model Components.....	61
5.2.1	PEM Fuel Cell Model .....	61
5.2.2	DC-DC Converter .....	62
5.3	Stand-alone Galley Model Description .....	63
5.4	Peaker Model Description.....	65
6	Results and Discussion .....	67
6.1	System Design and Feasibility .....	67
6.1.1	Location.....	67



6.1.2	System Design .....	72
6.1.3	System Performance .....	78
6.1.4	Cases 1a and 1b: Air Cooled.....	81
6.1.5	Cases 2a and 2b: Simple Water Cooled .....	82
6.1.6	Cases 3a and 3b: Water Cooled with Limited Heat Recovery.....	82
6.1.7	Cases 4a and 4b: Water Cooled with Maximum Heat Recovery .....	83
6.1.8	Case 5: Water Cooled with High Grade Waste Heat Recovery .....	83
6.1.9	Cases 6a and 6b: Fuel Cooled.....	84
6.1.10	Summary .....	84
6.2	System Performance with Current Technology .....	84
6.2.1	Mass .....	86
6.2.2	Volume .....	86
6.2.3	Performance.....	91
6.2.4	Summary .....	93
6.3	System Performance with DOE Target Technology .....	93
6.3.1	Mass and Volume.....	94
6.3.2	Performance.....	95
6.3.3	Summary .....	100
6.4	Electrical System Behavior .....	101
6.4.1	Stand-alone Galley Model Simulation Results .....	103
6.4.2	Peaker System Model Simulation Results.....	106
6.4.3	Summary .....	109
7	Conclusions, Recommendations, and Future Work.....	111
7.1	Conclusions and Recommendations.....	111
7.2	Future Work.....	113
	References .....	115
	Distribution .....	118

## Figures

Figure 1: The Boeing 787-8 is a “more electric airplane” with many of the conventional systems converted to electric power. This results in a high on-board electric generating capacity (nearly 1.5 MW). Image ©Boeing, used with permission. ....	22
Figure 2: The mission modeled for this study is a transcontinental flight between San Francisco International Airport (SFO) and John F. Kennedy International Airport (JFK).....	23
Figure 3: Ram-air inlet ducts on the 787 [16]. ....	25
Figure 4: Picture of a typical airplane galley indicating major electrical loads: ovens, hot water/coffee pots, and refrigeration units. ....	27
Figure 5: Layout of the 787-8 indicating typical locations of galleys (G) and lavatories (L). The actual configuration is customizable and highly dependent on the customer. The nose is to the left. Diagram from [11].....	27
Figure 6: Illustration of typical in-flight entertainment (IFE) seat-back devices. The total IFE load on a 787-8 could reach 20 kW during all phases of flight. Note: Picture is not from a 787.....	28
Figure 7: Schematic of the Boeing 787 electrical system. The system is complex yet offers many options for a fuel cell to tie-in. Figure taken from Nelson [13].....	30
Figure 8: Schematic diagram of a Proton Exchange Membrane (PEM) fuel cell. ....	38
Figure 9: Typical operating performance for the HyPM 12 power module. The left-hand chart shows voltage (blue line) and power (green line) as functions of current. The right-hand chart shows efficiency (LHV-basis) also as a function of current. Comparing the two figures reveals that the highest efficiency occurs at a low power level, and efficiency decreases as power increases. Note: “Available Current” and “User Current” are the same. Figure from [32]. ....	40
Figure 10: Mass of different hydrogen storage tanks as a function of the mass of hydrogen stored. Compressed gas storage at 350 bar (5,000 psi) offers the lowest mass solution for currently available methods. The proposed liquid storage methods are promising improvements for the future. References: [34-42].....	41
Figure 11: Volume of different hydrogen storage tanks as a function of mass of hydrogen stored. The compressed gas options require a larger volume than either the liquid or metal hydride options [34-41].....	41
Figure 12: Picture of Ovonics metal hydride storage tank. The nameplate indicates the system shown can store 3 kg (6.6 lb) of hydrogen, has a mass of 190 kg (419 lb), and a volume of 60 L (2.1 ft <sup>3</sup> ). From Chao et al. [36], see for more details. ....	43
Figure 13: Cut-away view of one of the current technology cryo-compressed hydrogen storage tanks. This design can store 10.7 kg (23.6 lb) of hydrogen at 345 bar (5,000 psi) with tank-only mass of 155 kg (342 lb) and volume of 297 L (10.5 ft <sup>3</sup> ). Figure and data from [34].....	43

Figure 14: The compressed gas hydrogen tanks from Lincoln Composites (left) and Quantum Technologies (right).....	44
Figure 15: Dimensioned outline drawing of the 787-8, showing location of the loads and options for the fuel cell and hydrogen storage. Dimensioned drawing (without locations) from [11]......	51
Figure 16: Comparison of the fuel cell model (blue solid line) using the parameters in Table 7, to the manufacturer’s data (red circles) as derived from Figure 9. The agreement is satisfactory for the entire operating range.....	58
Figure 17: Equivalent circuit of a fuel cell (from SimPowerSystems online product documentation).....	62
Figure 18: DC-DC converter schematic. ....	62
Figure 19: DC-DC converter controller.....	63
Figure 20: Graphical representation of the stand-alone galley model.....	64
Figure 21: Simulink code for the stand-alone galley model. ....	64
Figure 22: Graphical representation of the Peaker System model. ....	66
Figure 23: Simulink code for the Peaker model.....	66
Figure 24: The effect of location of the fuel cell and hydrogen storage systems on the piping and tubing mass. The chart reveals that the impact of not locating the fuel cell close to the load is small, but the mass increases several times when the fuel cell and hydrogen are separated.....	68
Figure 25: The effect of location of the fuel cell and hydrogen storage systems on the piping and tubing volume. The results show that the differences between cases are relatively small. Similar to the mass analysis, the worst cases are when the hydrogen and fuel cell are separated.....	69
Figure 26: Mass comparison of the $\pm 270$ VDC and 230 VAC systems, including wiring and equipment, assuming the fuel cell is in the fairing area. The $\pm 270$ VDC system has a lower mass in every case. ....	70
Figure 27: Volume comparison of the $\pm 270$ VDC and 230 VAC systems, including wiring and equipment, assuming the fuel cell is in the fairing area. The $\pm 270$ VDC system has a lower volume in every case. ....	71
Figure 28: Combined mass of the piping, tubing, and wiring assuming that the fuel cell and hydrogen are located together and that a 270 VDC electrical distribution system is used. Locating the system next to the load can save over 100 kg overall. The cumulative difference between locating the system in the fairing (158 kg total) or tail (148 kg total) is small. ....	71
Figure 29: Schematic for Case 1a, where the fuel cell’s internal liquid cooling system is air cooled and no heat recovery is utilized. ....	73

Figure 30: Schematic for Case 1b. The fuel cell’s internal liquid cooling system is air cooled. The hot cooling air is combined with the fuel cell exhaust and used to heat water. .... 73

Figure 31: Schematic for Case 2a. The fuel cell’s internal liquid cooling system is cooled by the airplane’s liquid cooling loop and no heat recovery is utilized. .... 74

Figure 32: Schematic for Case 2b. The fuel cell’s internal liquid cooling system is cooled by the airplane’s liquid cooling loop. The exhaust air from the fuel cell is used to heat hot water. .... 74

Figure 33: Schematic for Case 3a. The fuel cell’s internal liquid cooling system is used to heat a limited amount of hot water, and remaining heat is rejected to the airplane’s liquid cooling loop..... 75

Figure 34: Schematic for Case 3b. The fuel cell’s internal liquid cooling system is used to heat a limited amount of hot water, and remaining heat is rejected to the airplane’s liquid cooling loop. The exhaust air from the fuel cell is cooled by the airplane’s cooling loop in order to condense the water..... 75

Figure 35: Schematic for Case 4a. The fuel cell’s internal liquid cooling loop is used to heat a quantity of water not intentionally limited. Exhaust air from the fuel cell is used to pre-heat the water, and some water is condensed in the process, thereby maximizing water recovery. This design does not require any cooling by the airplane’s systems. .... 76

Figure 36: Schematic for Case 4b. The fuel cell’s internal liquid cooling loop is used to heat a quantity of water not intentionally limited. Exhaust air from the fuel cell is used to pre-heat the water, and some water is condensed in the process. The exhaust air is further cooled by the airplane’s liquid cooling loop to further condense and recover water. .... 76

Figure 37: Schematic for Case 5. The fuel cell’s internal liquid cooling loop is used to pre-heat a quantity of water not intentionally limited. The excess hydrogen from the fuel cell is kept separate from the air and instead combusted in a hydrogen furnace to produce high-temperature waste heat which is used to heat the galley ovens. The oven exhaust further heats the water. This design does not require any cooling by the airplane’s systems..... 77

Figure 38: Schematic for Case 6a. The fuel cell’s internal liquid cooling loop is used to heat the airplane’s fuel. No other waste heat recovery is utilized, and none of the airplane’s cooling systems are needed..... 77

Figure 39: Schematic for Case 6b. The fuel cell’s internal liquid cooling loop is used to heat the airplane’s fuel. Exhaust from the fuel cell is also used to heat the airplane’s fuel, producing condensed water in the process. A secondary coolant loop is used to prevent mixing of the airplane’s fuel with air or water. No other waste heat recovery is utilized, and none of the airplane’s cooling systems are needed. .... 78

Figure 40: Overall system efficiency of the eleven system case options for the 20 kW in-flight entertainment load. The cases with the most waste heat recovery (cases 4-6) have the highest overall system efficiencies..... 79

Figure 41: Summary of the mass analysis for each case. The different colors in the narrow bars represent different components. Quantities above the zero-line are for mass added to the system, and quantities below the zero-line are for mass credits. The net change (the sum of the added mass and mass credits) is shown by the wide hollow bar. For comparison, the “standard passenger” has a mass of 104 kg (230 lb) including luggage. .... 79

Figure 42: Summary of the volume analysis for each case. The volume of each component is shown by a different color. The larger volumes of the air-cooled cases (1a and 1b) are due to the larger heat exchangers required in addition to the increased fuel cell and hydrogen requirements. Because volume is most influenced by the size of the fuel cell and hydrogen tanks, the differences between the other cases are relatively small. For comparison, a typical galley beverage cart has a volume of 240 L (8.5 ft<sup>3</sup>)..... 80

Figure 43: The overall effect of the fuel cell system on airplane performance, as measured by the amount of additional Jet-A the fuel cell-equipped airplane needs to accomplish the same mission as the base airplane. The numbers in parenthesis express this amount as a percentage of total mission fuel. Only Cases 4a, 4b, and 5 results in a performance benefit..... 81

Figure 44: Mass distribution for Case 2a (water cooled, no heat recovery) for the different loads, using current technology for the fuel cell and hydrogen storage. The different colors in the narrow bars represent different components. Quantities above the zero-line are for mass added to the system, and quantities below the zero-line are for mass credits. The net change (the sum of the added mass and mass credits) is shown by the wide hollow bar. For comparison, the “standard passenger” has a mass of 104 kg (230 lb) including luggage. .... 87

Figure 45: Mass distribution for Case 3b (water cooled, water recovery, limited hot water) for the different loads, using current technology for the fuel cell and hydrogen storage. The different colors in the narrow bars represent different components. Quantities above the zero-line are for mass added to the system, and quantities below the zero-line are for mass credits. The net change (the sum of the added mass and mass credits) is shown by the wide hollow bar. For comparison, the “standard passenger” has a mass of 104 kg (230 lb) including luggage. .... 88

Figure 46: Mass distribution for Case 6a (fuel cooled) for the different loads, using current technology for the fuel cell and hydrogen storage. The different colors in the narrow bars represent different components. Quantities above the zero-line are for mass added to the system, and quantities below the zero-line are for mass credits. The net change (the sum of the added mass and mass credits) is shown by the wide hollow bar. For comparison, the “standard passenger” has a mass of 104 kg (230 lb) including luggage. .... 89

Figure 47: Summary of the volume analysis for Case 2a (water cooled, no heat recovery). The volume of each component is shown by a different color. For comparison, a typical galley beverage cart has a volume of 240 L (8.5 ft<sup>3</sup>)..... 90

Figure 48: Summary of the volume analysis for Case 3b (water cooled, water recovery, limited hot water). The volume of each component is shown by a different color. For comparison, a typical galley beverage cart has a volume of 240 L (8.5 ft<sup>3</sup>)..... 90

Figure 49: Summary of the volume analysis for Case 6a (fuel cooled). The volume of each component is shown by a different color. For comparison, a typical galley beverage cart has a volume of 240 L (8.5 ft<sup>3</sup>). ..... 91

Figure 50: The overall effect of the fuel cell system on airplane performance, as measured by the amount of additional Jet-A the fuel cell-equipped airplane needs to accomplish the same mission as the base airplane. The chart assumes current technology for the fuel cell and hydrogen storage systems. As a comparison, the base airplane on the base mission is estimated to carry 22,680 kg (50,000 lb) of Jet-A at takeoff. .... 92

Figure 51: Mass distribution for Case 2a (water cooled, no heat recovery) for the different loads, using DOE target technology for the fuel cell and hydrogen storage. The different colors in the narrow bars represent different components. Quantities above the zero-line are for mass added to the system, and quantities below the zero-line are for mass credits. The net change (the sum of the added mass and mass credits) is shown by the wide hollow bar. For comparison, the “standard passenger” has a mass of 104 kg (230 lb) including luggage. .... 94

Figure 52: Mass distribution for Case 3b (water cooled, water recovery, limited hot water) for the different loads, using DOE target technology for the fuel cell and hydrogen storage. The different colors in the narrow bars represent different components. Quantities above the zero-line are for mass added to the system, and quantities below the zero-line are for mass credits. The net change (the sum of the added mass and mass credits) is shown by the wide hollow bar. For comparison, the “standard passenger” has a mass of 104 kg (230 lb) including luggage. .... 95

Figure 53: Mass distribution for Case 6a (fuel cooled) for the different loads, using DOE target technology for the fuel cell and hydrogen storage. The different colors in the narrow bars represent different components. Quantities above the zero-line are for mass added to the system, and quantities below the zero-line are for mass credits. The net change (the sum of the added mass and mass credits) is shown by the wide hollow bar. For comparison, the “standard passenger” has a mass of 104 kg (230 lb) including luggage. .... 96

Figure 54: Summary of the volume analysis for Case 2a (water cooled, no heat recovery) with DOE target technology. The volume of each component is shown by a different color. For comparison, a typical galley beverage cart has a volume of 240 L (8.5 ft<sup>3</sup>). ..... 97

Figure 55: Summary of the volume analysis for Case 3b (water cooled, water recovery, limited hot water) with DOE target technology. The volume of each component is shown by a different color. For comparison, a typical galley beverage cart has a volume of 240 L (8.5 ft<sup>3</sup>). ..... 97

Figure 56: Summary of the volume analysis for Case 6a (fuel cooled) with DOE target technology. The volume of each component is shown by a different color. For comparison, a typical galley beverage cart has a volume of 240 L (8.5 ft<sup>3</sup>). ..... 98

Figure 57: The overall effect of the fuel cell system on airplane performance, as measured by the amount of additional Jet-A the fuel cell-equipped airplane needs to accomplish the same mission as the base airplane. The chart assumes DOE target technology for the fuel cell and hydrogen storage systems. As a comparison, the base airplane on the base mission is estimated to carry 22,680 kg (50,000 lb) of Jet-A at takeoff. .... 98

Figure 58: The amount of fuel required by the base airplane and the airplane with the fuel cell to generate electricity and heat for the different load scenarios. The base airplane uses the main engine generator with a fuel-to-electricity efficiency of 34%, while the fuel cell assumes the fuel cooled configuration with DOE target technology. The numbers are presented below in Table 14. .... 99

Figure 59: Yearly avoided CO<sub>2</sub> emissions for a fleet of 1,000 fuel cell-equipped airplanes operating 750 hrs/yr, using a fuel cooled fuel cell system (Case 6a) and renewable hydrogen, and comparing to the base airplane generating electricity via the main engines at 34% efficiency. .... 101

Figure 60: Allowed voltage transient for 28 VDC systems. During transients, the system voltage must not go higher than the top solid line or lower than the bottom solid line. (Figure 13 in MIL-STD-704F [61].)..... 102

Figure 61: Allowed voltage transient for 270 VDC systems. During transients, the system voltage must not go higher than the top solid line or lower than the bottom solid line. (Figure 16 in MIL-STD-704F [61].)..... 103

Figure 62: Stand-alone galley system simulation: voltage as measured at the load..... 104

Figure 63: Stand-alone galley system simulation: Detail of the voltage transient at 6 seconds, showing that voltage recovers to more than 22 V within about 0.0001 seconds, easily satisfying the MIL-STD-704F requirements. .... 105

Figure 64: Stand-alone galley system simulation: Power response from the fuel cell and the fuel cell + DC-DC converter..... 105

Figure 65: Peaker system simulation: Power responses. .... 106

Figure 66: Peaker system simulation: Voltage at the load. Detail of the transient at 2 seconds (where only the engine generator is supplying power) is shown in Figure 67. Detail of the transient at 4 seconds (where the fuel cell is supplying the additional power) is shown in Figure 68. The system is stable and the transients are all within the MIL-STD-704F specifications. .... 107

Figure 67: Peaker system simulation: Detail of the voltage transient at 2 seconds as shown in Figure 66. This load change is fully met by the engine generators. The transient recovers within the time specified by MIL-STD-704F. .... 108

Figure 68: Peaker system simulation: Details of the voltage transient at 4 seconds as shown in Figure 66. This load change is fully met by the fuel cell system. The transient recovers within the time specified by MIL-STD-704F, and has a much faster recovery than that of the engine generator alone (Figure 67). .... 108



## Tables

Table 1: Specifications of the base airplane and flight mission used in this study.....	24
Table 2: Source and estimated magnitudes of heat generation on board the base airplane that must be rejected to the atmosphere through the ram air cooling system.....	36
Table 3: Types of fuel cells.....	37
Table 4: The nine different load scenarios considered in this study. ....	46
Table 5: Design current required for the three electrical distribution options. The 50 VDC option would require currents that are too high for switching and circuit protection equipment. ....	47
Table 6: Wire sizes for the 270 VDC and $\pm 230$ VAC distribution systems.....	47
Table 7: Data for the modeled PEM fuel cell. Manufacturer’s data from [32, 51]. ....	57
Table 8: PEM fuel cell model parameters used in the stand-alone galley simulation.....	63
Table 9: Galley loads considered in the galley electrical system simulation, from Refs [52-57].....	63
Table 10: PEM fuel cell model parameters used in peaker simulation. ....	65
Table 11: Summary of the three cases selected from the screening analysis. Each system is designed to meet a constant 20 kW IFE electrical load operating for all phases of flight.....	85
Table 12: The nine different load scenarios considered in this study (Table 4 repeated for convenience). ....	85
Table 13: Savings data for Cases 3b and 6a, illustrating the more beneficial effect of saving Jet-A directly vs. saving mass. ....	93
Table 14: A summary of the numbers plotted above in Figure 58, and the calculated percentages, comparing the fuel needed by the base airplane and the fuel cell airplane to generate the required electricity. The percentage shows the amount of fuel required by the fuel cell airplane relative to that required by the base airplane. Percentages below 100% show a fuel savings of the fuel cell airplane, over 100% show a fuel penalty. ....	99
Table 15: Load increases during stand-alone galley simulation. ....	104

## Nomenclature

### Acronyms

ACH	Air Changes per Hour
APU	Auxiliary Power Unit
DOE	Department of Energy
ECS	Environmental Control System
FAA	Federal Aviation Administration
HHV	Higher Heating Value
IFE	In-flight Entertainment
LH <sub>2</sub>	Liquid hydrogen
MEA	More Electric Airplane (airplanes), or Membrane Electrode Assembly (fuel cells)
<i>MW</i>	Molecular weight
nm	nautical miles
PECS	Power Electronics Cooling Loop
PEM	Proton Exchange Membrane
PEMFC	Proton Exchange Membrane Fuel Cell
PI	Proportional-Integral
SCFM	Standard Cubic Feet per Minute
V-i	Voltage-current

### Symbols

$a$	Speed of sound
$c_T$	Thrust specific fuel consumption
$C_L$	Coefficient of lift
$C_D$	Coefficient of drag
$C_{DL}$	Drag due to the creation of lift
$C_{DO}$	Parasitic drag
$E$	Nernst Voltage
$F$	Faraday constant
$I$	Stack current
$i_L$	Limiting current density
$i_o$	Exchange current density
$K$	A constant
$M$	Mach number
$\dot{m}$	Mass flow rate
$N$	Number of cells in the stack
$n$	Number of electrons transferred per mole of reactant
$P$	Electrical and/or thermal power delivered by the system
$P_1$	Pressure upstream of the pump
$P_2$	Pressure downstream of the pump
$p_x$	Partial pressure of species X

$R$	Range of the airplane
$r$	Internal resistance
$U_f$	Fuel utilization
$U_{O_2}$	Oxygen utilization
$v$	Specific volume
$W_1$	Airplane starting weight (takeoff weight as used)
$W_2$	Airplane final weight (landing weight as used)
$W_{F,used}$	Fuel burned during the mission
$W_{F,reserve}$	Extra fuel that must be carried but is not used in normal missions
$W_{OEW}$	Operating empty weight
$W_p$	Payload, including passengers, their baggage, and cargo

### **Greek Letters**

$\Delta$	A change (e.g, $\Delta W_{F,used}$ is a change in fuel used)
$\alpha$	Charge transfer coefficient
$\eta$	Thermal efficiency
$\eta_{pump}$	Pump efficiency

# 1 Introduction

Fuel cells have become increasingly important as alternative sources of power, offering the potential for drastic reduction in emissions in particulate matter (PM), nitrogen oxides ( $\text{NO}_x$ ), and  $\text{CO}_2$ . In addition, they offer exceptionally quiet operation, highly efficient use of the fuel energy, and a high energy storage density compared to batteries. For a number of years, the manufacturers of commercial aircraft, most notably Boeing and Airbus, have realized that fuel cells may offer advantages for commercial aircraft operation. Apart from emissions reductions and thermal efficiency referenced above, they can constitute distributed power systems, enabling locating the power near the point of use (reducing wiring) and also reducing the power draw from the engines.

Recently the German Aerospace Center (DLR) has conducted successful flight tests of a fuel cell power system for hydraulic backup power [2], and a fuel cell-powered nose wheel drive motor [3]. In addition, Boeing has been examining the use of fuel cells for on-board electrical power generation for at least the past 10 years, including for distributed power systems [4-7]. A few years ago, Boeing sponsored a Sandia study which examined the use of a PEM fuel cell for a ram air turbine (RAT) emergency power backup system [8]. The results of that study (SAND report 2007-4542P) indicated that the fuel cell could successfully replace a conventional RAT, but offered little performance advantages.

Realizing that it may be difficult to introduce fuel cells directly on aircraft without some prior experience, there has been increasing interest in the use of fuel cells in aviation ground support equipment (GSE). Both Boeing and the US Department of Energy (DOE) have funded Sandia to design and construct a fuel cell based mobile lighting system to replace existing mobile lights that use diesel generators. This project has led to the first commercial offering of a fuel cell based piece of construction equipment (the fuel cell mobile light) by Multiquip, Inc.

Turning attention back to on-board uses, the DOE became interested in examining in a broad way if fuel cells might offer an operational advantage over traditional on-board power systems (generators based off the jet engines). The purpose was to go beyond the rather narrow application of a RAT, which itself is rarely used. The real question is if fuel cells offer operational advantages over traditional power in systems that are used routinely in flight, for example galley power, in flight entertainment, and to provide additional power to the aircraft electrical grid when “peaker” power is needed. This interest in the use of fuel cells is timely, as the electrical needs on-board are going up considerably as systems that were formerly hydraulic in operation are converted to electric operation [1]. For the new Boeing 787, the aircraft-wide electrical generation capacity is 1.5 MW – almost an order of magnitude larger than for previous designs. This study, then, is an initial investigation of the use of fuel cells on-board commercial aircraft. This study is limited to PEM fuel cells. We seek to understand how to physically deploy a fuel cell on an aircraft, understand the impact on system volume, weight, and to understand the impact on jet fuel consumption, both in relation to fuel currently devoted to electricity generation, and the overall fuel needed to fly a given mission.

## 1.1 Content of the Report

This introduction is meant to orient the reader to the topic, and also to the particular aspects that this study addresses. It includes background information on fuel cells used on airplanes, highlights of the insights learned from the study, and a description of the approach.

While this report assumes a general familiarity with fuel cells and energy systems, it does not assume anything beyond popular knowledge of commercial airplanes or airplane systems. Therefore, Chapter 2 introduces the reader to the key concepts needed to understand the airplane application. These concepts are useful to understand the context and implications of putting a fuel cell system on-board a commercial airplane. This includes the critical aspect of how to account for the effect of the fuel cell system on airplane performance.

Chapter 3 describes the components that make up the PEM fuel cell system and the issues related to recovering the waste heat and the system's location on the airplane. It includes background information on fuel cells and hydrogen storage, as well as the specific information needed to estimate the size and performance of the components. Estimated uses of waste heat are discussed. A description of the options for locating the system on the airplane along with pros and cons of each option are also described.

Chapters 4 and 5 gives the details on the thermodynamic and electrical models, respectively, used to simulate the different on-board systems. This includes specific model components, calculations, assumptions, and inputs.

Chapter 6 presents the results of the analyses. It begins with the results related to system design and feasibility; that is, how the system would be best installed on the airplane, the thermodynamic performance of the various heat recovery options, and the selection of systems that give the best overall performance benefit to the airplane. The second section of the chapter explores in more detail the systems selected from the first section for their performance serving combinations of the various possible electrical loads. The last section of the chapter shows the results using the exact same method, but with future technology assumed for the fuel cell and hydrogen storage, to forecast what the effect on the airplane would be if DOE targets for these technologies are met.

Finally, Chapter 0 provides the overall conclusions and recommendations that result from this study, as well as some suggestions on future work to further enable the energy efficiency benefits that may result from deploying PEM fuel cells on commercial airplanes.

Some questions that this report answers are:

- 1. Is it technologically feasible to install and operate a PEM fuel cell system on-board a commercial airplane?**
  - It is feasible and possible using today's technology for all components. However, a system made with today's fuel cell and hydrogen storage technology may not be able to provide an overall performance benefit to the airplane (see next question).
- 2. How does using future technology, such as DOE-target technology for the fuel cell and hydrogen storage, affect the results?**

- Contrary to systems using current technology, some systems using DOE-target technology for the fuel cell and hydrogen storage system were shown to offer performance benefits to the airplane.
3. **Because the fuel cell system is small compared to the entire airplane, can the effect of its size on the airplane's performance be neglected?**
    - No. The addition of a fuel cell system adds mass, and possibly drag, to the airplane. While this penalty may be small compared to the entire airplane, it is not small compared to the fuel cell's benefit. Quantification of this penalty and combining it with the fuel cell's benefit is necessary to determine the overall effect of the fuel cell system.
  4. **Does the addition of the fuel cell system adversely affect the airplane's existing electrical system?**
    - There is no adverse effect. The system remains stable and meets the specifications (MIL-STD-704F) for transient responses. In fact, the electrical system with a fuel cell attached was shown to have a faster transient response than the existing system.
  5. **How important is it to recover waste heat and liquid water from the fuel cell?**
    - Very important. Recovery of waste heat and liquid water is what may allow the fuel cell system to "pay for itself" (i.e., offset its weight increase) and possibly provide a performance benefit to the airplane.
  6. **How does the choice of load affect the fuel cell system's performance?**
    - A load that requires the fuel cell to operate as close as possible to full load throughout the flight will provide a larger performance benefit than one that operates at part load or only for portions of the flight. The reason is the recovery of waste heat and water, as indicated in the previous question. That being said, there may be other reasons to operate a fuel cell sparingly during flight, such as durability concerns.
  7. **What are some methods to recover the waste heat on-board the airplane?**
    - While heating water is one method, the amount of heat generated by the fuel cell exceeds the amount of hot water needed. Instead, heating the airplane's jet fuel absorbs all the fuel cell's heat and provides a performance benefit to the airplane's engine efficiencies.
  8. **Where should the fuel cell and hydrogen storage be located?**
    - The fairing (area around where the wings intersect the fuselage) and tail cone offer similar benefits, including available space. For this study, the fairing is chosen. Locating the fuel cell near the load could provide redundancy benefits and reduce piping, tubing, and wiring mass, but the effect is small and it is likely to occupy space that is currently used for other purposes.
  9. **What electrical distribution methods are feasible?**
    - A  $\pm 270$  Volt DC distribution system was found to be the lowest-mass system. However, either this or a 230 Volt AC system is feasible. Low voltage (e.g., 50 Volt DC) systems are not feasible due to very high current requirements.
  10. **What effect could a fuel cell system have on electrical generation efficiency and CO<sub>2</sub> emissions?**
    - Including the penalty associated with carrying the fuel cell system on-board, using a PEM fuel cell system could decrease the amount of jet fuel needed to generate electricity by over 30%. The amount of CO<sub>2</sub> that could be avoided by a fleet of PEM fuel cell equipped airplanes could be over 20,000 metric tons per year (assuming renewable hydrogen is used to power the fuel cell).

## 1.2 Analysis Approach

The purpose of this study is to find how deployment of a fuel cell on a commercial airplane in a number of different uses would affect the electrical infrastructure of the airplane and the overall performance of the aircraft. To accomplish this, two basic airplane designs were considered: one airplane without a fuel cell (the base airplane), and one airplane designed to perform the same mission as the first airplane, only carrying a fuel cell and associated hardware to fulfill a specific electrical need. The difference in the performance of these two airplanes is made quantitative by calculating the fuel required to fly the mission in the two cases, which requires understanding the influence of drag. Calculating the required fuel also allows us to assess fuel use as it directly relates to power generation on the airplane.

### 1.2.1 Base Airplane and Mission

The airplane selected as the basis for this study is a derivative of a Boeing 787-8, shown in Figure 1. “Derivative” means that while the specifications would be similar to a 787-8, the airplane on which a fuel cell is deployed would be a different model not currently planned by Boeing. This platform was selected primarily because it represents the state-of-the-art in “more electric airplane” (MEA) designs. The MEA differs from traditional airplanes in that many of its systems that were previously powered by pressurized air extracted from the main engines (bleed air) or by hydraulic power are now powered by electricity. These additional electrical loads include engine start, wing de-ice, cabin environmental control and pressurization, brakes, and flight controls [9]. This totally re-designed, much larger electrical system could potentially be more readily adapted to incorporate an on-board fuel cell. In addition, the larger electrical load means that the potential benefit to using fuel cells to replace current generators might be higher than for current, less-electric airplanes.



**Figure 1:** The Boeing 787-8 is a “more electric airplane” with many of the conventional systems converted to electric power. This results in a high on-board electric generating capacity (nearly 1.5 MW). Image ©Boeing, used with permission.



**Figure 2: The mission modeled for this study is a transcontinental flight between San Francisco International Airport (SFO) and John F. Kennedy International Airport (JFK).**

The mission we model is a transcontinental flight between San Francisco International Airport (SFO) and John F. Kennedy International Airport (JFK) in New York City, a distance of 4,139 km (2,235 nm) as shown in Figure 2 below. This choice was made as being a typical intermediate-length flight for a 787-8.

Three electric loads were considered for the application of a PEM fuel cell system: (1) the galley (see Section 2.2), (2) in-flight entertainment system (see Section 2.5), and (3) peaker (see Section 2.6). These systems currently draw power from the main engines. These applications were chosen as being likely first deployments of moderate sized (20 - 60kW) fuel cells. Boeing is currently assessing fuel cell-based galley systems in its own work [10].

It is important to review the system specifications for the “base aircraft” of the model. These specifications are indicated in Table 1 below. These specifications were obtained from Ref. [11] and from conversations with Dr. Joe Breit, Associate Technical Fellow of the Systems Concept Center of Boeing Commercial Airplanes.



Table 1: Specifications of the base airplane and flight mission used in this study.

<u>Airplane Specifications [11]</u>	
<b>Model</b>	Boeing 787-8 derivative
<b>Max Design Takeoff Weight</b>	227,930 kg (502,500 lb)
<b>Length</b>	56.72 m (186.1 ft)
<b>Wingspan</b>	60.12 m (197.25 ft)
<b>Seating Configuration</b>	Short to Medium Range, Dual Class
<b>Passengers as Configured</b>	291
<b>Maximum Passengers (for System Design)</b>	375
<u>Mission Specifications</u>	
<b>Route</b>	SFO <-> JFK
<b>Distance</b>	4,139 km (2,235 nm)
<b>Total Duration</b>	5 hr
<b>Fuel Required for Mission, including reserves</b> (see Section 2.7.2.1 for how this was determined)	22,680 kg (50,000 lb)
<b>Segments and Durations</b>	Ground Taxi: 8 min. Takeoff and Climb: 20 min. Cruise: 4 hr. Descent and Landing: 25 min. Ground Taxi: 7 min.
<u>Load Specifications</u> (from conversations with Joe Breit, Boeing)	
<b>Galley:</b>	
<b>Load</b>	40 kW (forward), 20 kW (mid), 60 kW (aft)
<b>Segments</b>	Initial Ground Taxi, Takeoff and Climb, and Cruise
<b>In Flight Entertainment:</b>	
<b>Load</b>	20 kW
<b>Segments</b>	All
<b>Peaker:</b>	
<b>Load</b>	75 kW per engine x 2 engines = 150 kW total
<b>Segments</b>	Only Descent and Landing

## 2 Airplane Systems and Concepts

An understanding of the airplane's systems and performance is required for finding a practical fuel cell system solution for this unique application. The relevant aspects of these are described in this chapter.

### 2.1 Environmental Control System

The purpose of the environmental control system (ECS) is to pressurize the cabin, provide a continuous source of clean air, and maintain the cabin at the desired temperature. Except as noted, the reference for the ECS information is [12].

#### 2.1.1 Pressurization

In the 787, outside air is pressurized by electrically-driven compressors to approximately 103 kPa (15 psia). Cabin pressure at a normal cruise altitude between 34,000 to 36,000 ft is maintained at or above 84.1 kPa (12.2 psia, corresponding to an altitude of 5,000 ft), and decreases to 81.4 kPa (11.8 psia, corresponding to an altitude of 6,000 ft) at cruise altitudes above 40,000 ft [13]. For reference, at 40,000 feet altitude, the outside air pressure is about 18.8 kPa (2.73 psia) [14]. The electrical load for pressurization is the largest single load of the airplane at cruise, consuming over 25% of the total electrical power by itself. The motors are +/- 270 VDC, adjustable speed. The air intake on the 787 is from intake manifolds on the outside of the aircraft, see Figure 3.

#### 2.1.2 Clean Air Supply

Federal Aviation Regulations (FARs) require 7.25 g/s (0.55 lbm/min; 11.9 SCFM) of fresh air per occupant [15]. It is assumed that the ECS system is sized to supply this flow for the maximum possible number of



Figure 3: Ram-air inlet ducts on the 787 [16].

passengers, 375, corresponding to a maximum fresh air supply of 2,719 g/s (4456 SCFM). The fresh air is mixed with approximately 50% of the air returned from the cabin, cleaned and filtered with high efficiency particulate air (HEPA) type filters, and sent to the cabin air supply system. Approximately 0.33% of the oxygen in the air is consumed in the cabin during normal operation. Of the air withdrawn from the cabin, the remaining 50% is exhausted overboard. To put this air flow in perspective, the entire volume of cabin air is replaced by fresh air about every five minutes. In terms familiar to buildings, this corresponds to about 12.5 air changes per hour (ACH) in a commercial airplane while building ventilation systems are typically designed for just 1 to 2.5 ACH.

### **2.1.3 Temperature Control**

The amount of heat generated within the cabin is greater than the amount that is dissipated through the airplane's skin. It is estimated that each passenger generates approximately 100 W of heat, and each piece of equipment within the cabin generates heat as well. The 787 is the first commercial aircraft with an all-composite hull, and the composite material makes it much more thermally insulating than a normal aluminum aircraft structure.

Cabin cooling is accomplished using the fresh air supply. Although the outside air at altitude is cold (approximately  $-57^{\circ}\text{C}$  ( $-70^{\circ}\text{F}$ )), the compression required for pressurizing this air will heat it to temperatures unacceptable for the cabin ( $95^{\circ}\text{C}$  ( $200^{\circ}\text{F}$ )) [17]. Therefore, after pressurization, the air is cooled using an air cycle machine (a refrigeration unit that uses air as the working fluid, see [12] for more details). This air is then mixed with the recirculated cabin air, cooling it. The effect is that the air cycle machine must reject heat not only from the pressurization process, but also all the heat being generated in the cabin. This heat rejection is accomplished through heat exchangers which utilize outside air captured by ram air inlets, a process referred to as ram air cooling. Because ram air cooling imposes an aerodynamic drag penalty on the airplane, the overall effect of any heat generated on the airplane is to increase aerodynamic drag (see Section 2.7.2.2).

## **2.2 Power Electronics Cooling System**

The 787-8 is unique in that it has a separate, liquid cooling system for its many electronic loads and galley refrigeration units [13]. The power electronics cooling system (PECS) uses propylene glycol as the coolant [17] and runs throughout the airplane. Like the air conditioning system, it is cooled by ram air effectively resulting in a drag penalty for any heat it absorbs.

## **2.3 Galley System**

Galleys provide heated and chilled beverages and food for the passengers, see Figure 4 below for an example. Configuration of the galleys is highly customizable and they are typically configured according to the customer (airline) desires. However, the 787 airplane is designed to meet the maximum customer requirements of electrical power, water, and waste from sinks and lavatories. A typical configuration of an airplane the size of a 787-8 is to have a large galley in the rear, abutting the rear bulkhead, a smaller (but still complete) galley at the front for servicing first or business class, and small sub-galleys near the midpoint used for chilled beverage storage. See Figure 5 below for this arrangement. Refrigeration units, ovens (convection and/or steam), and hot water/coffee pots can all be large electrical loads. In this study it is assumed that the maximum galley load of 120 kW is divided

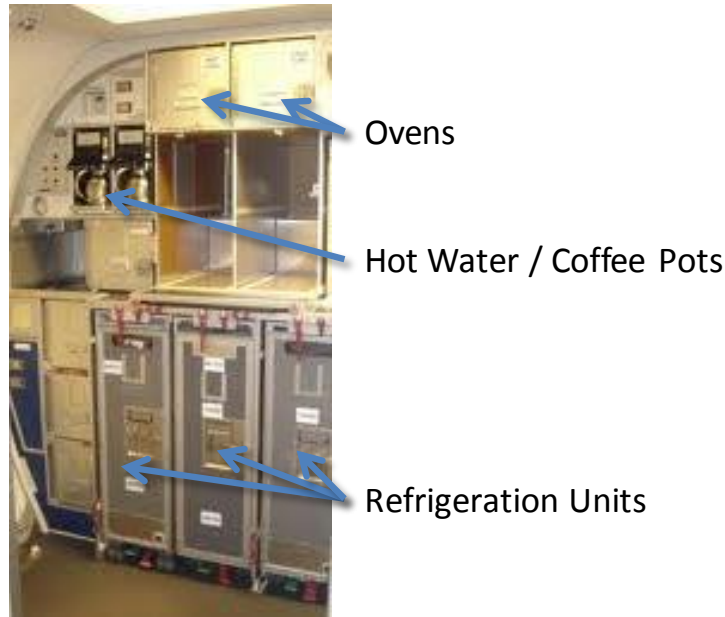


Figure 4: Picture of a typical airplane galley indicating major electrical loads: ovens, hot water/coffee pots, and refrigeration units.

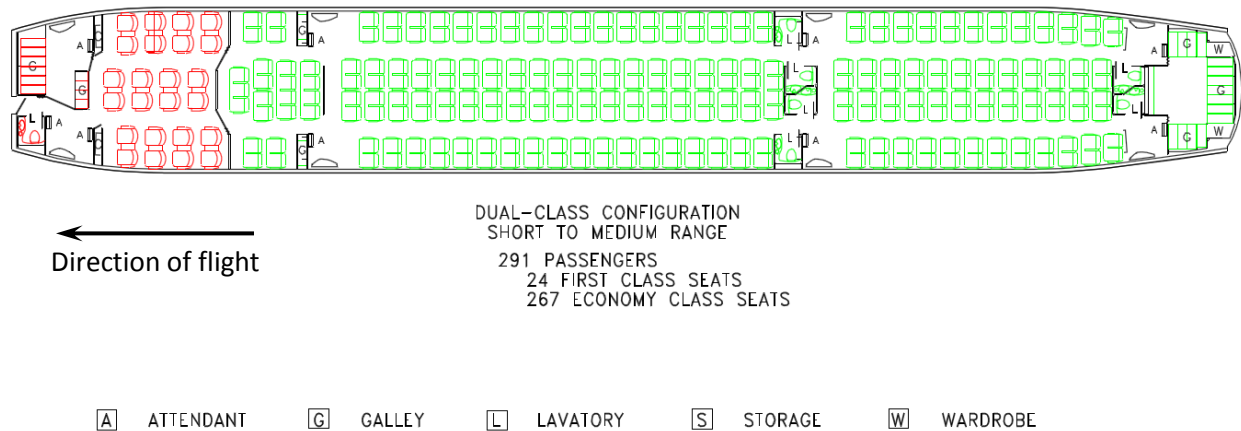


Figure 5: Layout of the 787-8 indicating typical locations of galleys (G) and lavatories (L). The actual configuration is customizable and highly dependent on the customer. The nose is to the left. Diagram from [11].

as 60 kW to the rear galley, 40 kW to the forward galley, and 20 kW for the mid galley. Galleys are active for all phases of flight except for descent, landing, and destination ground taxi. Galley ovens on the current 787 utilize 230 VAC and the other galley loads 115 VAC, all variable frequency (38-800 Hz).

## 2.4 Water System

The 787-8 has two 511 L (135 gal) potable water storage tanks located behind the bulk cargo compartment in the rear of the airplane [18]. Potable water from the airport is treated with ultraviolet light when it is uploaded to the airplane. From the on-board storage tanks, the water is pressurized by electric water pumps and distributed to the galleys and lavatories. Galley and lavatory water faucets are

equipped with electric water heaters for dish and hand washing. In the galleys, water intended for consumption is further treated with charcoal filters, and is heated using the hot water/coffee pots.

United flight attendants on a recent transcontinental flight (SFO – IAD) of a Boeing 777 were able to estimate actual hot water use on that and other flights. The data from these conversations were used to estimate that on a typical transcontinental flight of a 787 less than 62.4 L (16.5 gal) of hot water beverages would be used for a mission-averaged hot water flow of 0.21 LPM (0.055 gpm). Of course this number will vary from flight to flight, even on the same route, and this does not include hot water used for washing or lavatories. However, this gives a rough order-of-magnitude estimate of hot water use that is useful considering the lack of any measured data.

The 787-8 differs from other airplanes in that all waste water (everything that goes down a sink or toilet) is collected on board. The waste tank has a capacity of 1,628 L (430 gal).

## 2.5 In-flight Entertainment System

The in-flight entertainment (IFE) system (Figure 6) includes all electronics for providing movies, TV shows, and audio programming for the passengers, but excludes any electrical receptacles that may be provided for powering or charging laptops and other devices. We estimate that the IFE system consumes a maximum of 20 kW and is active for all phases of flight. The IFE utilizes 115 VAC variable frequency (380-800 Hz).

## 2.6 Electrical Power Generation and Distribution System

The 787-8 has two 250 kVA generators mounted on each propulsion engine, for a total of 1 MW of electrical generation capacity during normal flight. The auxiliary power unit (APU), used for ground power and in-flight emergency power, consists of two 225 kVA generators for an additional 550 kW of capacity [13]. The APU on the 787 is not considered to be operating during the normal mission profile and is ignored for the purposes of this study. However, the APU is another possible early deployment



Figure 6: Illustration of typical in-flight entertainment (IFE) seat-back devices. The total IFE load on a 787-8 could reach 20 kW during all phases of flight. Note: Picture is not from a 787.

application for fuel cell power, and has been examined in prior studies of aviation uses of fuel cells [19-22].

The two engine generators produce power at 230 VAC, and because they are variable speed the frequency depends on engine operation and can vary from 380-800 Hz. Each generator weighs approximately 90 kg (200 lb) [17].

One impact of having the main engines generate so much electrical power is that during periods of low engine load the amount of power needed to generate electricity is a large fraction of total engine output. This occurs primarily during descent and landing, when engines are often throttled back to idle. At these times, the engine is spinning slowly enough that if the power demand (either thrust or electrical generation) was to suddenly increase, the engine's compressor may cease to function properly, or stall, and the engine would shut down. The difference between the stall condition and the operating condition is referred to as the stall margin. It would be advantageous to remove some of the electrical burden on the engines during times of low engine power output. This would allow either a larger stall margin or a reduced engine size for the same stall margin.

An additional concern is that the engine efficiency decreases with decreasing power. This reduced efficiency extends to the generators on the engines. As the engine slows during descent and landing, its thermal efficiency decreases, making the overall electrical energy generation less efficient.

An alternative source of power that is only used for peak electrical loads (a "peaker") during descent and landing would provide dual benefit, increasing both stall margin and efficiency. In this study, two 75 kW peaker fuel cells (one per main engine), operating during descent and landing, is also considered. However, we do not assess the impact on stall margin or efficiency.

A schematic of the 787's electrical distribution system is shown in Figure 7. It can be seen that the airplane employs four distinct distribution voltages and types:

1. The 230 VAC system is used as the main bus, which all current generators feed into. Power from the 230 bus feeds some large loads, and the other three buses.
2. The  $\pm 270$  VDC system gets its power from the 230 VAC bus through an auto transformer rectifier unit (ATRU) and sends it to large motors on the airplane.
3. The 115 VAC system gets its power from the 230 VAC system through an auto transformer unit (ATU) and is used for many of the airplane's large and small loads.
4. The 28 VDC system gets its power from the 230 VAC bus through a transformer rectifier unit (TRU) and it is used for many of the airplane's large and small loads.

The complexity of the electrical system also has the advantage that there are many options regarding how to integrate a fuel cell. For example, inverting the fuel cell's output could allow it to tie-into the existing 230 VAC bus and serve any of the airplane's electrical loads. Or, simple DC-DC conversion could allow it to tie into either of the DC buses. In addition, several fuel cells could be distributed at the point of use, eliminating long wire lengths (and/or possibly eliminating the need for redundant buses), as described in a Boeing patent [5]. The implications of these options are explored further in Section 3.4.

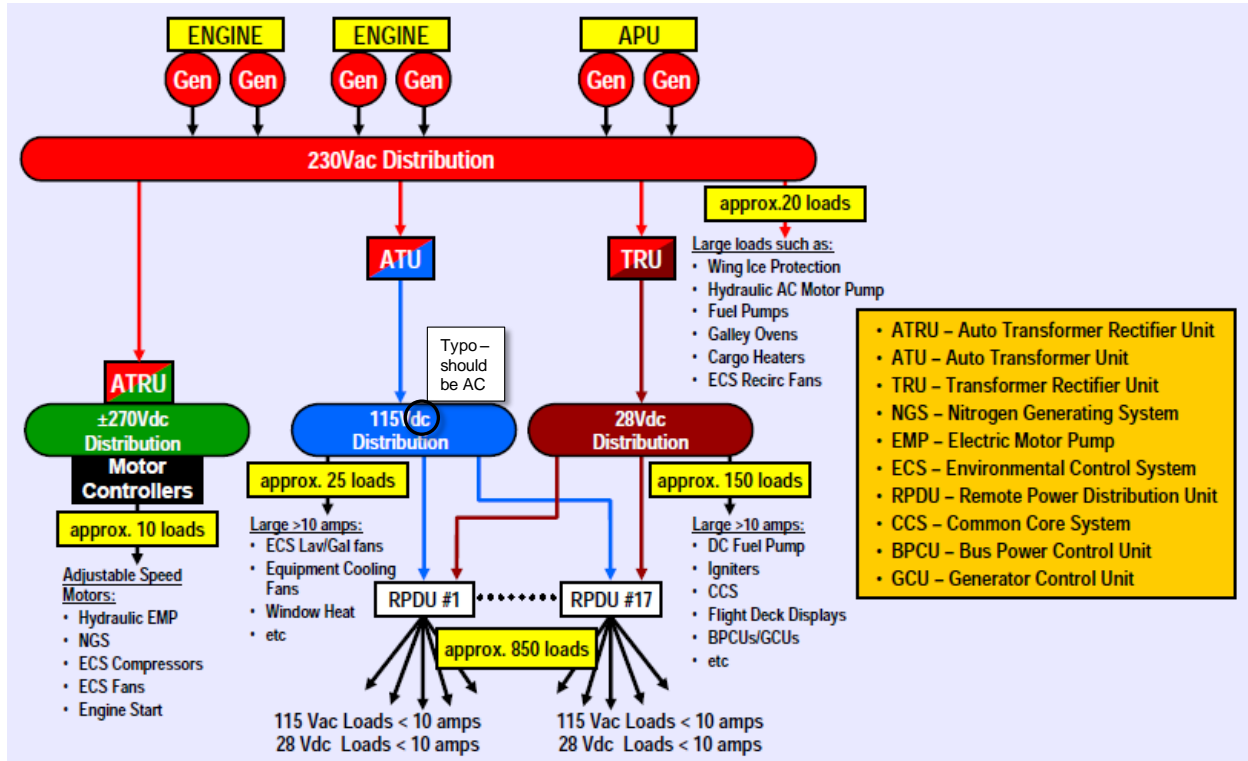


Figure 7: Schematic of the Boeing 787 electrical system. The system is complex yet offers many options for a fuel cell to tie-in. Figure taken from Nelson [13].

## 2.7 Airplane Performance

Many individual factors can be used to measure the performance of an airplane depending on the particular emphasis. These factors include fuel consumption, ratio of lift over drag, velocity (or Mach number), weight, and fuel capacity. Each of these may be more important than the others for a particular application. However, all of these factors can be combined together to give an expression for airplane range. The Breguet range equation is a classic method combining these factors, and can be expressed as [23]:

$$R = \frac{aM}{c_T} \frac{C_L}{C_D} \ln \frac{W_1}{W_2} \quad (1)$$

where  $R$  is the range,  $a$  the speed of sound,  $M$  the Mach number,  $c_T$  the thrust specific fuel consumption,  $C_L$  the coefficient of lift,  $C_D$  the coefficient of drag,  $W_1$  starting weight, and  $W_2$  the final weight. The equation can be used to determine range between any two points on a flight.

### 2.7.1 Base Airplane, Base Mission

A special case is where the Breguet equation is solved for the range of an entire mission. In this case,  $W_1$  is the weight of the aircraft at takeoff and  $W_2$  is the weight of the aircraft at landing.  $W_1$  can be expressed as the sum of its parts:

$$W_1 = W_{OEI} + W_P + W_{F,used} + W_{F,reserve} \quad (2)$$

$W_{OEW}$  is the operating empty weight, which is the weight of the structure, engines, furnishings, unusable fuel, other integral parts of the airplane configuration, and standard supplies, personnel, equipment necessary for full operations.  $W_P$  is the payload, including passengers, their baggage, and cargo.  $W_{F,used}$  is the fuel burned during the mission, and  $W_{F,reserve}$  is the extra fuel that must be carried but is not used in normal missions.

For this special case the airplane has used all of its fuel ( $W_{F,used}$ ) upon landing, so that  $W_2$  is:

$$W_2 = W_{OEW} + W_P + W_{F,reserve} \quad (3)$$

The minimum amount of reserve fuel is regulated by the FAA and depends on the mission length and destination. Airlines may add to this amount in accordance with their own policies. In general, the reserve fuel can be expressed as a fraction of the used fuel:

$$W_{F,reserve} = xW_{F,used} \quad (4)$$

Airplane drag ( $C_D$ ) has two components, induced drag ( $C_{DL}$ ) due to the creation of lift, and parasitic drag ( $C_{DO}$ ) due to all other effects including the shape, friction, etc. That is:

$$C_D = C_{DL} + C_{DO} \quad (5)$$

Combining equations (1) through (5) results in a range equation for the base airplane on the base mission:

$$R = \frac{aM}{c_T} \frac{C_L}{C_{DL} + C_{DO}} \ln \left( 1 + \frac{W_{F,used}}{W_{OEW} + W_P + xW_{F,used}} \right) \quad (6)$$

### 2.7.2 Effect of Weight and Drag Changes

As mentioned in Section 1.2.1, the effect of adding a fuel cell system to the airplane is quantified by comparing the performance of the base airplane to the performance of the airplane with the fuel cell. Since this study assumes a derivative of the existing 787 airplane, we assume there is no change to the overall shape or flight envelope of the airplane if fuel cells are utilized. This means that, for purposes of this study, all variables in the range equation are assumed constant between the base case and the case with the fuel cell system, with two exceptions. The first is the change in airplane weight  $W_2$  due to the additional fuel cell system weight, and the second is the change in the parasitic drag coefficient  $C_{DO}$  due to additional airplane cooling requirements (as explained in Section 2.1.3). In either case, the effect of using fuel cells can be quantified by the amount of extra fuel needed (or fuel saved) for the airplane to accomplish the same mission as the base airplane.

The first step in this analysis is to rearrange Eq (6):

$$R \frac{c_T}{aM} \frac{1}{C_L} = \frac{1}{C_{DO} + C_{DL}} \ln \left( 1 + \frac{W_{F,used}}{W_{OEW} + W_P + xW_{F,used}} \right) \quad (7)$$



Since all the terms on the left-hand side are the same for the base airplane and the airplane with the fuel cell, they can be combined to a single constant ( $K$ ):

$$R \frac{c_T}{aM} \frac{1}{C_L} = K \quad (8)$$

Combining equations (7) and (8) shows that:

$$K = \frac{1}{C_{DO} + C_{DL}} \ln \left( 1 + \frac{W_{F,used}}{W_{OEW} + W_P + xW_{F,used}} \right) \quad (9)$$

Equation (9) is then solved for the base airplane to determine the constant  $K$ .

We want to quantify the effect on the fuel used, so Eq. (9) can be rearranged to solve for  $W_{F,used}$ :

$$W_{F,used} = \frac{(W_{OEW} + W_P)(e^{K(C_{DO}+C_{DL})} - 1)}{1 + x(1 - e^{K(C_{DO}+C_{DL})})} \quad (10)$$

A change (from the base airplane) in operating empty weight  $\Delta W_{OEW}$  and/or parasitic drag  $\Delta C_{DO}$  will correspond to a change in the fuel used,  $\Delta W_{F,used}$ . Equation (10) can then be written as:

$$W_{F,used} + \Delta W_{F,used} = \frac{(W_{OEW} + \Delta W_{OEW} + W_P)(e^{K(C_{DO}+\Delta C_{DO}+C_{DL})} - 1)}{1 + x(1 - e^{K(C_{DO}+\Delta C_{DO}+C_{DL})})} \quad (11)$$

Solving for  $\Delta W_{F,used}$  and combining the drag terms using Eq. (5) gives:

$$\Delta W_{F,used} = \frac{(W_{OEW} + \Delta W_{OEW} + W_P)(e^{K(C_D+\Delta C_{DO})} - 1)}{1 + x(1 - e^{K(C_D+\Delta C_{DO})})} - W_{F,used} \quad (12)$$

This gives the additional fuel that must be carried for the airplane with the fuel cell system to achieve the same mission performance as the base airplane. By including the effect of both additional weight and drag, it automatically takes into account the interaction between the two. However, the disadvantage is only the combined effect can be seen.

To better understand the individual effects of the weight and drag, the results shown in this report solve Eq. (12) twice: once for a change in weight assuming no change in drag, and once for a change in drag assuming no change in weight. The fuel changes are then added. The slight error of using this method (less than 0.2% for values typical in this work) is considered acceptable so that the different effects can be seen.

### 2.7.2.1 Determining the Weight and Change in Weight

The operating empty weight ( $W_{OEW}$ ) of the current 787-8 is unknown at this time, as the airplane has not been finalized yet. Maximum takeoff weight, maximum fuel, and maximum payload figures are available from Boeing [11], but because of the trade-off between payload and fuel, simply adding or

subtracting these numbers will not give  $W_{OEW}$ . (As an example, the maximum takeoff weight is given as 227,930 kg (502,500 lb) and the maximum usable fuel is 101,894 kg (224,638 lb). Subtracting maximum fuel from maximum takeoff weight will give 126,036 kg (277,862 lb), which is the weight of the airplane plus some unknown amount of payload.) Unpublished reports, projections, and anecdotes estimate  $W_{OEW}$  will be close to 250,000 lb (113,399 kg), which is consistent with the example above. Therefore, this is what is used for the base airplane in this study.

Payload weight ( $W_p$ ) is estimated by considering a fully-loaded passenger flight with no revenue cargo. As mentioned in Table 1 and shown in Figure 5, the base airplane is assumed to be configured for 291 passengers. Assuming an average of 104 kg (230 lb) per passenger (including baggage)<sup>1</sup>, the payload will weigh 30,359 kg (66,930 lb).

The fuel used for the base airplane and mission ( $W_{F,used}$ ) is not known. However, current 787-8 data shows that the maximum range is 15,740 km (8,500 nm) [13] and the maximum usable fuel is 101,894 kg (224,638 lb) [11]. Assuming that maximum fuel is used to achieve maximum range, this gives an average fuel burn of 6.47 kg/km (26.43 lb/nm). Multiplying by the distance of the base mission, 4,139 km (2235 nm), gives a base mission fuel burn of 26,794 kg (59,070 lb). This method will surely give a high number, since as the Breguet equation shows, on a maximum range flight proportionally more fuel is needed to carry the fuel than on the base mission.

For another estimate of fuel burn, Boeing claims the 787 to be 20% more efficient than a 767 [4, 24]. This efficiency gain can be combined with a Boeing report that shows that the fleet-wide average fuel consumption for all 767s to be 1.45 kg/s (11,537 lb/hr) [25], resulting in a predicted 787 average fuel consumption of 1.16 kg/s (9,229 lb/hr). For the base mission of 5 hrs, this comes to 20,933 kg (46,150 lb).

Combining these two estimates, a reasonable assumption is that the base mission will require about 50,000 lb (22,680 kg) of fuel to be burned.

A typical reserve fuel amount ( $W_{F,reserve}$ ) is based on a recent newspaper article showing that American Airlines has historically used a fleet average of between 88 to 95 minutes of reserve fuel on their flights [26]. Therefore, 90 minutes is used in this study, which for a 5-hr base mission gives a value of  $x = 1/3$  in Eq. (4) and a reserve fuel amount of 7,560 kg (16,667 lb).

Adding all these components together gives a total airplane weight of 173,998 kg (383,598 lb) at takeoff ( $W_1$ ), and 151,318 kg (333,597 lb) at landing ( $W_2$ ).

The change in operating empty weight ( $\Delta W_{OEW}$ ) is simply the weight of the entire fuel cell system minus any weight savings. The weight of the fuel cell system includes the fuel cell, hydrogen storage, heat exchangers, pumps, blowers, piping, and accessories. It also includes additional Jet-A needed to provide the increased demand for pressurized air required by the fuel cell. Weight savings that are considered in this study are reductions in engine generator size, reduction in the amount of water carried (due to

---

<sup>1</sup> Conversation with Andy Bayliss of Boeing, Nov. 3, 2010.

production of water from the fuel cell), and reductions in Jet-A carried that is no longer needed for generating the heat and/or electricity that the fuel cell provides. Details of how the fuel cell system component weights were determined and the specific values used are given in Chapters 3 and 6.

Using the above numbers and solution procedure, Eq. (12) shows that every 1 kg (or lb) increase in operating empty weight will require an additional 0.16 kg (or 0.35 lb) of Jet-A fuel to accomplish the same mission as the base airplane.

### **2.7.2.2 Determining the Drag and Change in Drag**

Equation (5) revealed that drag is made up of two major components: drag induced by the lift force, and parasitic drag. Parasitic drag is made up of many components: Roskam and Lan [23] have an 11-component equation of which the last term is “miscellaneous” and accounts for at least eight more components. It is beyond the scope of this report to detail all these different drag components. However, because the airplane with the fuel cell system is assumed to have the same shape and structure as the base airplane, all of these components are considered constant with one exception: the drag due to cooling air. The need for cooling air was explained in Sections 2.1.3 and 2.2, but to summarize:

- Any heat generated within the airplane, including the fuel cell waste heat, must be rejected to the environment or the cabin will become intolerably hot.
- Heat transfer through the skin of the airplane is small due to the low density of air at flight altitudes and the composite structure of the 787.
- Except for the small amount of heat lost through the skin, all heat must eventually be rejected to the atmosphere by ram air cooling.
- Ram air cooling adds parasitic drag to the airplane.

The key idea is that every watt of heat generated on the airplane requires some ram air cooling, which adds to the parasitic drag of the airplane.

Cooling drag is not a major part of overall drag and accordingly estimates of its magnitude are not available in the literature. Even airplane designers may not be sure of this number: according to Roskam and Lan [23], typically drag from the “major contributors” is calculated or measured if possible, then the drag of the entire airplane is measured and the difference between these is attributed to the “miscellaneous” category without too much concern for how that is distributed.

In light of this, we must estimate the cooling drag from what is known, by the following procedure:

1. Assume the total drag coefficient ( $C_D$ ) for the 787-8 is 0.022. This is in the range for jet transport airplanes. It is less than the older A-300B (0.024 according to Roskam and Lan [23]) and at the limit of current technology according to Fillippone [27].
2. Assume parasitic drag ( $C_{D0}$ ) accounts for 60% of total drag<sup>2</sup>. This gives a parasitic drag component of 0.0132. This seems reasonable when compared to other transport airplanes:

---

<sup>2</sup> Conversation with Andy Bayliss of Boeing, October 29, 2010.

0.0131 for a Boeing 707-320, 0.0165 for an Airbus A-340, and 0.0135 for a Boeing 767 [23]. Being lower than the similarly-sized 767 is expected since the 787 is claimed to have utilized several drag reduction strategies [28].

3. Assume miscellaneous drag accounts for 7% of parasitic drag. This is an average of the estimates from Roskam and Lan (9%, Ref. [23]) and Fillippone (5%, Ref. [27]).
4. Assume cooling air drag accounts for 5% of the total miscellaneous drag. This is an engineering estimate based on consideration and knowledge of the other components of the miscellaneous drag category. This results in a drag coefficient of 0.0000462 due to ram air cooling for the base airplane.

To relate the drag number to an amount of heat rejection, we need to estimate how much heat is rejected in the base airplane. Again, this number is not known but must be estimated. The generated heat that must be rejected by the ram air cooling system is divided into three categories:

1. Heat generated by passengers, absorbed by the cabin air and rejected through the air conditioning units,
2. Heat generated by electronics and galley equipment in the cabin, that is absorbed by cabin air and rejected through the air conditioning units, and
3. Heat generated by electronics and galley equipment that is absorbed by the liquid cooling system (power electronics cooling loop, PECS).

Estimates of the magnitudes of these categories are given in Table 2. It shows that approximately 360 kW of heat must be rejected through the current ram air cooling system. To relate this to the drag coefficient, it is assumed that there is a linear relationship between the drag coefficient and the heat rejection. This results in a drag coefficient of 0.000000129/kW. Therefore, given a change in cooling demand, we can calculate the change in parasitic drag ( $\Delta C_{DO}$ ) by this relationship and solve Eq. (12) to find the corresponding change in fuel requirements. This reveals that every 1 kW of additional heat to be rejected will require an additional 0.15 kg (0.33 lb) of Jet-A to overcome the additional parasitic drag as a result of fuel cell deployment and achieve the same performance as the base airplane.

**Table 2: Source and estimated magnitudes of heat generation on board the base airplane that must be rejected to the atmosphere through the ram air cooling system.**

<b>Passenger Heat Generation</b>			
Number of Passengers	Heat per Passenger	Heat Generated	
375 (maximum design)	100 W	37.5 kW	
<b>Cabin Electronics and Galley</b>			
Load	Electrical Demand	Efficiency	Heat Generated
IFE	20 kW	50%	10 kW
115 VAC	140 kW	50%	70 kW
Galley	120 kW	75%	30 kW
Line Ohmic Heating	280 kW	96%	11.2 kW
SUB-TOTAL			121.2 kW
<b>Liquid-cooled Electronics and Galley</b>			
Load	Electrical Demand	Efficiency	Heat Generated
ATRU	432 kW	90%	43.2 kW
ECS Motor Controller	360 kW	80%	72 kW
Hydraulics Motor Controller	40 kW	80%	8 kW
Ram Air (ECS) Fan	32 kW	50%	16 kW
Galley Refrigeration Unit	n/a	n/a	60 kW
SUB-TOTAL			199.2 kW
<b>TOTAL RAM AIR HEAT LOAD</b>			<b>357.9 kW</b>

### 3 Fuel Cell System Hardware and Concepts

The purpose of the engineering analysis was to determine the feasibility of a PEMFC system on board a commercial airplane with respect to:

- Major component options and sizes
  - Fuel cell
  - Hydrogen storage
  - Heat exchangers, blowers, and water pumps
- Waste heat recovery methods
- System location possibilities

Our analysis is meant to be a rather rigorous “first-cut” at determining the feasibility. Due to limitations in scope, we were unable to delve into some topics in great depth. Nonetheless, the analysis below provides sufficient detail that this study can be used to reliably assess the impacts of using current PEM fuel cell technology onboard commercial aircraft for the purposes indicated.

#### 3.1 Fuel Cells

An excellent review of fuel cell systems can be found in Larminie and Dicks [29]. A fuel cell provides, in an electrochemical environment, a way to combine gaseous hydrogen and oxygen to form water (typically as a liquid), as indicated by Eq. (13):



The hydrogen fuel is not literally burned. Rather, the reaction proceeds electrochemically, producing electrical energy and waste heat. The efficiency of the electrochemical process can be significantly higher than traditional combustion. Lutz et al. [30] compared conventional  $\text{H}_2/\text{O}_2$  combustion with the “electrochemical combustion” provided in a fuel cell. Whereas traditional combustion has a thermal efficiency of  $\cong 35\%$ , limited primarily by the temperatures achievable in traditional combustion systems, the thermal efficiency of the electrochemical process can be  $\cong 50\%$ . Wright [31] has also compared fuel cell efficiency with that of heat engines.

Over the years, there have emerged five general classes of fuel cell systems, which are viable and commercially available. Table 3 briefly describes these five types.

Table 3: Types of fuel cells

Fuel Cell Type	Mobile Ion	Operating Temp
Proton exchange membrane (PEM)	$\text{H}^+$	50 – 100 °C (122 – 212 °F)
Alkaline (AFC)	$\text{OH}^-$	50 – 200 °C (122 – 392 °F)
Phosphoric Acid	$\text{H}^+$	$\cong 220^\circ\text{C}$ (430°F)
Molten Carbonate	$\text{CO}_3^{2-}$	$\cong 650^\circ\text{C}$ ( $\cong 1200^\circ\text{F}$ )
Solid Oxide	$\text{O}^{2-}$	500 – 1000 °C (930 – 1832 °F)

The fuel cell types can be divided into two regimes of operating temperature: low-temperature fuel cells that operate in the range 50°C to 220°C (122 – 392°F) (proton exchange membrane, alkaline, and phosphoric acid fuel cells), and high-temperature fuel cells that operate above 650°C (1200°F, molten carbonate, and solid oxide fuel cells). In a related study being performed by the Pacific Northwest National Lab (PNNL), solid-oxide high temperature fuel cells are being examined for their usefulness on-board commercial aircraft.

In this study, we examine the low temperature fuel cells. Alkaline fuel cells are damaged by the small amounts of CO<sub>2</sub> in the air and are not practical for this application. Phosphoric acid fuel cells have typically lower efficiencies and lower power densities than proton exchange membrane (PEM) fuel cells. This leaves a PEM fuel cell as the only practical fuel cell candidate for low-temperature fuel cell operation on-board a commercial aircraft. A description of the PEM fuel cell is found below.

### 3.1.1 PEM Fuel Cell: Background

Figure 8 below shows the relevant reactions in a PEM fuel cell. At the PEM anode (site of oxidation) hydrogen gas ionizes (oxidizes), releasing protons and electrons for the external circuit. Simultaneously, at the cathode (site of reduction), oxygen molecules are reduced in an acidic environment by electrons from the circuit, forming water molecules. Protons pass through the proton exchange membrane, from anode to cathode, completing the circuit.

PEM fuel cells deliver high power density and offer lighter weight and smaller volume than other fuel cell systems. Traditional PEM fuel cells use a solid proton conducting polymer membrane called Nafion, a type of polyfluorinated sulfonic acid (PFSA) material, which allows proton transfer between the anode and cathode. Porous carbon electrodes containing a platinum catalyst act as the membrane electrode assemblies (MEA). PEMs require only hydrogen and oxygen to operate and water to humidify the polymer membrane.

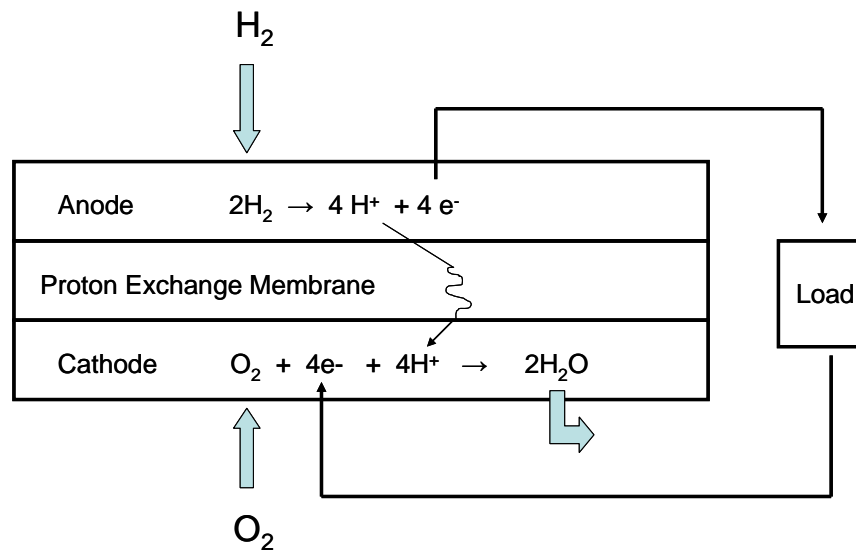


Figure 8: Schematic diagram of a Proton Exchange Membrane (PEM) fuel cell.

Nafion-based fuel cells operate at low temperatures, around 80°C (180°F). The low-temperature operation provides for rapid start-up, which is essential for aircraft power applications. However, for temperatures at or below 80°C, the reaction product is liquid water, making management of liquid water an important issue. The MEAs in PEM fuel cells require a Pt catalyst, which is sensitive to CO poisoning. If properly designed, PEM fuel cells have a low sensitivity to orientation which is particularly favorable for aircraft applications.

It is envisioned that further advances in PEM stack design, materials, and new PEM materials may enable fuel cell stack operation temperature in excess of 100°C (212°F) in order to increase its efficiency, improve heat rejection, further decrease the size of the heat exchanger, and operate the stack at a state where the water produced at the cathode is water vapor versus liquid. This would significantly reduce the balance of plant (BOP), since gaseous water vapor is easier to handle than liquid water.

For this study, we will assume the current state of the commercial PEM systems for nearly all the analysis, only considering planned technology in the final section to illustrate the impacts of improvements in weight and volume reduction. Furthermore, we make no consideration of fuel cell system cost, as this is likely to change drastically as fuel cells become more widespread and manufacturing costs drop.

### **3.1.2 PEM Fuel Cell: Specifics for the Study**

A survey of available PEM fuel cells from various manufacturers was conducted emphasizing those products that offer high power density (Power/Volume) and high specific power (Power/Mass), are available in capacities on the order of the loads in this study (> 10 kW), and are provided as modules requiring only hydrogen fuel, ambient air, and external cooling. That is, they include all equipment required for cathode air compression, heat management, and control.

The module chosen for the basis of the study is the Hydrogenics HyPM HD 12 Power Module. The nominal power output of this PEM fuel cell is 12 kW and the specifics of its operating characteristics are given in the Thermodynamic Analysis section (Table 7, Section 4.1.1). It should not be inferred that this is the only product or manufacturer that will work for this application but is taken as the representative technology and serves well the function of this engineering analysis.

To determine the physical sizes of the fuel cells required to meet the loads in this study, it was assumed that an appropriately-sized module based on technology identical to the HyPM 12 could be built, and its size would be proportional to its power in the same ratio as the HyPM 12. However, the maximum rated capacity was not used to determine this ratio for the HyPM 12. This is because efficiency, and therefore fuel consumption, changes with power so that a fuel cell operating at high power will consume more fuel on a per kW basis than one at lower power (see Figure 9). This affects the hydrogen storage system, changing its weight and volume. So the optimal operating point from a weight and volume perspective must consider the combined fuel cell + hydrogen storage system and not just the fuel cell itself.

In light of this, the lightest system (hydrogen and fuel cell) mass and lowest system volume operating point for the fuel cell was calculated to be that which gives an efficiency of  $\eta_{HHV} = 40.9\%$  ( $\eta_{LHV} = 48.4\%$ ),



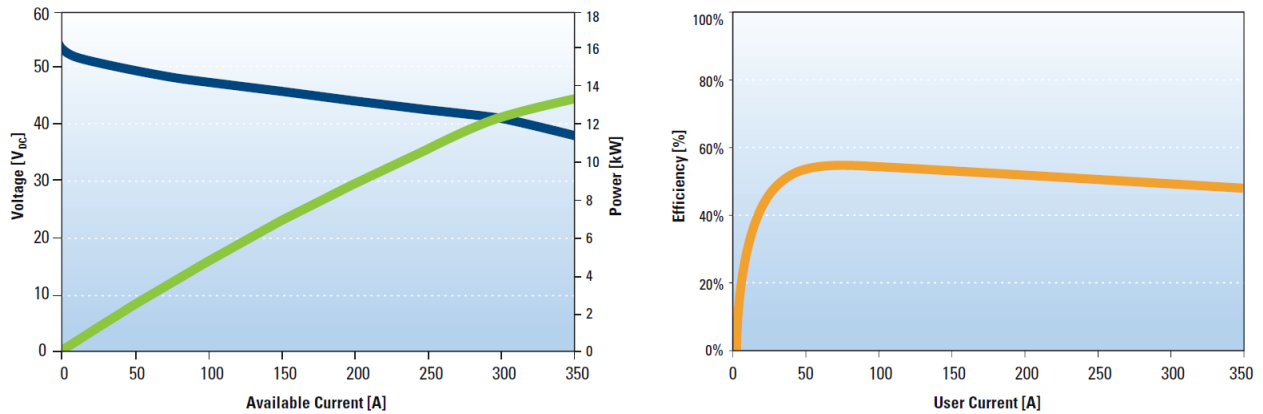


**Figure 9: Typical operating performance for the HyPM 12 power module. The left-hand chart shows voltage (blue line) and power (green line) as functions of current. The right-hand chart shows efficiency (LHV-basis) also as a function of current. Comparing the two figures reveals that the highest efficiency occurs at a low power level, and efficiency decreases as power increases. Note: “Available Current” and “User Current” are the same. Figure from [32].**

which corresponds to a power of approximately 12.8 kW for the Hydrogenics module. This in turn gives the specific power of the fuel cell module is 149 W/kg (67.6 W/lb) and the power density is 103 W/L (2,920 W/ft<sup>3</sup>). These values may be lower than stated for some manufacturers’ products but it must be emphasized that not only is the modeled module a “high power” unit and contain the necessary accessories in addition to the stack but also the fuel cell is not operating at its maximum rated power.

This study also examines the use of DOE-target technology for the fuel cell system. The 2015 targets for 80 kW integrated transportation fuel cell power systems operating on direct hydrogen are 650 W/kg (295 W/lb) gravimetric density and 650 W/L (18,400 W/ft<sup>3</sup>) volumetric density [33], and these values are used in the DOE Target Technology Analysis (Section 6.2.4).

Once the gross fuel cell power required for a given system was determined from the thermodynamic analysis, the relationships (given above) for mass and volume were used to calculate the necessary size of the fuel cell module.

### 3.2 Hydrogen Storage

The hydrogen storage options considered are:

1. Metal Hydride
2. Liquid
3. Compressed gas: 350 bar (5,000 psi) and 700 bar (10,000 psi)

Figure 10 and Figure 11 provide comparisons between these options in terms of storage mass and volume, respectively, for given amounts of hydrogen stored. Each of these options is described below in this context.

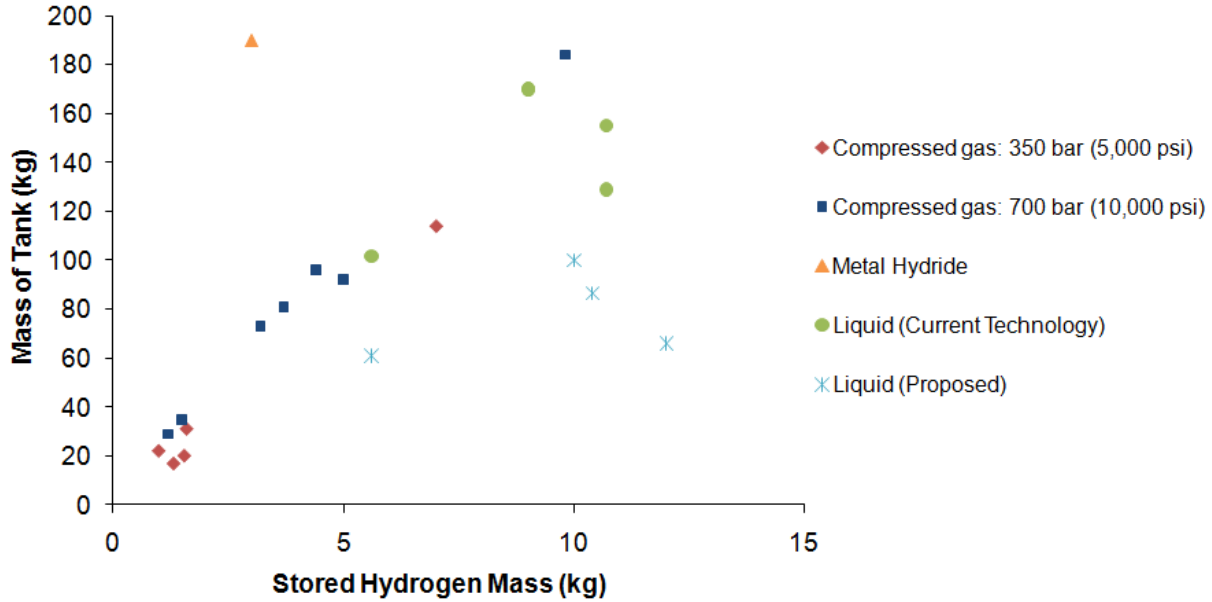


Figure 10: Mass of different hydrogen storage tanks as a function of the mass of hydrogen stored. Compressed gas storage at 350 bar (5,000 psi) offers the lowest mass solution for currently available methods. The proposed liquid storage methods are promising improvements for the future. References: [34-42].

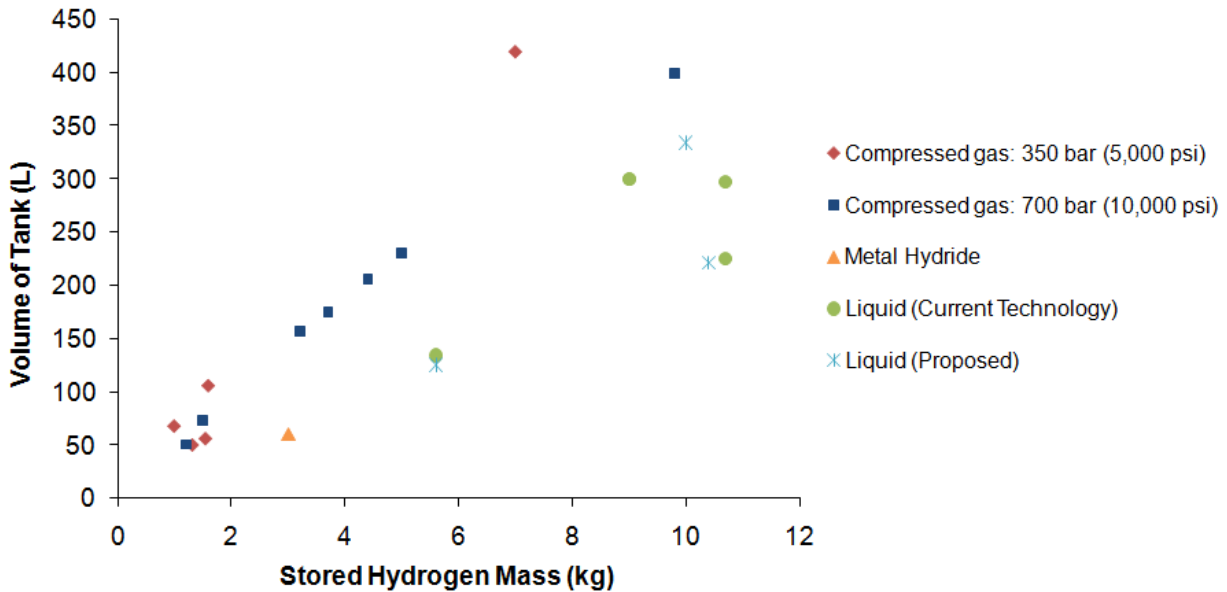


Figure 11: Volume of different hydrogen storage tanks as a function of mass of hydrogen stored. The compressed gas options require a larger volume than either the liquid or metal hydride options [34-41].

### 3.2.1 Metal Hydride

An alternative to storing hydrogen as either a gas or liquid is to store it in a compound as a metal hydride. Metal hydrides have been investigated for many years for their interesting technical properties [43]. Over the years, a number of classic “interstitial” metal hydrides have been studied, and are commercially available. Examples include  $\text{LaNi}_5$ , Fe-Ti-V alloys, and many others. These materials are kinetically fast, fully reversible, but typically their gravimetric capacity is low (typically about 2%),

because heavy metals are employed. This poor gravimetric capacity is particularly troublesome for applying classic metal hydrides in weight-sensitive applications, for example in automobiles or on-board aircraft.

More recently, metal hydrides have been investigated as a way of storing hydrogen for automobile applications. For example, Sandia has been the lead laboratory for The Metal Hydride Center of Excellence (MHCoE, [www.ca.sandia.gov/MHCoE/](http://www.ca.sandia.gov/MHCoE/)), a DOE-funded center comprised of nine universities, six national laboratories, and four companies, all collaborating to develop advanced materials for automotive applications that reversibly store hydrogen with high weight percent and improved volumetric density. A number of interesting high capacity materials have been developed, for example  $\text{AlH}_3$  (10 wt. %) and  $\text{Mg}(\text{BH}_4)_2$  (14 wt. %). All of these materials are at this point research materials only, not ready for use in a practical near term aviation system. One of the best-known of the higher capacity metal hydrides is Ti-doped sodium alanate,  $\text{NaAlH}_4$  [44]. As a practical matter, only a maximum of approximately 4.5 wt. % percent is released from the material. This gravimetric capacity is an improvement over the classic metal hydrides with a weight percent typically of 2 wt. %.

In order to release hydrogen from  $\text{NaAlH}_4$ , one needs to heat the material to temperatures around  $150^\circ\text{C}$  ( $300^\circ\text{F}$ ). Recently, Sandia has completed a project in which the engineering issues associated with building a 5 kg (11 lb)  $\text{NaAlH}_4$  automotive tank, with all the attendant heat transport and kinetic issues, have been worked out [45]. However, such a tank is at an R&D stage, and not really ready for a near-term commercial aviation applications.

The only metal hydrides that are readily commercially available are the interstitial metal hydrides, and so, we report on the weight and volumetric capacities of a commercially available metal hydride (OV 679) made by Ovonic Hydrogen Systems. It is a proprietary mixture of nominal formula  $\text{AB}_2\text{H}_3$ , where  $\text{A} = \text{Ti}$  and  $\text{Zr}$ , and  $\text{B} = \text{V}$ ,  $\text{Cr}$ , and  $\text{Mn}$ . The weight and volume estimates we make also include the tank shell and internal structure including heat exchange tubing. A picture of the system used for the data is shown in Figure 12. We do not go into detail on these considerations, as it can be seen from Figure 10 that metal hydrides are simply too heavy to be reasonably used for an on-board aviation application.

### 3.2.2 Liquid

Hydrogen has been stored for decades in large quantities as a cryogenic liquid (“ $\text{LH}_2$ ”) for industrial and space applications. For much smaller quantities of hydrogen, there are no liquid hydrogen storage tanks suitable for transportation applications that are available on the open market. However, some  $\text{LH}_2$  storage systems have been demonstrated in either prototype form or in small quantities. The size characteristics of these are labeled as “Liquid (Current Technology)” in Figure 10 and Figure 11 and it is assumed that these could be produced if needed. It can be seen that the current technology of liquid tanks is comparable to the 350 bar pressurized tanks in terms of weight, and less than either pressurized tanks in terms of volume.

There are two categories of liquid storage. The first is where the hydrogen is stored at approximately 20 K ( $-424^\circ\text{F}$ ), but the pressure above the liquid is simply the equilibrium vapor pressure established by the  $\text{LH}_2$  at that temperature. A second type of liquid storage is one in which the tank containing the liquid

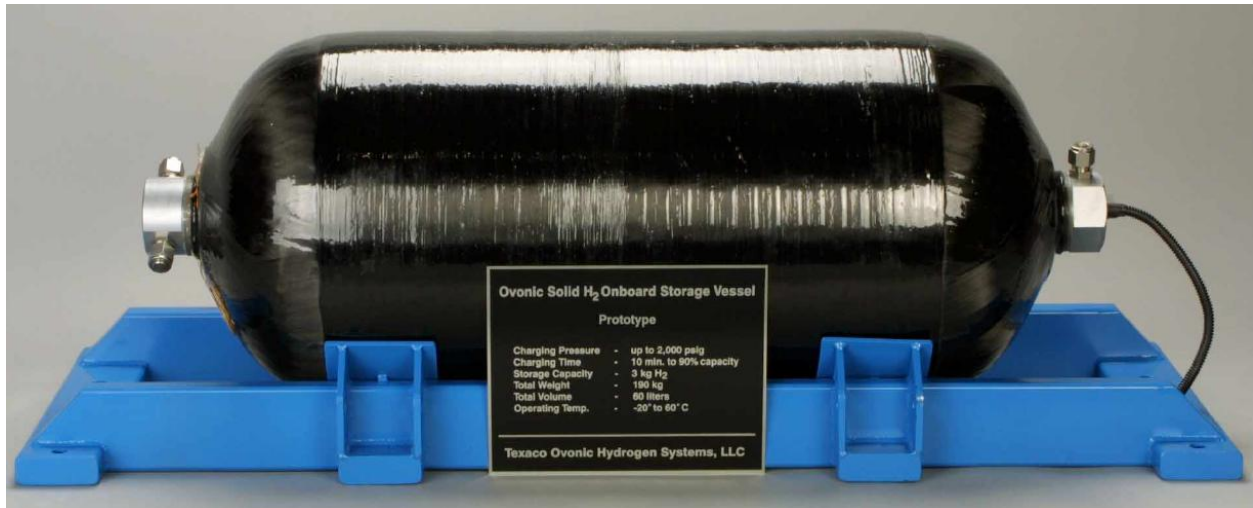


Figure 12: Picture of Ovonic metal hydride storage tank. The nameplate indicates the system shown can store 3 kg (6.6 lb) of hydrogen, has a mass of 190 kg (419 lb), and a volume of 60 L (2.1 ft<sup>3</sup>). From Chao et al. [36], see for more details.

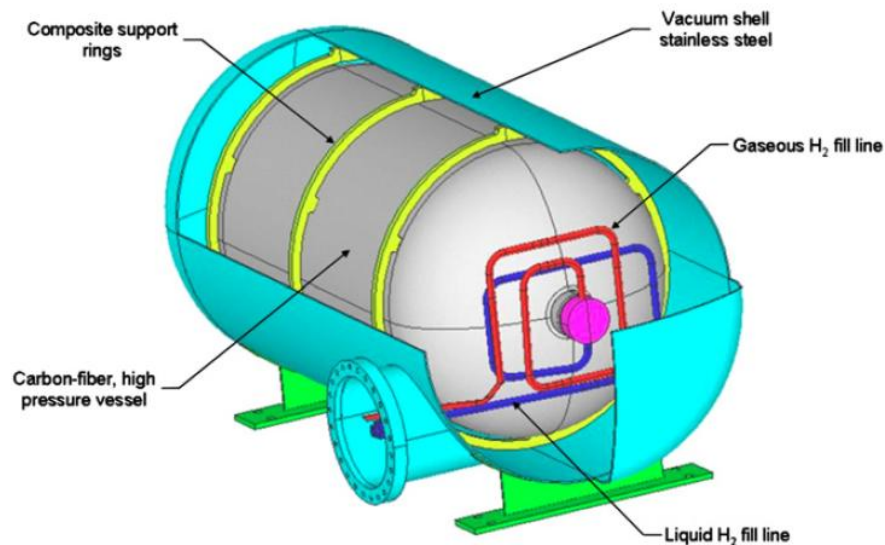


Figure 13: Cut-away view of one of the current technology cryo-compressed hydrogen storage tanks. This design can store 10.7 kg (23.6 lb) of hydrogen at 345 bar (5,000 psi) with tank-only mass of 155 kg (342 lb) and volume of 297 L (10.5 ft<sup>3</sup>). Figure and data from [34].

hydrogen is pressurized and the hydrogen exists as a supercritical fluid. The latter is referred to as cryo-compressed and offers improved gravimetric and volumetric storage density over an atmospheric pressure LH<sub>2</sub> vessel. A current version of the cryo-compressed tank is shown in Figure 13.

There are several improvements to the cryo-compressed tanks that are under development, and they are included in the “Liquid (Proposed)” category in the figures. These proposed liquid tanks offer a large weight reduction over other storage methods, being approximately half the weight of the current liquid

technology. The improvements to this new technology, namely optimizing the pressure vessel and shell designs thereby reducing wall thicknesses and changing to lighter materials, are rather straightforward, and should lead to robust commercially available cryo-compressed hydrogen tanks in the future.

One potential drawback of a liquid hydrogen storage system is the fact that the liquid will absorb heat from the surroundings and evaporate, leading to pressure rise within the vessel. When the pressure builds to the maximum level allowed, the hydrogen is vented to the atmosphere so an un-used liquid hydrogen tank will exhaust itself over time. However, the cryo-compressed design averages less than 0.5% loss per day. Furthermore, this loss becomes negligible in the airplane application where the hydrogen only needs to be stored for the several hours to complete the mission. Of course another consideration for LH<sub>2</sub> is the fact that it takes a lot of energy to liquefy hydrogen: up to 30% of the combustion energy of LH<sub>2</sub> must be consumed in order to produce hydrogen at T = 20K. This represents a drawback from LH<sub>2</sub> being widely available as part of a growing H<sub>2</sub> infrastructure.

Cryo-compressed hydrogen offers promise for future systems, especially if the issues of liquid hydrogen generation, storage, and refueling are satisfactorily solved. However, for this study even these potentially minor issues are not worth the slight increase in gravimetric storage density vs. compressed gas (see Figure 10), and the cryo-compressed storage option was not considered further.

### 3.2.3 Compressed Gas

The compressed gas storage tanks analyzed for this study are composite tanks with polymer liners, also known as Type IV tanks. They are the highest pressure, lightest weight tanks available on the market. The data for the 350 bar (5,000 psi) and 700 bar (10,000 psi) tanks shown in Figure 10 and Figure 11 come from two commercial vendors, Lincoln Composites and Quantum Technologies. Pictures of the Lincoln and Quantum tanks are shown in Figure 14. Compressed gas at 700 bar (10,000 psi) was eliminated during preliminary screening because although it has a smaller volume than 350 bar (5,000 psi) tanks, the weight is more and it has additional safety and fuel logistics concerns. The 350 bar tanks are feasible for use on-board the airplane and were selected for use in the engineering analysis.

For use in this study, 350 bar compressed gas hydrogen tanks were sized according to the linear trend observed in Figure 10 and Figure 11. It is assumed that a custom-designed tank would be used for the

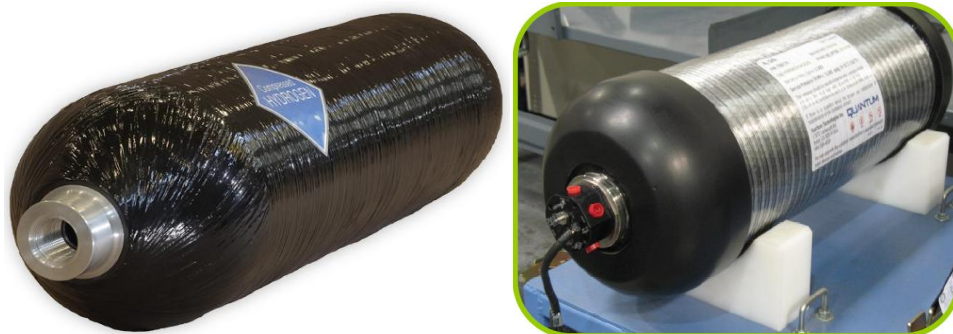


Figure 14: The compressed gas hydrogen tanks from Lincoln Composites (left) and Quantum Technologies (right).

airplane application and it would have similar characteristics to the off-the-shelf models that are depicted in the figures. Therefore the equation used to size the tank mass is the one used to linearly fit the manufacturers' data:

$$\textit{Tank Mass} = 16.19 * H_2 \textit{ Mass} + 0.3862 \quad (14)$$

For 6 kg (13.2 lb) of hydrogen, this leads to a tank mass of 98 kg (216 lb), or about 6.1% gravimetric density. Similarly for volume, the linear fit to manufacturers' data shows that the relationship between hydrogen mass and volume for the 350 bar (5,000 psi) compressed gas tanks is 17.0 gH<sub>2</sub>/L (1.06 lb/ft<sup>3</sup>).

This study also examines the use of DOE-target technology for the hydrogen storage system. The "ultimate" targets of on-board hydrogen storage systems for light-duty vehicles are 7.5% gravimetric density and 70 gH<sub>2</sub>/L (4.37 lb/ft<sup>3</sup>) volumetric density [46], and these values are used in the DOE Target Technology Analysis (Section 6.2.4).

Once the amount of hydrogen required for a given system was determined from the thermodynamic analysis, the relationships (given above) for mass and volume were used to calculate the necessary size of the storage tank.

### **3.3 Heat Exchangers, Blowers, and Water Pumps**

A fuel cell system requires a number of components for operation, including pumps, blowers, fans, and heat exchangers. The primary method to determine the fuel cell system component sizes (weight and volume) was to use the thermodynamic analysis of the system to find the performance requirements, and then consult with manufacturers for the appropriate available or planned product that will satisfy those requirements.

Representative heat exchanger sizes were found by consulting with Lytron Inc., a manufacturer that offers a standard and custom products for both air/liquid and liquid/liquid applications. Although sizes may differ from one manufacturer to another, the differences are expected to be small given the thermodynamic and heat transfer constraints of typical heat exchangers. In the sizing process, the type and flow rates of both fluids along with the ratio of required heat transfer to initial temperature difference (Q/ITD) were taken from the thermodynamic analysis. These numbers were used to find the appropriate heat exchanger from the Lytron catalog and its associated weight and volume.

Blowers are used to feed air into the cathode input on the fuel cell, and for supplying cooling air in the air-cooled system cases. Representative blowers were sized by using the required pressure rise and flowrate from the thermodynamic analysis to find commercially available blowers that would meet these needs. The product line available from Ametek Technical & Industrial Products, a supplier of a variety of blowers including those specific for fuel cell applications, was taken as representative of the type that would be deployed in an actual system.

For the pumps, water flowrate and required pressure head were calculated by the thermodynamic model. Similar to the blower, appropriately-sized, commercially available water pumps from Ametek were used as representative of the size of pump that would be deployed in the actual system.

### 3.4 Electrical Load and Components

The fuel cell size depends on the power load that it must serve, and the hydrogen tank depends on the amount of energy it must store to meet that given load for the specified time. Because all other components in the system must be sized to go along with the fuel cell’s requirements, they also depend on the load. Therefore, to find the system size and performance, it is necessary to specify the load for which it is designed. Table 4 shows the nine load scenarios that considered in this study. More information on each load can be found in Section 2.3 (galley), Section 2.5 (IFE), and Section 2.6 (peaker).

The choice of distribution voltage and type (AC or DC) can impact the number and size of the wires required, so this must be determined before wire mass and volume is estimated. Three possible distribution methods were considered:

1. Low voltage (50 Volt) DC. A DC system has the advantage of not requiring a DC-AC inverter and needs two wires compared to a three-phase AC system. A voltage lower than 50 V provides safety and maintenance advantages. However, wire diameters will be the largest of all options. The 787 does not currently have a 50 VDC distribution system (see Figure 7 in Section 2.6), so this option is mainly considered for stand-alone configuration (a dedicated fuel cell and load circuit independent of the existing electrical system).

**Table 4: The nine different load scenarios considered in this study.**

ID	Load Description	Maximum Electrical Demand	Phases of Flight
1	In-flight entertainment (IFE)	20 kW	All
2	Mid-galley	20 kW	Initial taxi, takeoff and climb, and cruise
3	Forward galley	40 kW	Initial taxi, takeoff and climb, and cruise
4	Aft galley	60 kW	Initial taxi, takeoff and climb, and cruise
5	All galleys combined	120 kW	Initial taxi, takeoff and climb, and cruise
6	Single peaker	75 kW	Descent and landing
7	Both peakers	150 kW	Descent and landing
8	All galleys (5) and both peakers (7)	150 kW	120 kW during initial taxi, takeoff and climb, and cruise; 150 kW during descent and landing
9	All loads (1, 5, and 7)	170 kW	140 kW during initial taxi, takeoff and climb, and cruise; 170 kW during descent and landing, 20 kW during final taxi

2. High voltage ( $\pm 270$  Volt) DC. This system has the advantage of being DC, but requires more attention to safety during maintenance than the 50 VDC system. The 787 already has a  $\pm 270$  Volt distribution bus (see Figure 7) so this will not add any additional requirements and will allow the fuel cell system to tie directly into the existing system.
3. 230 Volt AC. This is the main electrical distribution bus on the 787 (see Figure 7). While this system requires a DC-AC inverter, the electricity from the fuel cell sent to this bus can be used in all airplane loads.

Table 5 shows the amperage requirements for the three options and the different possible loads. The AC current calculations assume a 0.95 power factor. Note that 3-phase AC power inherently requires less current per wire than equivalent DC power. The 50 VDC option has very large currents, and high-current DC may not allow application of proper switching and protection equipment. Therefore, 50 VDC is eliminated from further consideration.

Table 6 shows the appropriate wire sizes based on the design current. It is assumed that an AC

**Table 5: Design current required for the three electrical distribution options. The 50 VDC option would require currents that are too high for switching and circuit protection equipment.**

Load (kW)	Design Current (150% Rated Amps)		
	50 VDC	$\pm 270$ VDC	230 VAC
75	2250	417	297
60	1800	333	238
40	1200	222	159
20	600	111	79

**Table 6: Wire sizes for the 270 VDC and  $\pm 230$  VAC distribution systems.**

<u><math>\pm 270</math> VDC Wire Selection</u>				
Load (kW)	AWG	Number of Conductors	lb per 1,000 ft.	Dia (in)
75	4/o	2	486.8	1.238
60	3/o	2	404.0	1.134
40	1	2	216.7	0.81
20	6	2	79.4	0.496
<u>230 VAC Wire Selection</u>				
Load (kW)	AWG	Number of Conductors	lb per 1,000 ft.	Dia (in)
75	2/o	3	321.4	1.02
60	1/o	3	258.4	0.91
40	2	3	171.5	0.734
20	6	3	79.4	0.496



distribution system will utilize the existing grounding bus running throughout the 787, so only three conductors are needed. Note that there would be two 75 kW units for the Both Peakers load, resulting in a total of four conductors for the DC case and six conductors for the AC case.

Because of the difference between the two system types (DC vs. AC), it is necessary to also consider the difference in equipment; that is, the size of the DC-DC converter for the DC system vs. the size of the DC-AC inverter for the AC system. Commercially available equipment was used to estimate these sizes. For the DC-DC converter, we used an aviation-optimized 60 kW unit manufactured by AeroVironment has a specific power of 3.8 kW/kg and a power density of 2.8 kW/L [47]. For the DC-AC inverter, we used a 30 kW transportation unit manufactured by US Hybrid has a specific power of 1.07 kW/kg and a power density of 1.12 kW/L [48]. These values were linearly scaled by the power of each load to find the sizes for this study.

### **3.5 Piping and Tubing**

Gaseous hydrogen is assumed to be distributed at approximately 446 kPa (50 psig) by stainless steel (type 316L or 304L) seamless tubing with a low pressure drop over the length of the run. This resulted in nominal tubing sizes of ½-inch and ¾-inch OD (outside diameter). Standard tubing wall thicknesses of 0.035 inch and 0.045 inch for the ½-inch and ¾-inch diameter tubing, respectively, were used. This provides a minimum design pressure of 13,890 kPa (2,000 psig). Although this is well above the intended distribution pressure, it provides a safety margin in case of regulator failure, and mitigates the effect of possible tubing wear in the high-vibration environment of an airplane. As customers and passengers feel more comfortable with hydrogen safety, it may be reasonable to reduce the wall thicknesses or possibly switch to a non-metallic tubing to optimize the weight.

Supply and exhaust air streams are assumed distributed by 4-inch (nominal diameter) PVC ducts, and water by ¾-inch (nominal diameter) nylon-reinforced silicone tubing. Either medium could be used to transfer heat from the fuel cell to the heat load, but preliminary analysis revealed that conveying heat via hot water greatly reduced the weight and volume of the piping compared to using hot air. Furthermore, heat exchangers and fans/pumps are more efficient when handling water. For these reasons, conveying heat via hot air was rejected and not considered in any further analysis.

The size of the regulator is taken to be 0.6 L (36.6 in<sup>3</sup>) and weigh 2.3 kg (5 lb). Each hydrogen tank is assumed to have one regulator, and to find the number of regulators required, it is assumed that the maximum capacity per tank is 7 kg (15.4 lb).

### **3.6 Fuel Cell Waste Heat Recovery Options**

The PEM fuel cell generates two streams of waste heat. One is the exhaust of oxygen-depleted air after it passes through the electrochemically active portion of the stack (the cathode), and the other is the hot liquid in the cooling loop that is used to maintain stack temperature at an acceptable level. In this study, the stack was assumed to operate at 70°C (158°F) meaning that both the air and hot cooling water are expected to come out at this temperature. The cooling water carries a significantly higher proportion of the heat load: over 90% of the total heat rejected is through the cooling water.

The fuel cell also releases a small amount of hydrogen. In modern stacks this amount is so small that it is safely mixed with the oxygen-depleted air within the fuel cell module and released with that stream. One additional concept that was considered is taking this small amount of hydrogen and, instead of combining it with the air exhaust, burning it in a combustor to create a high-temperature waste heat stream. Because the combustor would realistically need to be located in the fire-rated tail section, the application of this concept is limited to the heat loads in the rear of the aircraft.

The remainder of this section describes the places on the airplane that may be able to utilize fuel cell waste heat, and options for fuel cell system configurations that supply varying degrees of waste heat.

### **3.6.1 On-board Uses of Waste Heat**

There are few places on the airplane that require heat. The largest load is for wing de-icing. On the 787 this is handled by electrical resistance heaters on the leading edges of the wing, with an electric demand of 30-85 kW per wing<sup>3</sup>. While heating the leading edges with hot air is common on commercial aircraft, doing this on the 787 using the hot air derived from fuel cell waste heat would require a significant re-design of the wing. Therefore, this potential use of waste heat was not considered.

In the cabin, there are three uses of heat: (1) hot water for washing in lavatories and galleys, (2) hot water for beverages, and (3) food service ovens. Low-grade waste heat from the fuel cells could provide wash water at an acceptable temperature (45°C, 115°F), and could pre-heat the beverage water and/or the food service ovens. The high temperature waste heat concept (burning the hydrogen, described above) could be constructed using a hydrogen-fueled furnace arrangement, with the resulting hot air stream used to fully heat the galley ovens, completely replacing their electrical needs. (The effectiveness of this concept is analyzed for the rear galley ovens as Case 5 in this report, see Section 6.1.)

It should be noted that the air conditioning needs of the cabin are entirely cooling-related, as the heat released from passengers is in excess of that naturally lost to the surroundings. This effect is compounded in the 787 due to its all-composite fuselage which is more insulating than the traditional aluminum structure. The transition to the more electric airplane architecture has also added heat loads in the form of the inefficiencies of increased electronics and power handling equipment. In fact, the 787 differs from other commercial airplanes in that it employs a liquid cooling loop extending throughout the fuselage to help reject the large amount of generated heat (see Section 2.2).

If liquid hydrogen (LH<sub>2</sub>) storage is used, it is required to add heat to the storage tank to maintain the pressure at a level high enough for fueling and to pre-heat the hydrogen from its 20 K (nominal) storage temperature to that usable by the fuel cell. As an example, simulation results (described in Chapter 6) show that a 20 kW fuel cell system requires approximately 345 g/s (2740 lb/hr) of hydrogen gas. Thermodynamic calculations reveal that this flow rate requires 1.22 kW to heat the hydrogen from 20 K to 300 K (-424°F to 80°F), and an additional 0.12 kW of heat is needed to maintain the storage tank pressure (using data from Ahluwalia et al. [35]), for a total of 1.34 kW of heat required. The 20 kW fuel cell module produces approximately 20 kW of waste heat, so using some of this heat to pre-heat the

---

<sup>3</sup> Conversation with Joe Breit of Boeing, July 21, 2010.

cold hydrogen fuel is beneficial from a system standpoint, as less of the fuel cell's waste heat needs to be rejected to the surroundings. However, the heat requirement is small compared to the amount of waste heat the fuel cell produces (approximately 7% of the waste heat is needed), and the heat exchangers required for this will add to the system weight and volume. Thus, the overall effect of using the waste heat to warm the hydrogen gas from the liquid hydrogen supply system is ignored in this work.

A remaining use of heat is to heat the airplane's propulsive fuel (Jet-A). Any addition of heat to the fuel will decrease the amount of fuel burned by the engines, resulting in an efficiency gain. Military aircraft commonly use this strategy with a variety of on-board heat sources, while on commercial airplanes the practice is common within the engines themselves, where the fuel is pre-heated by the engine oil. The only drawbacks are a slightly higher pressure drop in the fuel system due to the heat exchangers, and the danger of volatilizing the fuel if its temperature becomes too high. The former problem can be easily solved by appropriately sizing the fuel pump. For the latter issue, simulation results in this work reveal that for a 20 kW fuel cell system and the flight-averaged Jet-A flowrate of 1.26 kg/s (24.9 gpm), the fuel temperature would increase by about 7 °C (13 °F). For a 170 kW fuel cell, the fuel temperature would increase by about 54 °C (97 °F). Jet-A begins to boil at approximately 200 °C (392 °F) [49], so Jet-A volatilization should not be a concern except for much larger fuel cell systems.

### **3.7 Location Options for On-board Fuel Cell Systems**

There are five main location categories that were considered in this study:

1. Fuel cell and hydrogen near load (base case)
2. Fuel cell and hydrogen in fairing or "pack bay"
3. Fuel cell and hydrogen in tail
4. Hydrogen in the fairing, fuel cell at the loads
5. Hydrogen in the tail, fuel cell at the loads

A dimensioned outline of the 787-8 is given in Figure 15 showing each of these locations.

The issues influencing the choice of the optimal location of a fuel cell are:

1. Available space on the airplane
2. Safety of the installed systems
3. Tubing, ducting, and wiring mass and volume
4. Fuel cell waste heat recovery
5. Rejection of waste (warm and moist air from the cathode, condensed water, hot coolant, and/or excess hydrogen)

These factors are described below, along with the screening procedure

#### **3.7.1 Available Space on the Airplane**

There are two locations on the airplane where there is a significant amount of empty space due to the aerodynamic requirements of the airplane shape: the fairing (where the wing joins the body) and the tail cone. These two locations have the advantage of being able to host excess equipment volume without compromising interior space or changing the external shape.

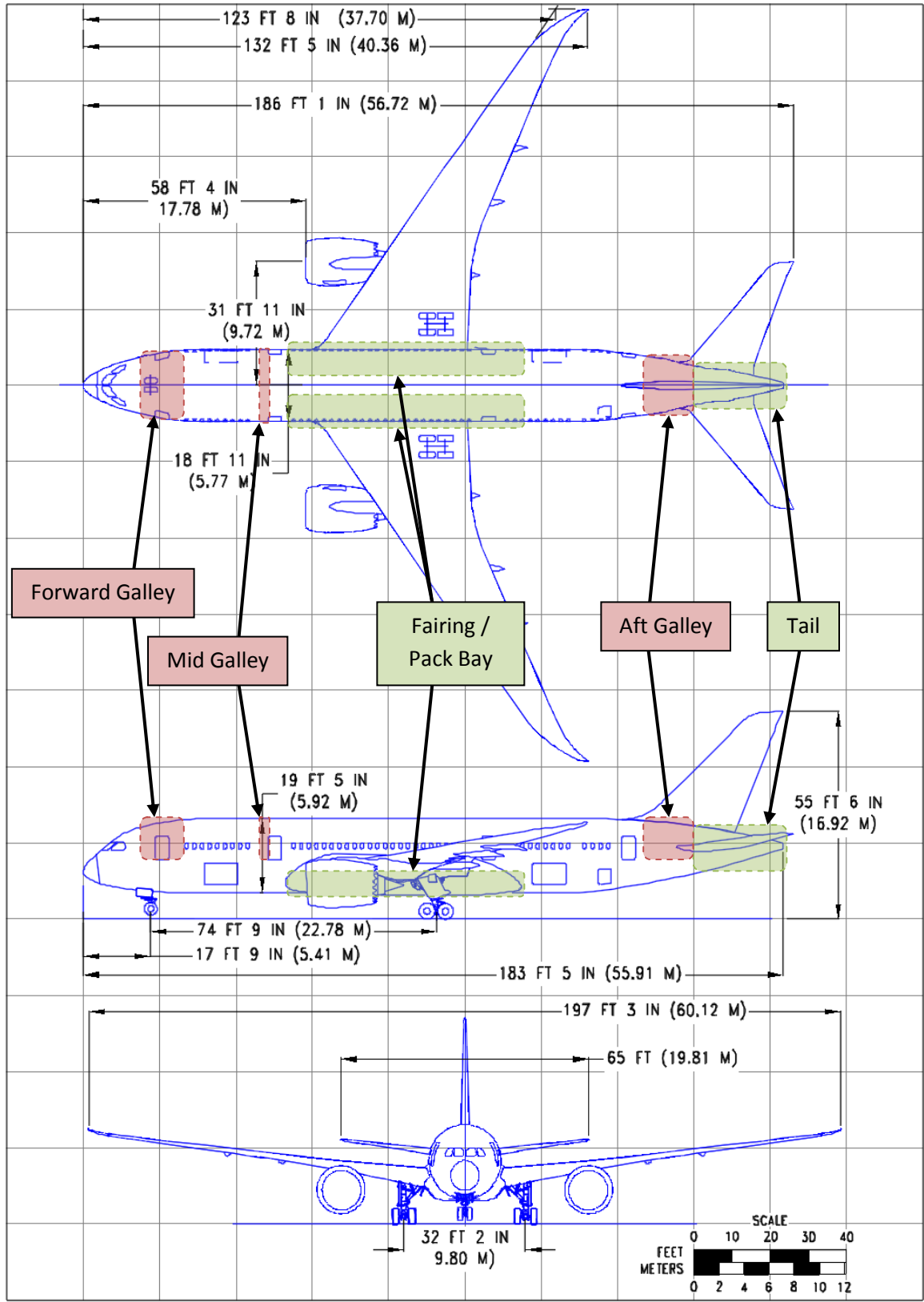


Figure 15: Dimensioned outline drawing of the 787-8, showing location of the loads and options for the fuel cell and hydrogen storage. Dimensioned drawing (without locations) from [11].

If the fuel cell and/or hydrogen is located outside of the fairing or tail cone, and instead is located near the load, it must displace an existing or planned piece of equipment such as part of a galley, overhead storage, under-floor cargo space, or passenger seat space. The inconvenience to an airline customer may make this option less attractive. For example, a typical galley cart occupies approximately 240 L (8.5 ft<sup>3</sup>). The 40 kW system sized for the forward galley would occupy approximately 1150 L (40 ft<sup>3</sup>), meaning it would displace an equivalent of nearly five galley carts. By comparison, the available volume in the tail cone area is estimated to be over 2,800 L (100 ft<sup>3</sup>), and possibly more in the fairing area.

### **3.7.2 Safety of the Installed Systems**

While fuel cells and hydrogen storage systems have in many respects a successful safety record, the aviation application exposes the travelling public to this technology in a very proximate way. The relative locations of people and hydrogen technology hardware strongly influences where such technology would likely be deployed on the airplane. From a safety perspective, the fire-rated section of the tail has a significant advantage in that it is behind a firewall and the space is rated for fire hazards, such as might be a concern for a hydrogen fuel – fuel cell system. This firewall does not currently exist in the fairing area, although such an upgrade is certainly possible and reasonable. These safety issues will be important considerations for early adoption onto an aircraft from both regulatory and customer acceptance points of view.

The separation of hydrogen storage from the fuel cell requires hydrogen to be piped through the airplane to the point of use. While all-welded tubing and fail-safe shutoff valves at the source should mitigate the safety issues, the perceived increase in risk may make this option less attractive.

Fueling the system might be more difficult if the tank was located in the tail, which is approximately 5 m (15 ft) above the ground, especially if liquid hydrogen is used.

### **3.7.3 Tubing, Ducting, and Wiring**

The details of the tubing and ducting for hydrogen delivery and fuel cell thermal management systems was described in Section 3.5, and the electrical wiring in Section 3.4. The location of the fuel cell system relative to the hydrogen tank, the heat load, and the electrical load will affect the length of these components and therefore the overall mass and volume. This impact for different location options is quantified in the Results section (Chapter 6).

### **3.7.4 Waste Heat Recovery**

The fuel cells generate a large amount of heat in the form of hot cooling water and gas exhaust streams. Except for the case with the hydrogen combustor, the streams are hot enough to heat, but not boil, water and would be suitable for heating tap water for washing, preheating hot water for beverages, and pre-heating oven systems. The case with the hydrogen combustor can provide hot enough waste heat for supplying an oven with all its thermal needs.

In all cases, the closer the fuel cell is to the load, the easier it is to utilize the waste heat. The reason for this is that the uses of waste heat are near the electrical loads in many cases (for example the galleys require both electricity for refrigeration and heat for hot water). The alternative is to pipe hot water or air from the location of the fuel cell to the load. This adds a marginal amount of weight (see the Piping

Weight and Volume section) but also reduced the amount of useful heat due to heat loss along the length of the hot pipe.

### 3.7.5 Rejection of Waste Streams from the Fuel Cell

The fuel cell has between one and four waste streams (depending on the design):

1. Warm, moist, oxygen-depleted air from cathode.
2. Water condensed from the cathode stream (only if the cathode stream is subsequently cooled below the dewpoint).
3. Hot cooling water (some fuel cells are cooled in other ways).
4. Small amount of excess hydrogen exhaust from anode (most PEM fuel cells do not exhaust any hydrogen, or mix it with the large quantity of excess air from the cathode to present no fire hazard).

As mentioned in the Waste Heat Recovery section (Section 3.7.4), the heat from (1) and (3) and energy from (4) may be utilized for other purposes before discharged into the environment. This would reduce, but not eliminate the waste generated by the fuel cell. There will always be oxygen-depleted air at above-ambient temperature that needs to be discharged, and in most cases this will also contain a very small amount of hydrogen (see Section 3.6). The amount of oxygen in this stream would typically not be above 15% and probably 10% or lower for modern stack designs, meaning it is not breathable and could not be exhausted into the cabin. Furthermore, exhausting it into the cabin would add to the heat load on the cabin air conditioning system. So it must be sent overboard and should be ducted to the same line which exhausts cabin air.

If the cathode exhaust is cooled before discharging, some water will condense. This water should be “pure” although any contaminants in the air stream may also enter the water. However, a simple in-line filtration system and, if needed, ultraviolet purification (as currently used for the potable water supply on commercial airplanes) could be applied before sending this stream to the potable water storage tank on board. The advantage of capturing this water instead of sending it to the waste tank is that it enables the airplane to carry less water at takeoff, lowering its takeoff weight. As shown in the discussion of the impact of weight on range and fuel consumption in Section 2.7.2.1, for every 1 L of water (= 1 kg) less on takeoff, the airplane could carry 0.16 kg L less of jet fuel and achieve the same mission.

Over 90% of the heat generated by the fuel cell is carried away by its internal cooling water system. For a typical PEM fuel cell operating condition, this amount can be approximated by the net electrical power of the stack (e.g., for a 10 kW stack, approximately 10 kW of heat will be exhausted through the cooling water). Because we assume the internal cooling system is closed-loop, this heat must be rejected to one of the airplane’s cooling systems and/or to a waste heat recovery option.

Because the internal cooling system is closed-loop, this heat must be rejected to one of the airplane’s cooling systems and/or to a waste heat recovery option.

The amount of hydrogen exhausted from the stack is small compared to the cathode exhaust containing oxygen-depleted air and water vapor. Commercial fuel cells will simply combine this with the cathode exhaust and send to the atmosphere. The resulting mixture will not be flammable due to the small

amount of hydrogen and the reduced oxygen concentration in the cathode exhaust. Alternatively, the excess hydrogen could be kept separate from the cathode exhaust stream and burned with an appropriate amount of air in a combustor to eliminate this exhaust stream entirely. If waste heat recovery is utilized, this has the added benefit of producing a high temperature waste heat stream.

## 4 Thermodynamic Analysis Method

Thermodynamic analysis was performed by utilizing the Matlab Simulink modeling platform. Dynamic (time-variant) modules coupled with the thermodynamic properties database and equilibrium composition solvers from Chemkin (commercial software originally developed by Sandia) were modified where needed and combined to model the complete aircraft PEM fuel cell systems. The system models contain the following blocks, which are subsequently described in detail:

- Fuel cell module
- PEM fuel cell
- Fuel flow controller
- Cooling water block
- Air flow controller
- Hydrogen storage vessel
- Heat exchangers
- Furnace
- Efficiency calculator
- Compressor/blower
- Pump

In addition, the following basic components are commonly used. They are based on simple principles and not described further:

- Fluid stream mixer
- Fluid stream splitter
- Separator (gas/gas or gas/liquid)

### 4.1 Fuel Cell Module

The purpose of the fuel cell module model is to accurately model and predict the hydrogen, air, and cooling requirements of a fuel cell that provides the electrical power demand specified by the load.

#### 4.1.1 PEM fuel cell

The PEM fuel cell model consists of electrochemical, heat transfer, and mass transfer calculations. The electrochemical calculations follow the typical engineering equations as found in common references on fuel cells [29, 50]. As a summary, on the single cell level the system of equations is:

$$V_{Operating} = E - V_{Activation} - V_{Ohmic} - V_{MT} \quad (15)$$

where the Nernst voltage ( $E$ ) is:

$$E = E^{\circ} + \frac{RT}{nF} \ln \frac{p_{H_2}(p_{O_2})^{1/2}}{p_{H_2O}} \quad (16)$$

Where  $p_x$  is the partial pressure of species  $X$ ,  $n$  is the number of electrons transferred per mole of reactant (2 in the case of hydrogen oxidation), and  $F$  is the Faraday constant.



The activation loss is (assuming a charge transfer coefficient ( $\alpha$ ) of 0.5):

$$V_{Activation} = \frac{2RT}{nF} \sinh^{-1} \left[ \frac{i}{2i_o} \right] \quad (17)$$

The ohmic loss is:

$$V_{Ohmic} = r_{cell} * i \quad (18)$$

And the mass transfer loss is:

$$V_{MT} = -\frac{RT}{nF} \ln \left[ 1 - \frac{i}{i_L} \right] \quad (19)$$

The three semi-empirical parameters,  $i_o$ ,  $r$ , and  $i_L$  are the exchange current density, internal resistance, and limiting current density. The exchange current density is a measure of how electrochemically active are the reaction sites, the resistance includes resistance of electrons through the electrodes and ions through the electrolyte, and the limiting current is a measure of the mass transfer losses from the bulk reactants through the electrodes to the reaction sites (and in the opposite direction for products).

These parameters can also be used as curve-fitting variables to match modeled and actual fuel cell performance as measured by voltage-current (V-i) curve generation methods. As opposed to purely mathematical curve-fitting methods, the advantage of using these three parameters along with their associated equations is that they represent the actual construction of the fuel cell. This means that they are relatively independent of operating condition and can be used to simulate cell performance at conditions not represented by measured V-i curves.

While a wealth of V-i measurements is available in the literature, the vast majority of these are on research-level and/or single cells at tightly controlled and optimized conditions. There will be some differences introduced between the V-i curves (and thus  $i_o$ ,  $r$ , and  $i_L$ ) for single cells versus those for stacks and modules even if they are made from the single cell: without exception, performance is degraded once the cell is made into a stack. For these reasons, to capture realistic performance at the stack level, the curve fitting should be done on stacks. And to make the study as practical as possible, the stacks should be commercially available (or at pre-commercial status).

The stack chosen to model for this study is the Hydrogenics HyPM module. Relevant manufacturer's data for the Hydrogenics HyPM HD 12 Power Module, used as the scalable unit for this study, is shown in Table 7. Voltage-current performance and efficiency at the stack level as given by the manufacturer can be seen in Figure 9. Combining this with knowledge about the stack construction [51] and curve fitting the data to the system of equations (15) through (19) produced the parameters shown in Table 7. A comparison of the model based on these parameters and the manufacturer's data can be seen in Figure 16. It should be noted that other PEMFC manufacturers have similar-performing units so choosing a different manufacturer for the fuel cell should not have a large impact on the results.

Table 7: Data for the modeled PEM fuel cell. Manufacturer's data from [32, 51].

Manufacturer's Data	
Model	HyPM HD 12
Maximum Continuous Power	12.5 kW
Voltage Range	30 to 60 VDC
Maximum Operating Current	350 A
Volume	124 L (4.38 ft <sup>3</sup> )
Mass	86 kg (190 lb)
Cooling	Water-cooled, includes pump, requires external heat exchanger
Air	Includes blower
Number of Cells	60
Cell Active Area (approximate)	500 cm <sup>2</sup> (77.5 in <sup>2</sup> )
Modeled Data	
Hydrogen Utilization	95%
Oxygen Utilization	50%
Operating Temperature	70 °C (158 °F)
Anode, Cathode, and Coolant Exhaust Temperatures	70 °C (158 °F)
Anode and Cathode Operating Pressure	1 atm (0.17 atm above ambient inside airplane)
Cathode Blower Efficiency	60%
Exchange Current Density ( $i_o$ )	0.00045 mA/cm <sup>2</sup>
Cell Resistance ( $r$ )	0.00015 kΩ*cm <sup>2</sup>
Limiting Current Density ( $i_l$ )	740 mA/cm <sup>2</sup>

#### 4.1.2 Fuel flow controller

The fuel flow controller specifies the mass flow rate of fuel to send to the stack depending on the power demand and the fuel utilization through the equation:

$$\dot{m}_{H_2} = \frac{1}{U_f} \frac{MW_{H_2} I N}{nF} \quad (20)$$

Where  $U_f$  is the fuel utilization,  $MW$  is the molecular weight,  $I$  is the stack current [A],  $N$  is the number of cells in the stack,  $n$  and  $F$  are as described in the fuel cell section, and the flowrate is given in g/s.  $U_f$  for commercial PEMFCs is typically close to 1, and in this study is assumed to be 95%.

#### 4.1.3 Air flow controller

The air flow controller is designed similarly to the fuel flow controller in that it calculates the amount of air to send to the stack depending on the power demand and the oxygen utilization  $U_{O_2}$ . The equation it uses is:

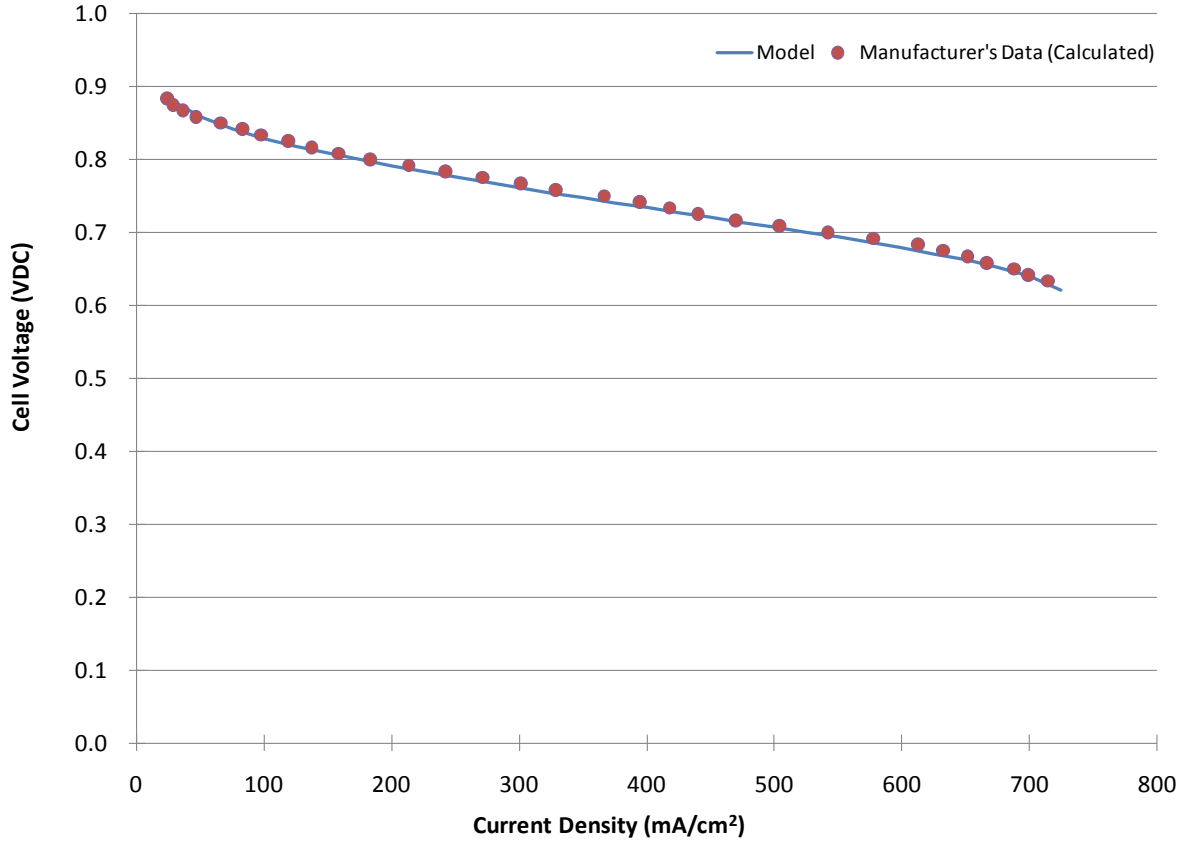


Figure 16: Comparison of the fuel cell model (blue solid line) using the parameters in Table 7, to the manufacturer's data (red circles) as derived from Figure 9. The agreement is satisfactory for the entire operating range.

$$\dot{m}_{Air} = \frac{1}{U_{O_2}} \frac{MW_{Air} IN}{nF} \quad (21)$$

Note that in this case  $n = 4$  because it is considering the oxygen reduction reaction.

The air control block also incorporates a compressor/blower model to find the power required to supply the calculated amount of air at 0.17 atm above ambient pressure at a specified efficiency. In addition, to account for the range limitations of most blowers, a minimum airflow was set so that even if the stack is operating at low load the blower must supply a minimum amount of airflow. This is common for commercial stacks and is the reason for the large drop in efficiency as current is reduced (as seen in Figure 9).

#### 4.1.4 Cooling water block

The PEM fuel cell calculates the amount of heat that must be absorbed by the cooling system. The cooling water block uses this amount of heat to find the amount of cooling water needed to absorb it. Because the stack operates at 70 °C (158 °F) it is assumed the cooling water out of the stack will be 65 °C (149 °F). With the inlet temperature a given, energy conservation is used to calculate the required flow rate. A pump is also modeled to provide the pressure head required for the cooling water loop and the power requirement of this pump is an output.

## 4.2 Hydrogen storage vessel

The hydrogen storage vessel block integrates the hydrogen flow rate to find the total amount used for the mission and adds additional un-used hydrogen to ensure that the tank pressure will be at a specified minimum value (in this case, 100 psig) when the fuel needed is used up. It models the hydrogen as a real gas and finds the required storage volume for the specified pressure.

## 4.3 Heat exchangers

The purpose of the heat exchanger block is to calculate the required heat exchanger performance that can be used to find realistic weight and volume estimates from commercial products. The parameters in the heat exchanger block are temperature in and out and mass flow for each of the two fluid streams. Knowing any five of these parameters the block uses conservation of energy to calculate the sixth. It also outputs the amount of heat transferred ( $Q$ ) and the temperature difference between the two inlet streams (initial temperature difference, ITD). The ratio  $Q/ITD$  is used as an indicator of the required heat exchanger performance and to match the modeled heat exchanger with a realistic one for weight and volume estimates.

A version of the heat exchanger with only one fluid stream is used to model the galley oven.

## 4.4 Furnace

The furnace block is used to find the high temperature waste heat stream that results from burning the excess hydrogen. It has the input of fuel, air, and the desired outlet temperature. In the combustion section of the block, it calculates the stoichiometric amount of air needed for complete combustion of the fuel, and uses the specified equivalence ratio (Actual air/fuel ratio divided by stoichiometric air/fuel ratio, 1.5 in this study) to separate that amount of air out of the inlet stream. It mixes the fuel and air and performs an equilibrium calculation on the mixture to simulate combustion and outputs the combustion products at the adiabatic flame temperature. The combustion products are then mixed with a calculated amount of excess air to achieve the specified outlet temperature of the furnace. In this way, the flowrate and temperature of the hot air going into the oven are determined.

## 4.5 Efficiency calculator

The efficiency of the fuel cell system is an important measure of performance. The equation used to calculate the thermal efficiency ( $\eta$ ) is:

$$\eta = \frac{P}{(\dot{m}HV)_{fuel}} \quad (22)$$

Here,  $P$  is the electrical and/or thermal power delivered by the system. That is, it includes both the electricity supplied by the fuel cell and the heat generated by the fuel cell if it is utilized for a useful purpose. (For example, if a fuel cell system delivers 20 kW of electricity to the load and rejects 20 kW of heat to the environment, the heat rejected is not used so it is not included and  $P = 20$  kW. However, if a fuel cell system delivers 20 kW of electricity, and 10 kW of heat is used to heat hot water, and 10 kW of heat is rejected to the environment,  $P = 30$  kW.)  $\dot{m}$  is the mass flow rate of hydrogen going into the fuel cell, and  $HV$  is the heating value of hydrogen. Because the product of a PEM fuel cell often comes out in

the form of liquid water, the higher heating value (HHV) of the fuel is usually used, and this convention is followed in this work.

#### **4.6 Compressor/blower**

The compressor takes a specified inlet air stream, outlet pressure, and efficiency and uses variable specific heat analysis to find the properties of the outlet (compressed) air stream and the compressor work, ignoring changes in potential and kinetic energy.

#### **4.7 Pump**

The purpose of the pump model is to accurately account for issues of pressure drop and work associated with circulating the cooling water. The pump model assumes that the fluid is incompressible. It uses the following equation to calculate pump power given the required pressure rise and fluid flow:

$$P_{pump} = \dot{m} \frac{v(P_2 - P_1)}{\eta_{pump}} \quad (23)$$

Where  $\dot{m}$  is the mass flow rate,  $v$  is the specific volume,  $P_1$  is the pressure upstream of the pump,  $P_2$  is the pressure downstream of the pump, and  $\eta$  is the pump efficiency.

## 5 Electrical System Analysis Method

The primary issue addressed in the electrical analysis is to assess if the fuel cell can indeed perform the electrical function asked of it, and in a way compatible with the remainder of the airplane electrical infrastructure. The dynamic behavior of any power system, including that of an aircraft, is influenced by the dynamic interactions of its components. Therefore, even if a power system is stable in a steady state, adding additional components may cause the system to become unstable. The objective of this analysis is to analyze the consequences of integrating a fuel cell to the existing electrical generation and distribution of an aircraft through modeling tools. Physical testing, although beneficial and critical, is expensive and time consuming. The modeling approach in the initial scoping stage provides an early indicator of the feasibility of fuel cell use on an airplane in addition to possible challenges that should be addressed with hardware testing.

### 5.1 Approach

As previously stated (Section 1.2.1), an on-board PEM fuel cell system was considered for the galley and IFE loads. An additional case where the fuel cell augments the power from the main engine and APU generators during times when the load demand is high was also analyzed as a Peaker concept. The case of the fuel cell powering only the galley loads and IFE loads is a simpler integration proposition, whereas the Peaker concept presents greater challenges because it has to seamlessly integrate into the main distribution bus and interact with the larger, more critical loads of the aircraft.

Initial analysis of the galley and IFE loads indicated that there may be advantages in designing the distribution system for 28 VDC, and that is the voltage in the simulation of this system. However, the electrical transient and stability results would be nearly the same for other DC distribution voltages including +/- 270 VDC. The higher power requirements of the Peaker concept required higher voltages of either 230 VAC or  $\pm 270$  VDC. Converting the native DC voltage of the fuel cell to AC imposes further weight/space penalties to accommodate the DC/AC inverter. Consequently, the Peaker concept was analyzed based on a  $\pm 270$  VDC network which eliminated the DC/AC inverter. (The analysis described in Section 6.1.1.2 illustrates the impact of different distribution voltages on overall system weight and volume.)

### 5.2 Major Model Components

This section describes the major components of the electrical system models, namely the fuel cell and DC-DC converter.

#### 5.2.1 PEM Fuel Cell Model

A PEM fuel cell stack model from the MATLAB/SimPowerSystems Toolbox library was used. The MATLAB model implements a generic hydrogen fuel cell stack. Within the model there is the option of using the simplified or the detailed model. The detailed model allows parameters such as temperature, pressures, flow rates, fuel rates, etc. to vary. The simplified model was used for this project and represents the fuel cell stack during nominal conditions. Figure 17 shows the equivalent circuit of a fuel cell stack that is the basis for the simplified PEM fuel cell stack model within MATLAB/SimPowerSystems.

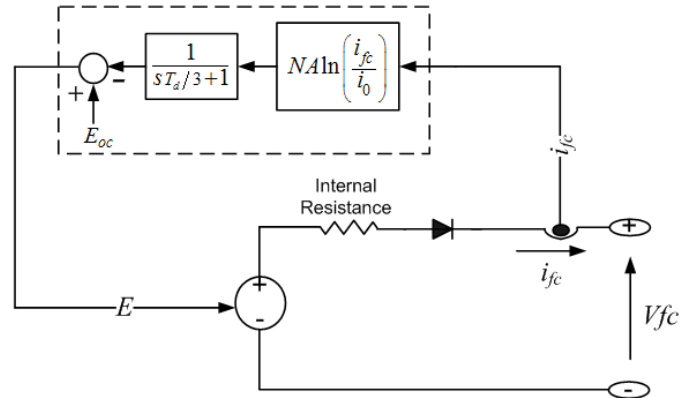


Figure 17: Equivalent circuit of a fuel cell (from SimPowerSystems online product documentation)

In Figure 17,  $T_d$  is the fuel cell response time (seconds),  $N$  is the number of cells,  $A$  is the Tafel curve slope,  $i_{fc}$  is the fuel cell current,  $E_{OC}$  is the open circuit voltage and  $i_o$  is the exchange current. More information on the fuel cell stack model can be found in the SimPowerSystems documentation on the MathWorks website.

Examination of the two models' code and sample results revealed little difference when used for the purposes of the electrical simulation study. Therefore, the simplified model was chosen.

### 5.2.2 DC-DC Converter

The purpose of the DC-DC converter is to convert and stabilize the variable DC fuel cell power to DC bus power at a different, constant voltage. The DC-DC buck converter model used was replicated from one of the MATLAB/SimPowerSystems demos and is shown in Figure 18. Slight modifications to the model were made to convert it from a current-regulated to a voltage-regulated converter. The duty cycle is controlled with a simple PI (Proportional-Integral) type controller, shown in Figure 19.

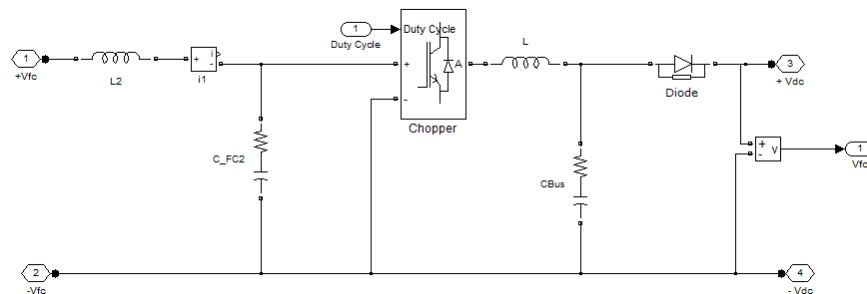


Figure 18: DC-DC converter schematic.

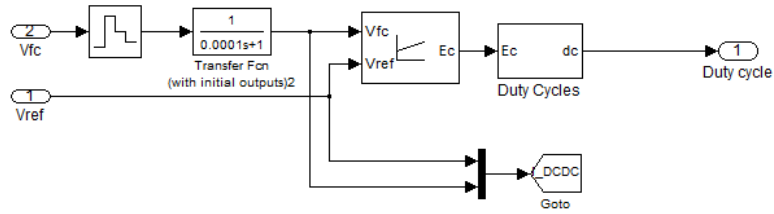


Figure 19: DC-DC converter controller.

### 5.3 Stand-alone Galley Model Description

The stand-alone galley model consists of a 60 kW fuel cell, a DC-DC converter and several galley loads. A graphical representation of the system is shown in Figure 20. Figure 21 shows the system code as modeled using MATLAB/Simulink/SimPowerSystems.

Fuel cell parameters used for the galley simulation can be found in Table 8. The DC-DC buck converter is used to step down the fuel cell voltage from about 625 V DC to 28 V DC.

Table 9 lists the power consumption for each galley load type included in the simulation. The loads were modeled as simple resistive loads and range between 1,600 and 4,340 Watts. The number of galley loads turning on at any one time was limited to two. Supervisory controls to enforce this rule can easily be implemented in the actual system and would ensure that the inrush currents resulting from turning additional loads simultaneously would be minimized. This kind of sequencing would also be transparent to the flight attendant.

Table 8: PEM fuel cell model parameters used in the stand-alone galley simulation.

Parameter	Value
Voltage at 0 A	900 V
Voltage at 1 A	895 V
I <sub>nom</sub> (A)	160
V <sub>nom</sub> (V)	625
I <sub>end</sub> (A)	230
V <sub>end</sub> (V)	430
Fuel Cell Response Time	5 sec

Table 9: Galley loads considered in the galley electrical system simulation, from Refs [52-57].

Load Type	Power Consumption (Rated)
Endura Water Boiler	4,240 Watts
Thermoelectric Refrigerator	1,620 Watts
DS3000 Steam Oven	3,800 Watts
Espresso/Cappuccino Maker	1,600 Watts
Endura Beverage Maker	2,760 Watts
DF3000 Convection Oven	3,800 Watts



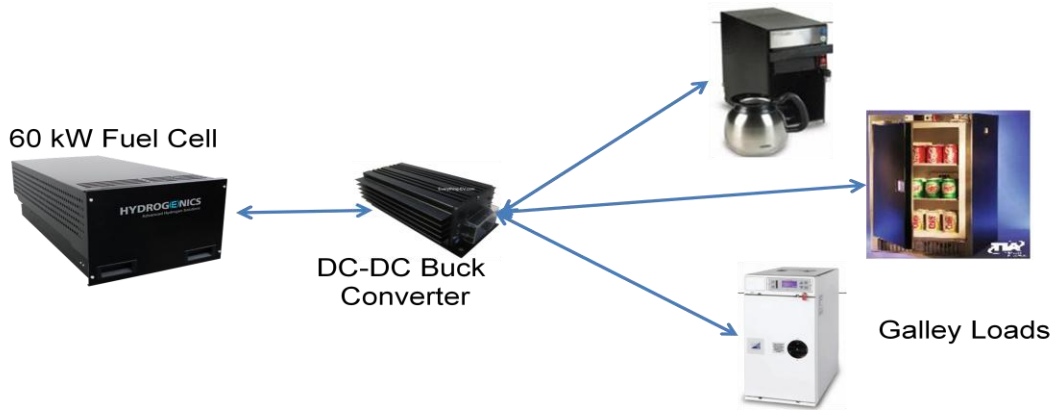


Figure 20: Graphical representation of the stand-alone galley model.

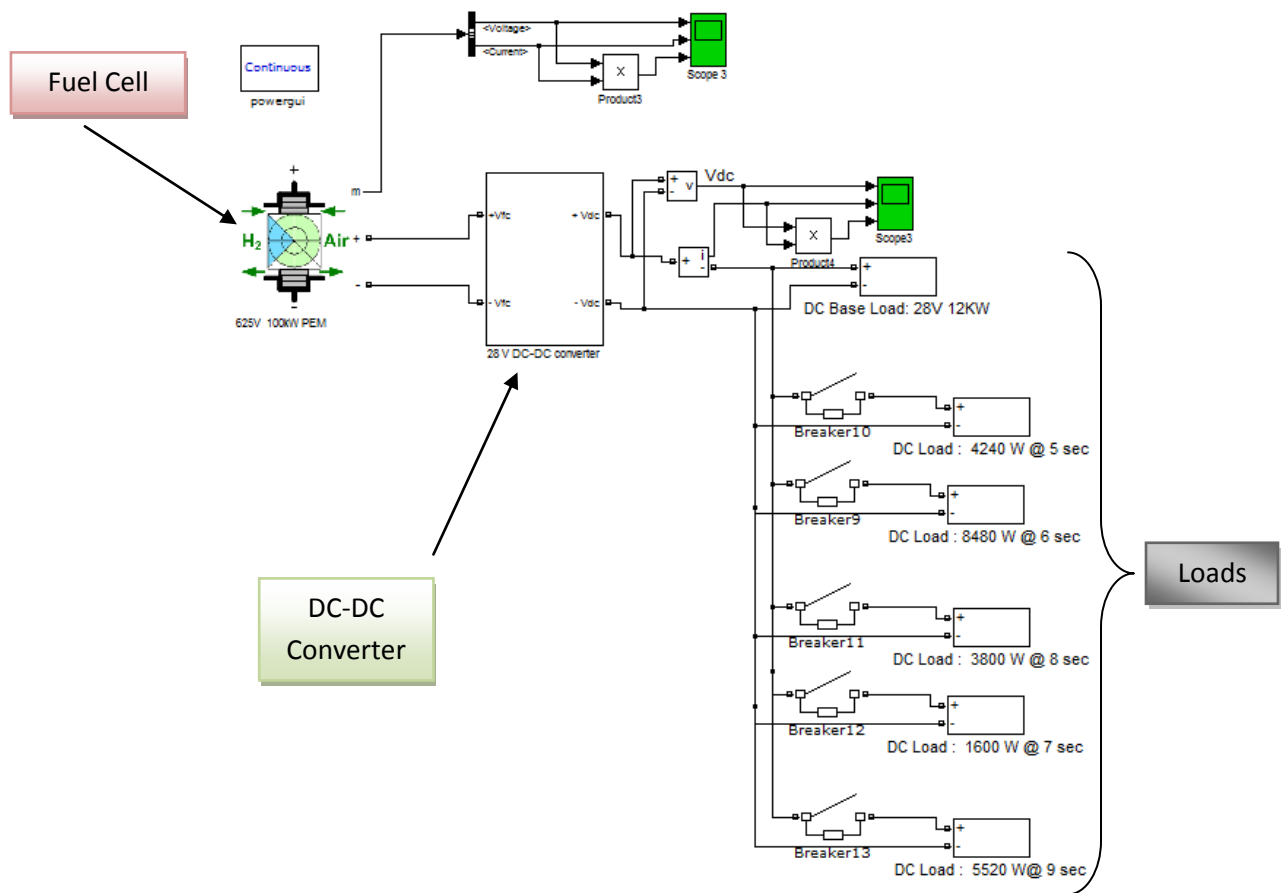


Figure 21: Simulink code for the stand-alone galley model.

The in-flight entertainment (IFE) system was also designed as a stand-alone system. The architecture of the IFE system would be identical to the galley system. Therefore, no additional electrical model was created for the IFE system, since its behavior would be nearly identical to the galley system model. In other words, the electrical simulation results for the galley system are directly applicable to the IFE system.

## 5.4 Peaker Model Description

The Peaker system consists of a 75 kW fuel cell and DC-DC converter, and interacts with other larger and more critical loads connected to the existing  $\pm 270$  VDC bus of the aircraft. A graphical representation of the system is shown in Figure 22. Figure 23 shows the Simulink code for the model. Recall that there are two peaker fuel cell systems contemplated for the 787 airplane.

As stated earlier (Section 2.6), the function of the fuel cell as a peaking unit is to decrease power burden on the main engines during periods of low engine power output. For example, during descent and landing the main engine output decreases, thus reducing either the output from the two generators on each engine or the stall margin on the compressor. Incorporating the Peaker concept would take some burden off the main engines, allowing either a larger stall margin during this flight period, or a reduced engine size for the same stall margin. In the Peaker function, the fuel cell will meet the power demand only when the engine generator limits have been met, and the fuel cell does not operate when the loads are lower than a pre-determined threshold.

Fuel cell parameters used for the peaker simulation can be found in Table 10. The DC-DC converter was used to step down the fuel cell voltage from about 625 Volts to 270 Volts.

A generic aircraft electrical distribution model demonstration included with SimPowerSystems was modified and used to model the  $\pm 270$  VDC bus of the aircraft. The aircraft electrical distribution model consists of a signal representing the mechanical input (engine speed) going into the 200 kVA generator and a Generator Control Unit (GCU) responsible for regulating voltage to 230 VAC (the main distribution voltage). Only one generator was modeled but in reality there are two generators per engine. There are also several components (transformer, rectifier, etc.) representing the Auto Transformer Rectifier Unit (ATRU) that is responsible for rectifying the 230 VAC to  $\pm 270$  VDC.

The total peaker load was estimated to be between 50 kW and 100 kW based on information from Boeing. Because the peaker ties into a bus, and the loads attached to that bus are widely varied, for purposes of this simulation all of the loads were modeled as simple resistive loads and the load increases varied between 25 and 35 kW. If motors or other inductive loads were modeled, the effect would be slightly different but applicable; i.e., the transients would change but there would not be any stability issues.

**Table 10: PEM fuel cell model parameters used in peaker simulation.**

<b>Parameter</b>	<b>Value</b>
<b>Voltage at 0 A</b>	900 V
<b>Voltage at 1 A</b>	895 V
<b>I<sub>nom</sub> (A)</b>	120
<b>V<sub>nom</sub> (V)</b>	625
<b>I<sub>end</sub> (A)</b>	326
<b>V<sub>end</sub> (V)</b>	230
<b>Fuel Cell Response Time</b>	5 sec

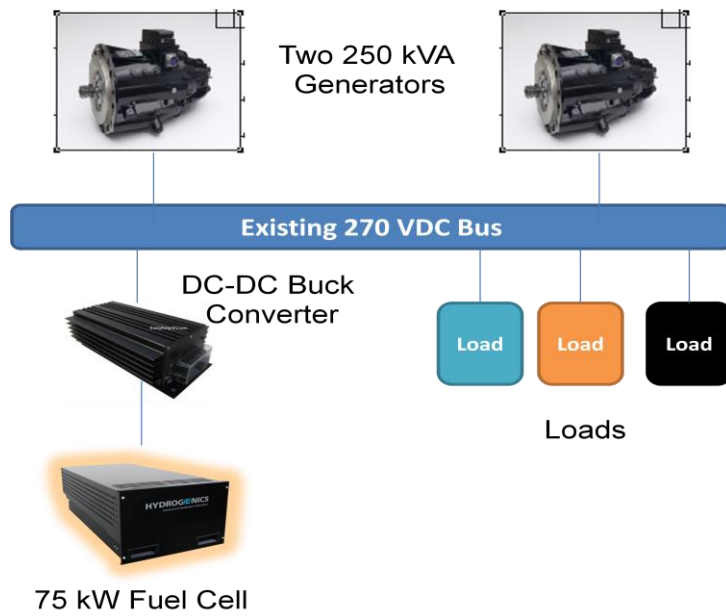


Figure 22: Graphical representation of the Peaker System model.

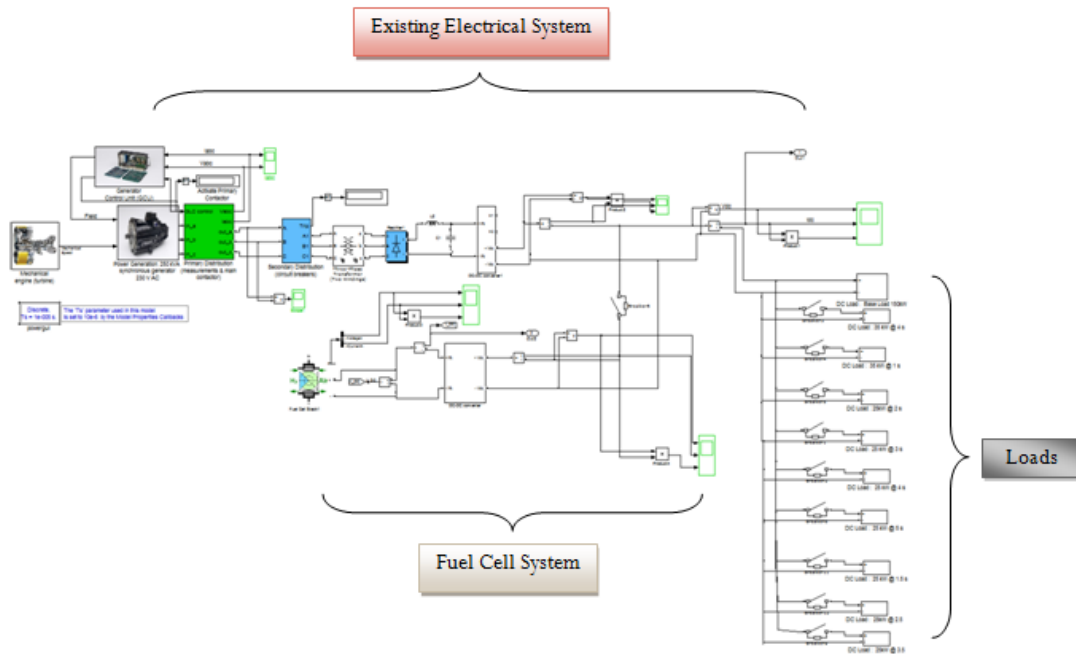


Figure 23: Simulink code for the Peaker model.

## 6 Results and Discussion

The main purpose of the first section in this chapter is to show whether or not a fuel cell system could be feasibly implemented on board an airplane, and what some of the design aspects and trade-offs are. This is done by examining different possible system configurations; that is, both how the components of the system are arranged relative to each other and the arrangement of the whole system on the airplane. This part of the study considers a fuel cell system supplying electricity to the in-flight entertainment (IFE) load, a 20 kW load constant for the entire flight. Considering only one of the nine possible load scenarios (see Table 4 in Section 3.4) is acceptable because the conclusions related to feasibility are the same for all of them. Besides the basic determination of feasibility, another product of this section is the recommendation of the three system configurations that make the most sense.

The goal of the second section in this chapter is to compare and contrast the effect of different loads on the system, and therefore, overall airplane performance. This is done by analyzing the three recommended system configurations from the first part in more detail, considering each possible load scenario. This enables not only a recommendation of the preferred system configuration, but also the preferred implementation strategy with regards to a specific load.

The goal of the last section of this chapter is to show what the possible performance benefits for the airplane may be in the future, if DOE targets for the fuel cell and hydrogen storage technologies are met. This is done by repeating the analysis of the second part, but using DOE target technology for the fuel cell and hydrogen storage components as described at the end of Sections 3.1.2 and 3.2.3, respectively.

### 6.1 System Design and Feasibility

This section shows the results that deal with system location, design, and performance, all leading to a determination of feasibility.

#### 6.1.1 Location

Many of the concepts related to system location were covered in Section 3.7. This section shows the quantifiable results that relate the effect of location on the mass and volume of tubing, ducting, and wiring. Combining these results with the qualitative reasoning discussed earlier, a recommended location is determined.

##### 6.1.1.1 Tubing and Ducting

The tubing and ducting is used to distribute the fuel, air, water, and waste heat streams associated with the fuel cell system. Depending on the location of the various system components, the required length of each tube or duct was determined from the airplane dimensions (see Figure 15). A factor of 1.5 was multiplied by this length to account for changes in elevation, bends and turns, fittings, and valves. The resulting “effective length” was multiplied by the weight per length and volume per length to find the size of each required tube or duct.

A summary of the piping mass implications of each arrangement is shown in Figure 24. First an overall comment. The magnitude of the piping masses (< 50kg (110 lb)) is not a very large addition to the mass of the aircraft. Recall from Section 2.7.2.1 that the estimated takeoff weight of the base airplane is

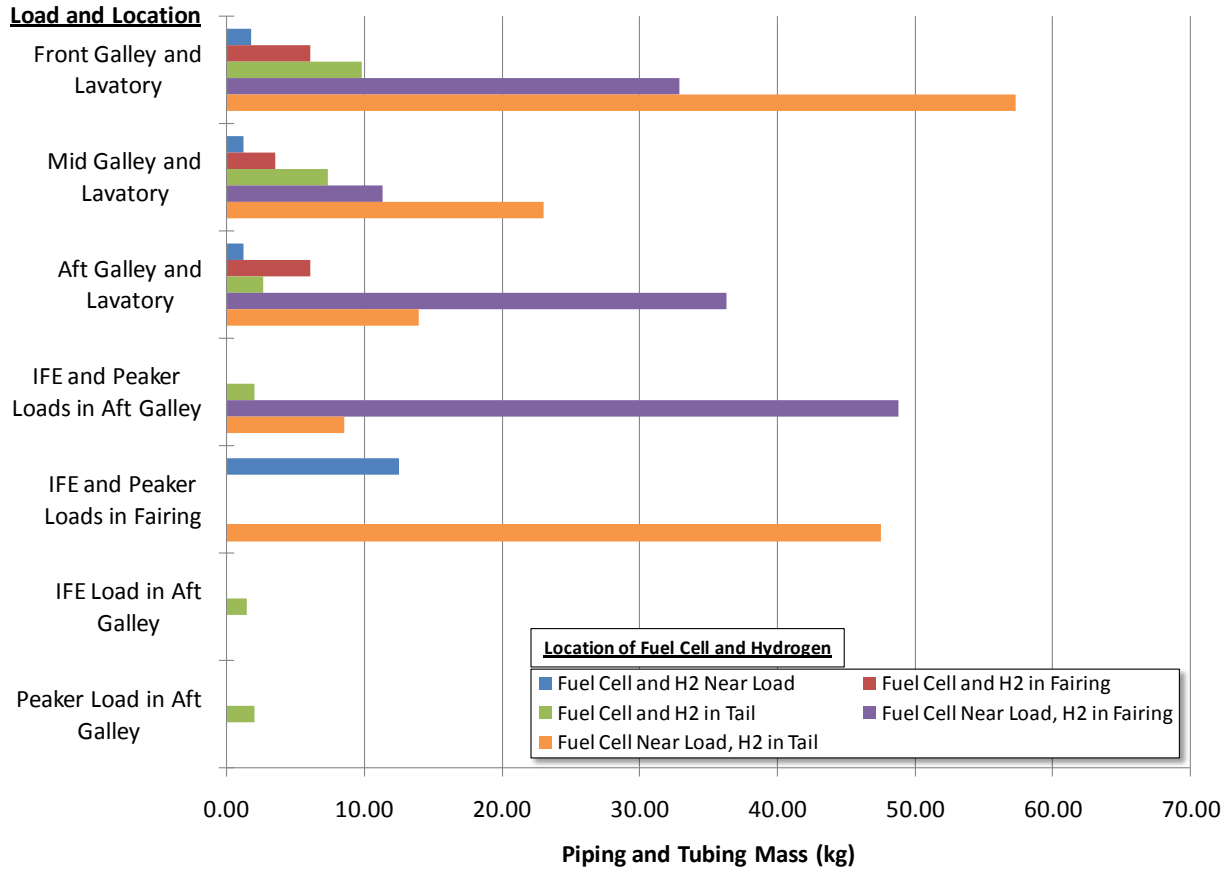


**Figure 24: The effect of location of the fuel cell and hydrogen storage systems on the piping and tubing mass. The chart reveals that the impact of not locating the fuel cell close to the load is small, but the mass increases several times when the fuel cell and hydrogen are separated.**

173,998 kg (383,598 lb). So, for each fuel cell system, the plumbing mass is minor. Placing each fuel cell and hydrogen system near the load it serves (blue bars) is the lightest option. However, the added mass of locating both the fuel cell and hydrogen system either in the fairing (red bars) or in the tail (green bars) is small and may be worth the convenience of utilizing existing empty space. The purple and orange bars show the effect of separating the fuel cell from the hydrogen: the large increase in mass is due to the long runs of stainless steel tubing that are required to distribute the hydrogen to the fuel cell. Again, it may be possible to reduce the wall thickness of this tubing and/or change to a non-metallic material. This would decrease, but not eliminate the penalty of separating the fuel cell from the hydrogen.

The results of the corresponding analysis for volume are shown in Figure 25. The overall impact of the piping and tubing on volume is rather small, with the worst case only adding approximately 18 L (0.64 ft<sup>3</sup>) of volume compared to the best case. However, some trends can still be observed. The volume has less variation than the mass, mainly because the 3/4" water tubing has a greater impact than the 1/2" stainless steel tubing, whereas on the mass basis the latter is more important. However, on long runs of hydrogen the volume increase is evident. The worst case is when the IFE and peaker hydrogen supply

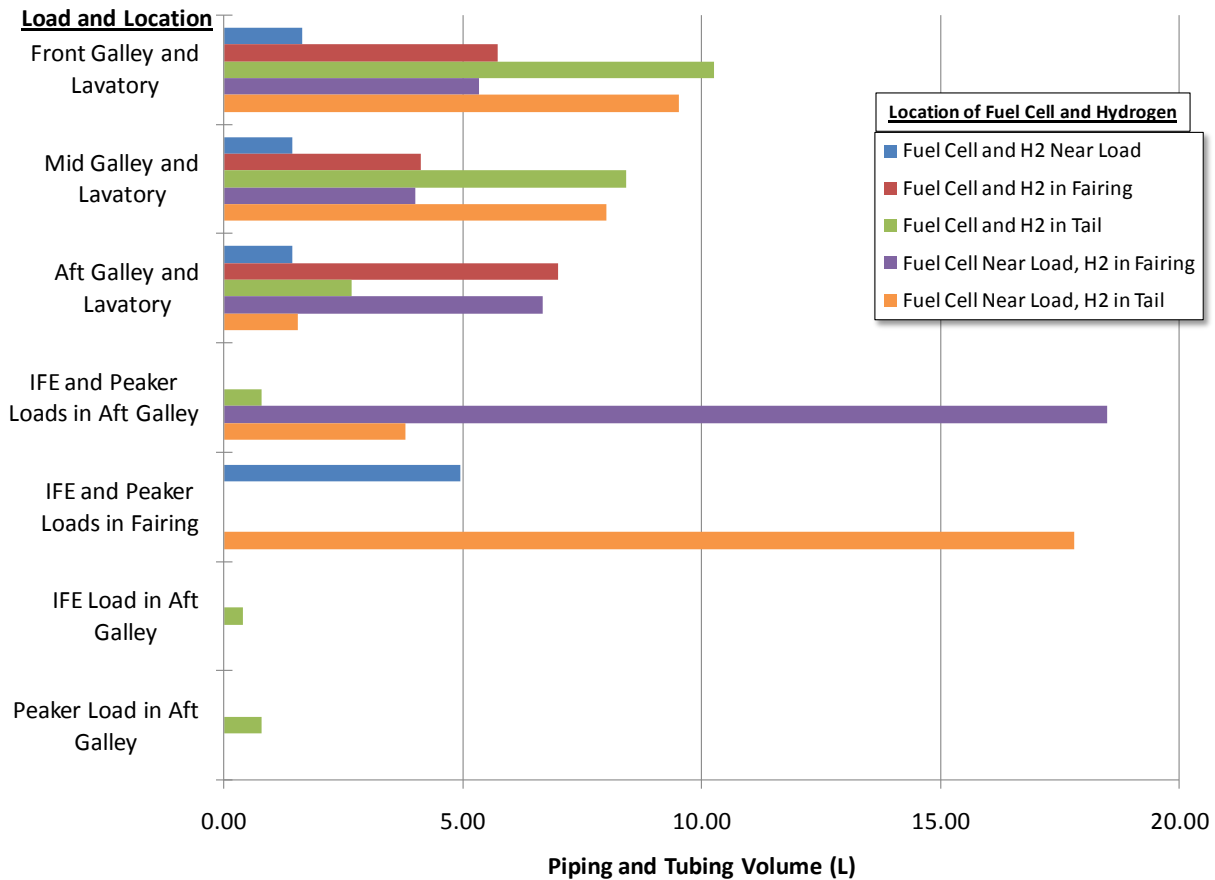


**Figure 25: The effect of location of the fuel cell and hydrogen storage systems on the piping and tubing volume. The results show that the differences between cases are relatively small. Similar to the mass analysis, the worst cases are when the hydrogen and fuel cell are separated.**

tubing is combined and the hydrogen is far from the fuel cell. These cases require ¾" tubing to keep the pressure drop within acceptable levels, but the increase in volume is nearly double all other cases.

The mass and volume analyses shown assume the use of waste heat recovery. When there is no waste heat recovery, the mass will decrease by about 2 kg (4.4 lb) for the cases where the fuel cell is close to the load, up to 10 kg (22 lb) when the fuel cell is furthest from the load. The analyses also assume that heat is distributed to the loads via hot water, not hot air. If hot air is used instead, the volume figures will increase many times.

The overall result from the piping and tubing analysis is that the piping system mass and volume can be minimized by keeping the hydrogen and fuel cell as close to each other as possible. The location of the fuel cell relative to the load will impact the results but the overall change is small and other location factors should be considered first.

### 6.1.1.2 Wiring

The combined masses of the wiring and DC-DC converter or DC-AC inverter for the different loads and locations around the airplane are shown in Figure 26. The distances between locations were estimated to be the same as in the piping and tubing analysis (previous section), including a factor of 1.5 to

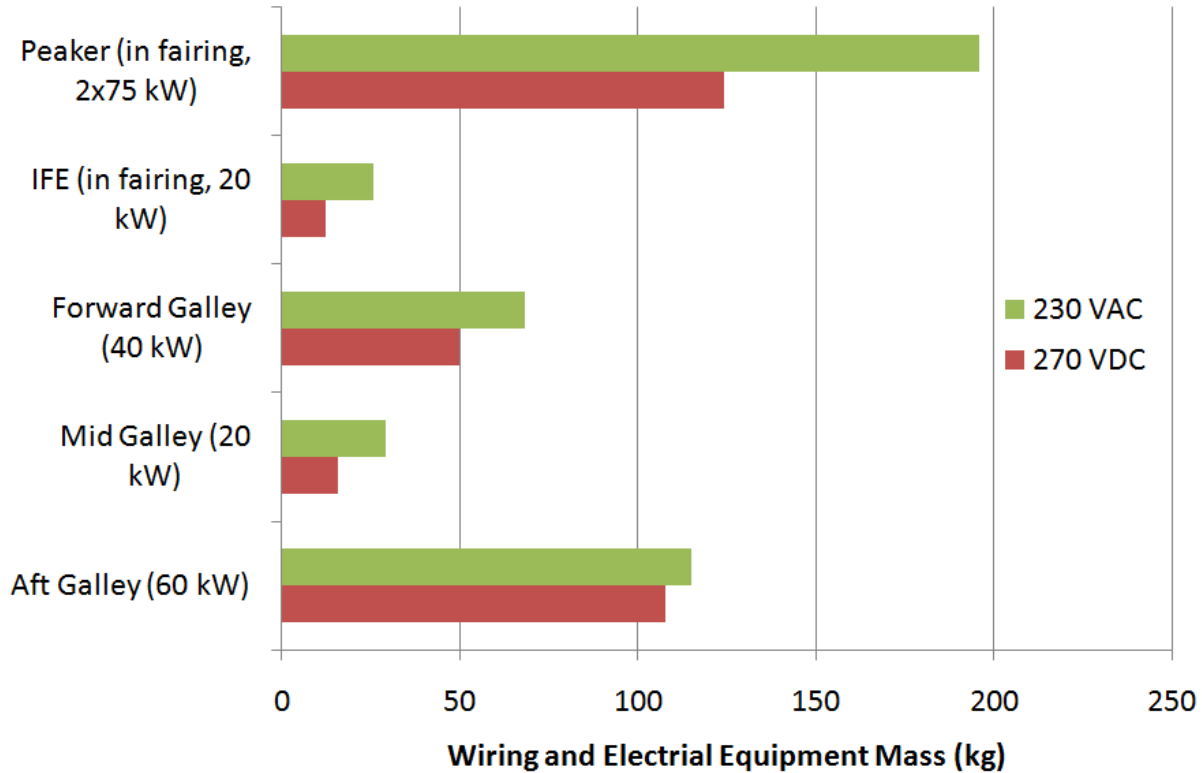


Figure 26: Mass comparison of the  $\pm 270$  VDC and 230 VAC systems, including wiring and equipment, assuming the fuel cell is in the fairing area. The  $\pm 270$  VDC system has a lower mass in every case.

account for bends, connectors, etc. This assumes that the output of the fuel cell is converted to the distribution system voltage right at the fuel cell module – there is no wiring allowance for the part between the fuel cell and the conversion device.

From the figure it is clear that the  $\pm 270$  VDC system has a lower overall mass than the 230 VAC system in every case. This is mainly due to the difference between the size of the DC-DC converter and the DC-AC inverter. While these results assume that the fuel cell is located in the fairing area, the trend is the same for any fuel cell location.

Figure 27 is a comparison of the volume of the two distribution systems. From this figure it can be seen that the  $\pm 270$  VDC system has a similar advantage in terms of volume as it did in terms of mass.

### 6.1.1.3 Summary of System Location Findings

A combination of the piping and wiring size analysis results is shown in Figure 28. The sum of all the loads for the fairing and tail are 158 kg (348 lb) and 148 kg (326 lb), respectively, showing that the total difference is small between these two options if all the loads are being considered. It can also be seen that locating the fuel cell system next to all the loads can save nearly 150 kg (331 lb) compared to locating it in either the fairing or tail sections. This figure does not include the IFE or Peaker, because it is assumed that the location of those loads is flexible and will be near the fuel cell no matter where it is located.

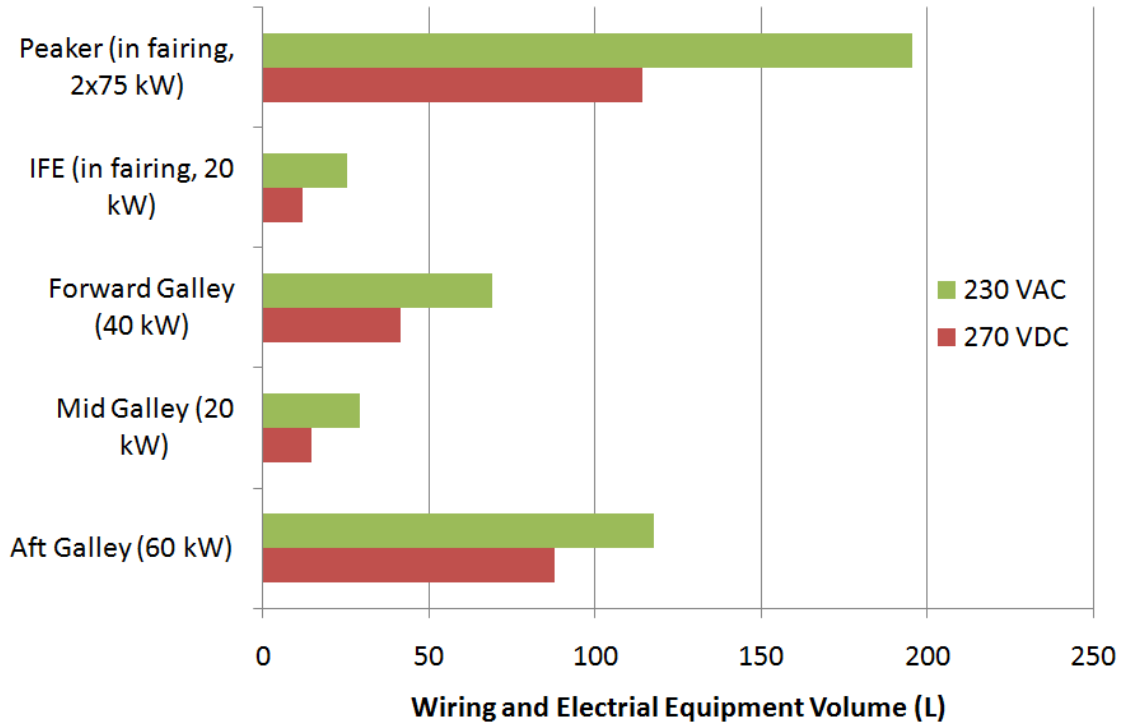


Figure 27: Volume comparison of the  $\pm 270$  VDC and 230 VAC systems, including wiring and equipment, assuming the fuel cell is in the fairing area. The  $\pm 270$  VDC system has a lower volume in every case.

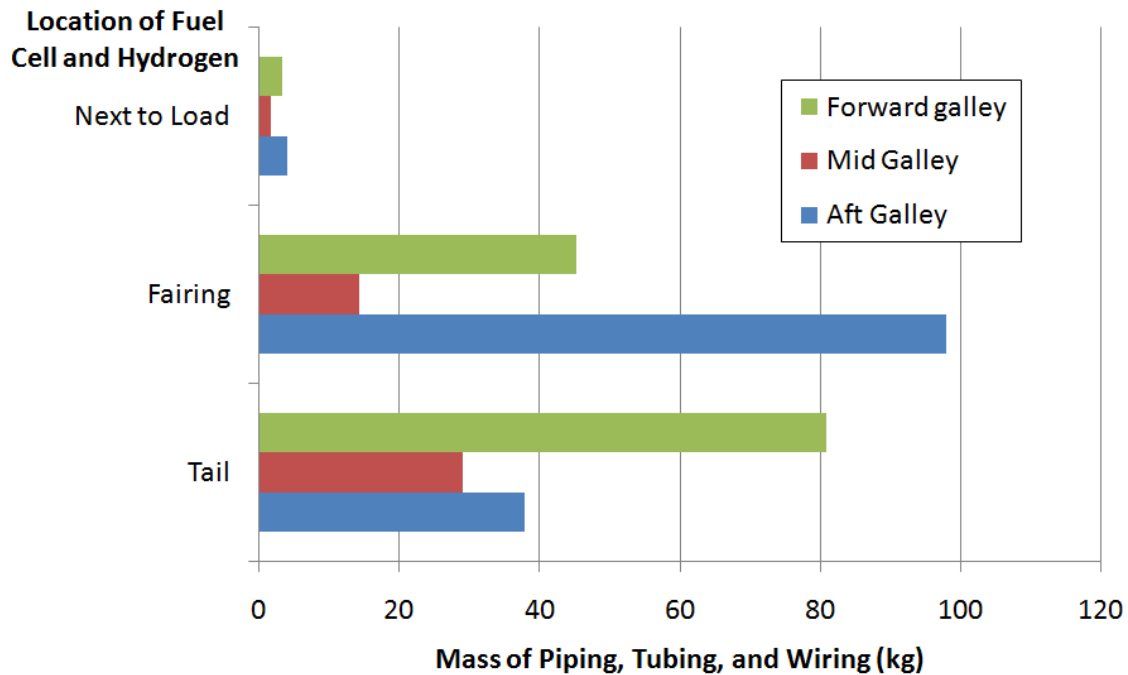


Figure 28: Combined mass of the piping, tubing, and wiring assuming that the fuel cell and hydrogen are located together and that a 270 VDC electrical distribution system is used. Locating the system next to the load can save over 100 kg overall. The cumulative difference between locating the system in the fairing (158 kg total) or tail (148 kg total) is small.



Co-locating the fuel cell and hydrogen storage in either the fairing or tail section provides logistical advantages to the deployment and maintenance of the fuel cell system. The fire-rated sub-section of the tail offers an added safety, and possibly regulatory, benefit, but the space in this sub-section is limited. The fairing may be safer for refueling activities since it is lower to the ground.

For these reasons, and the small difference in mass and volume between locating the system in the fairing or tail, the fairing section is chosen as the location for the remainder of this study. Because the differences in weight and volume between the fairing and tail locations are small, performing the analysis assuming the system is located in the tail area would lead to very similar results.

### **6.1.2 System Design**

Arrangement of the major components of a fuel cell system (see Chapter 3) into a practical working system depends primarily on the method of fuel cell cooling and waste heat recovery. Many possible configurations were attempted on paper and of these, eleven “Cases” warranted additional investigation. These were considered as they all represent possible deployment configurations, with different interfaces to the aircraft cooling systems and a variety of uses of the waste heat. In all of them, it is assumed that any air needed by the fuel cell system, whether for cooling or for oxygen supply, comes from the cabin. It is also assumed that all hot air coming out of the fuel cell module, whether exhaust from the fuel cell or air used for cooling, is routed to the cabin exhaust system and eventually rejected to the atmosphere.

Brief descriptions of the cases, followed by schematics, are:

- Cases 1a (Figure 29) and 1b (Figure 30) are air-cooled PEM fuel cell modules, with and without simple waste heat and water recovery.
- Cases 2a (Figure 31) and 2b (Figure 32) are water-cooled modules, with and without simple waste heat and water recovery. In 2b, we are assuming the exhaust air stream from the fuel cell is routed to an Air/Water heat exchanger, which is used to heat potable water.
- Cases 3a (Figure 33) and 3b (Figure 34) are similar to 2a and 2b but limit the amount of generated potable hot water to a reasonable level and as a consequence, require more cooling from the airplane’s cooling system to fully dissipate the waste heat from the fuel cell. Case 3b also shows the case for maximum potable water generation, as the warm, moist, oxygen-depleted air stream from the fuel cell is cooled to condense the water, which is then sent to the potable water system.
- Cases 4a (Figure 35) and 4b (Figure 36) do not limit the amount of hot water generated. Case 4a does not require any cooling from the airplane’s system while case 4b requires cooling only to condense the water from the warm, moist, oxygen-depleted air stream from the fuel cell.
- Case 5 (Figure 37) is configured to generate high-grade waste heat via combustion of excess hydrogen and use it for heating galley ovens and hot water (as described in the previous section).
- Cases 6a (Figure 38) and 6b (Figure 39) are cooled by the airplane’s fuel system. Case 6b is the same as 6a but with water recovery. This represents a particularly important configuration as

we will see. Enhancing the energy content of the Jet A by adding the fuel cell waste heat improves the turbine engine efficiency.

### Case 1a: Air Cooled

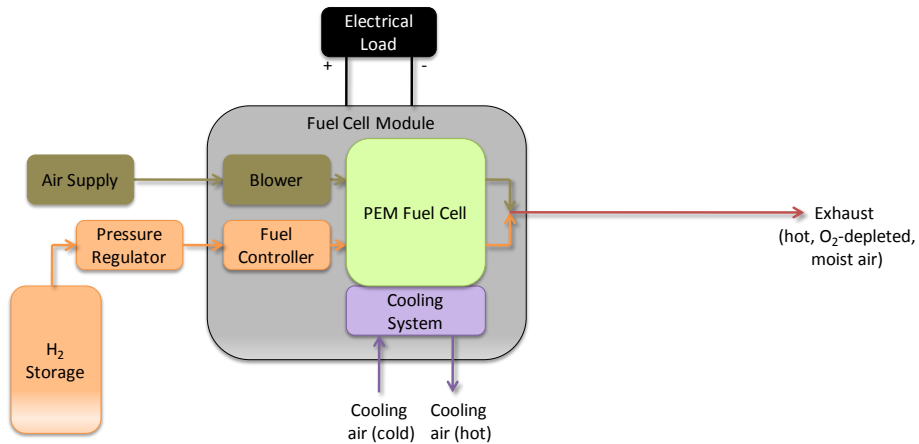


Figure 29: Schematic for Case 1a, where the fuel cell's internal liquid cooling system is air cooled and no heat recovery is utilized.

### Case 1b: Air Cooled, Hot Water

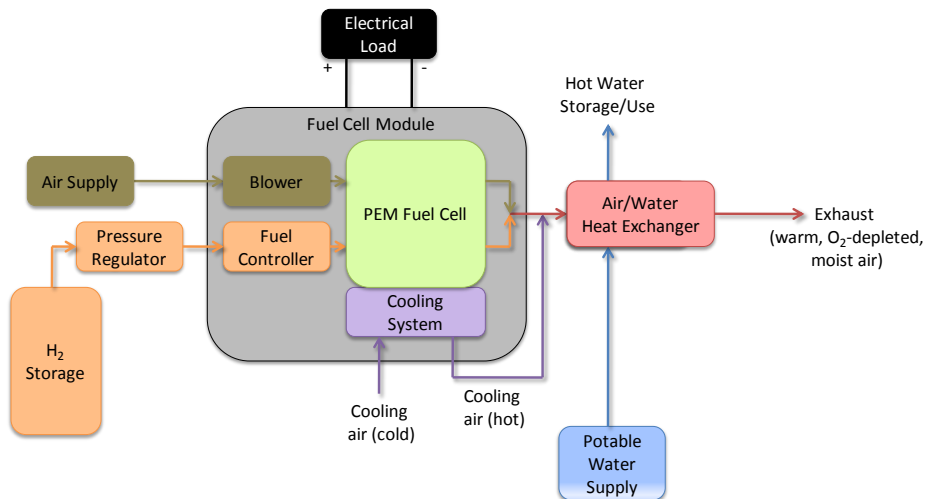


Figure 30: Schematic for Case 1b. The fuel cell's internal liquid cooling system is air cooled. The hot cooling air is combined with the fuel cell exhaust and used to heat water.

Case 2a: Water Cooled

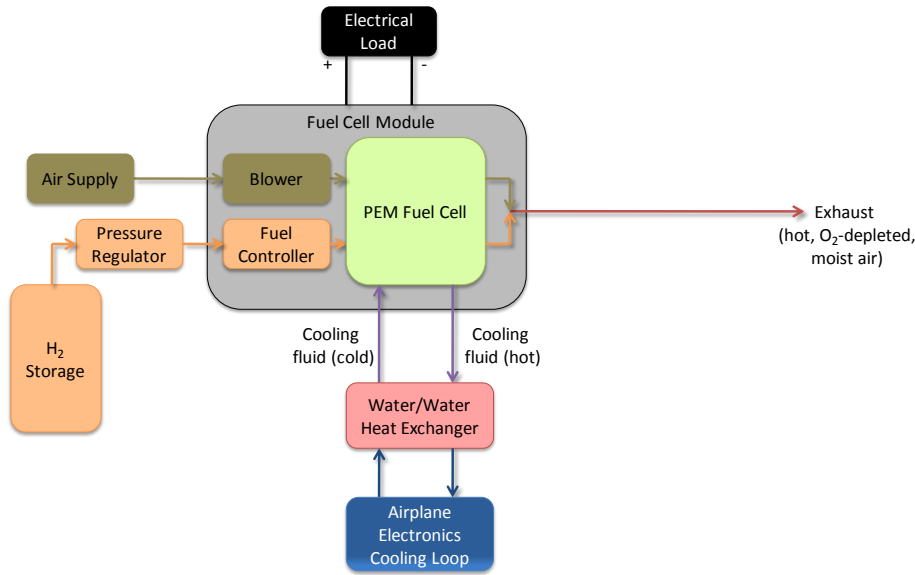


Figure 31: Schematic for Case 2a. The fuel cell’s internal liquid cooling system is cooled by the airplane’s liquid cooling loop and no heat recovery is utilized.

Case 2b: Water Cooled, Hot Water

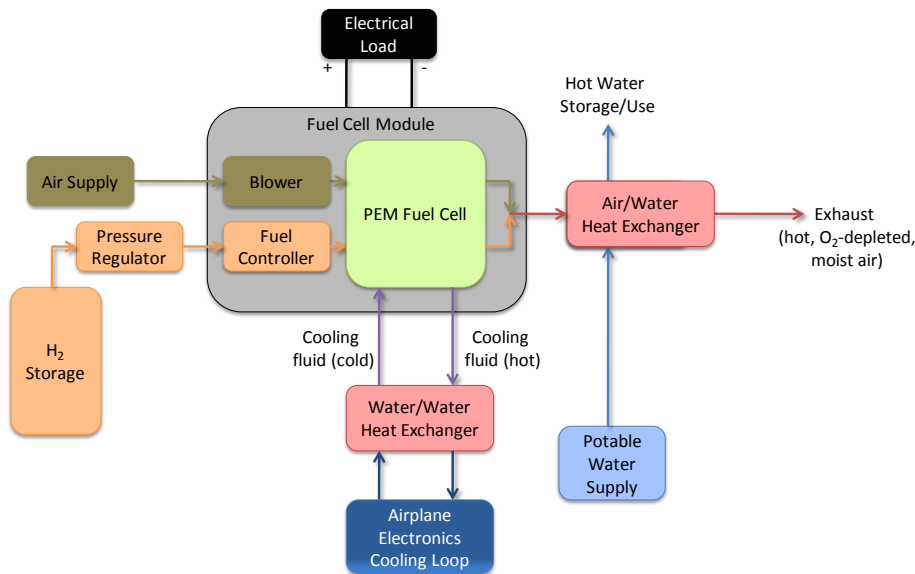


Figure 32: Schematic for Case 2b. The fuel cell’s internal liquid cooling system is cooled by the airplane’s liquid cooling loop. The exhaust air from the fuel cell is used to heat hot water.

### Case 3a: Water Cooled, Limited Hot Water

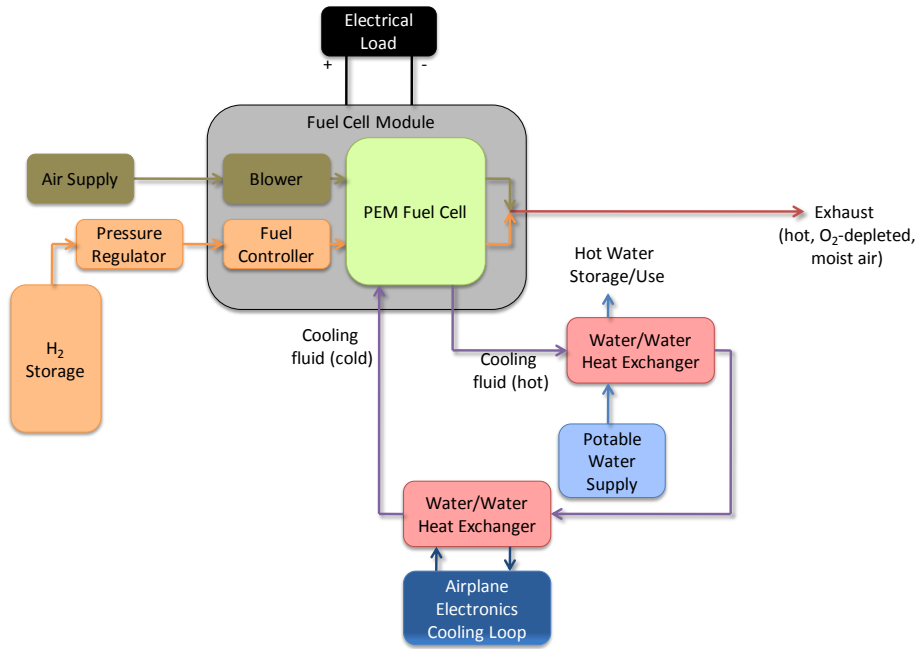


Figure 33: Schematic for Case 3a. The fuel cell’s internal liquid cooling system is used to heat a limited amount of hot water, and remaining heat is rejected to the airplane’s liquid cooling loop.

### Case 3b: Water Cooled, Limited Hot Water, Max Water Recovery

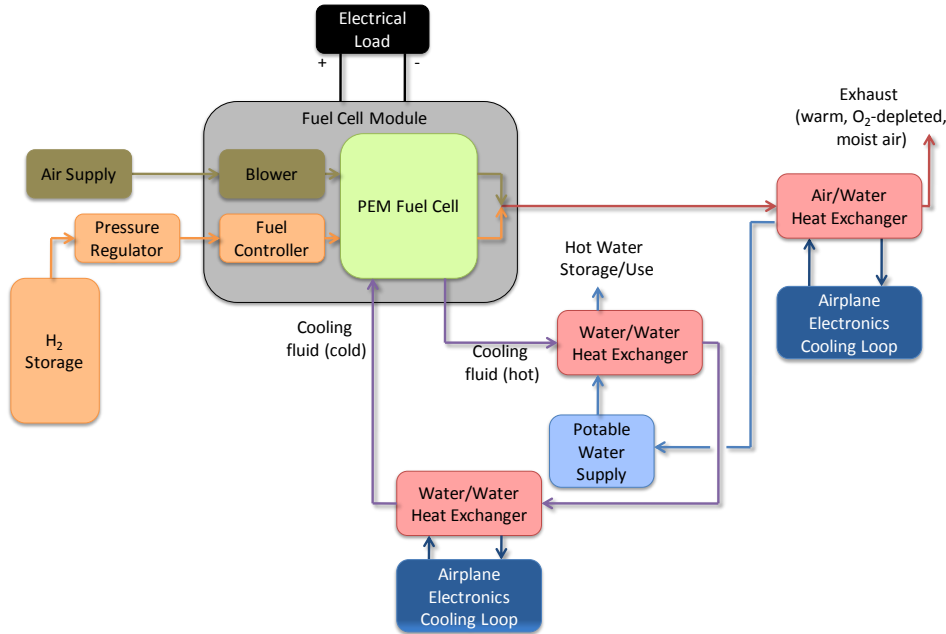


Figure 34: Schematic for Case 3b. The fuel cell’s internal liquid cooling system is used to heat a limited amount of hot water, and remaining heat is rejected to the airplane’s liquid cooling loop. The exhaust air from the fuel cell is cooled by the airplane’s cooling loop in order to condense the water.

Case 4a: No External Cooling, Max Hot Water, Water Recovery

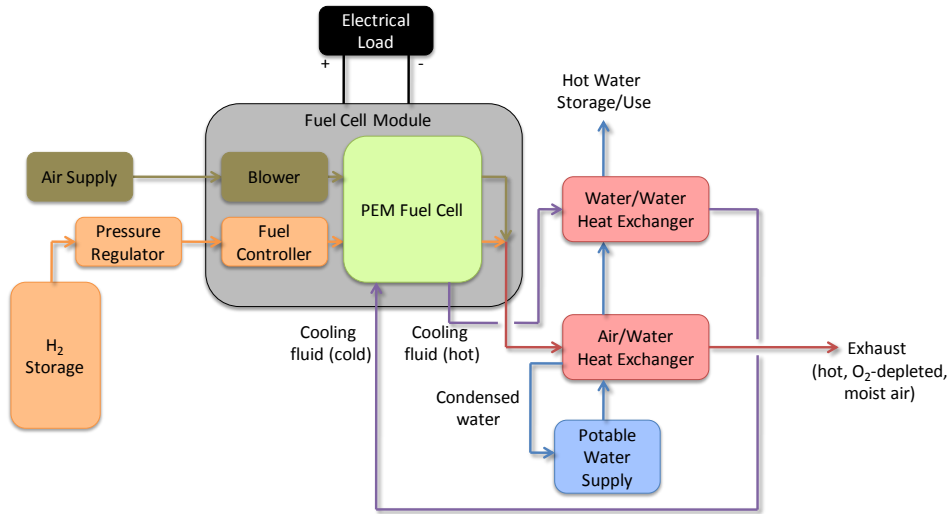


Figure 35: Schematic for Case 4a. The fuel cell’s internal liquid cooling loop is used to heat a quantity of water not intentionally limited. Exhaust air from the fuel cell is used to pre-heat the water, and some water is condensed in the process, thereby maximizing water recovery. This design does not require any cooling by the airplane’s systems.

Case 4b: No External Cooling, Max Hot Water, Max Water Recovery

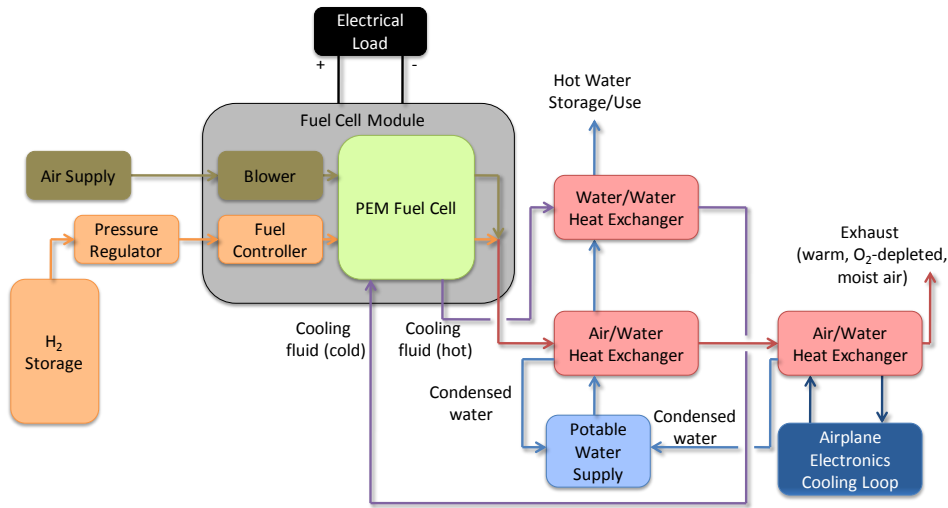


Figure 36: Schematic for Case 4b. The fuel cell’s internal liquid cooling loop is used to heat a quantity of water not intentionally limited. Exhaust air from the fuel cell is used to pre-heat the water, and some water is condensed in the process. The exhaust air is further cooled by the airplane’s liquid cooling loop to further condense and recover water.

Case 5: No External Cooling, High-Grade Waste Heat, Max Hot Water

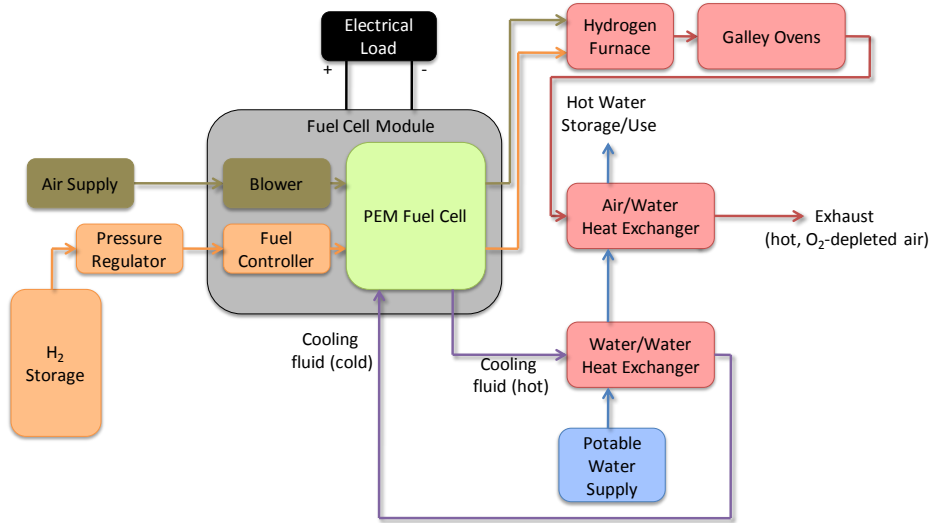


Figure 37: Schematic for Case 5. The fuel cell’s internal liquid cooling loop is used to pre-heat a quantity of water not intentionally limited. The excess hydrogen from the fuel cell is kept separate from the air and instead combusted in a hydrogen furnace to produce high-temperature waste heat which is used to heat the galley ovens. The oven exhaust further heats the water. This design does not require any cooling by the airplane’s systems.

Case 6a: Fuel Cooled

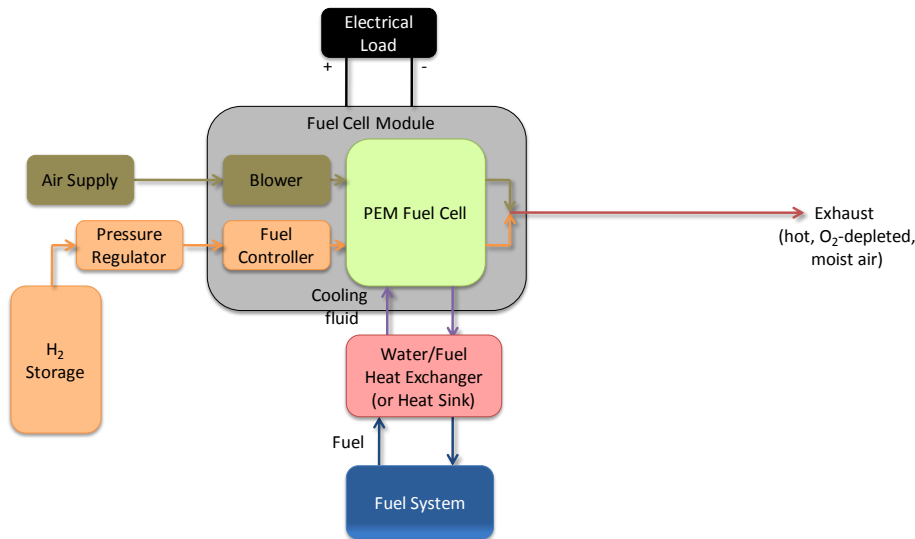
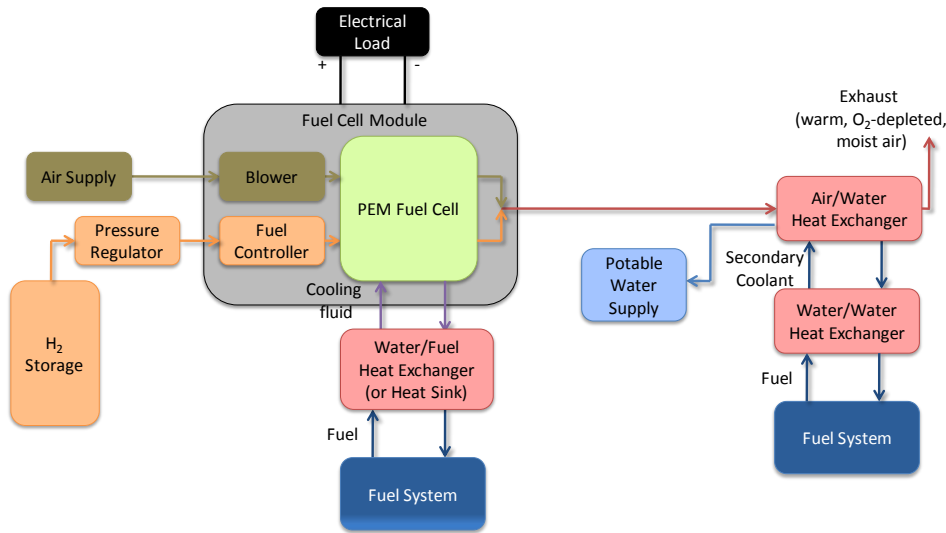


Figure 38: Schematic for Case 6a. The fuel cell’s internal liquid cooling loop is used to heat the airplane’s fuel. No other waste heat recovery is utilized, and none of the airplane’s cooling systems are needed.

## Case 6b: Fuel Cooled with Water Recovery



**Figure 39: Schematic for Case 6b.** The fuel cell’s internal liquid cooling loop is used to heat the airplane’s fuel. Exhaust from the fuel cell is also used to heat the airplane’s fuel, producing condensed water in the process. A secondary coolant loop is used to prevent mixing of the airplane’s fuel with air or water. No other waste heat recovery is utilized, and none of the airplane’s cooling systems are needed.

### 6.1.3 System Performance

The eleven different system configurations (“Cases”) were simulated to find the thermodynamic performance when meeting the in-flight entertainment (IFE) load of 20 kW for the entire flight. Figure 40 plots the fuel cell system thermal efficiencies, which as explained in Section 4.5 is the ratio of electrical and heat delivered by the fuel cell to the energy content of the hydrogen fuel. The highest efficiency cases are the ones that utilize the most waste heat, either through heating water (Cases 4a and 4b), heating galley ovens (Case 5), or heating the airplane’s fuel (Cases 6a and 6b).

Figure 41 summarizes the mass analysis including a component-by-component breakdown. The blue outline bars show the net system mass. For comparison, the “standard passenger” used by the airplane industry has a mass of 104 kg (230 lb) including luggage. The mass analysis includes physical hardware requirements and operating requirements. The physical hardware includes the fuel cell, hydrogen, hydrogen storage, piping and accessories, heat exchangers, pumps, and blowers, and electrical hardware and wiring. The increases in mass due to operating requirements includes increases in Jet-A due to additional system mass, cooling drag, and electrical power required by the ECS system to supply the necessary air for the fuel cell. The decrease in mass due to operating requirements includes a decrease in Jet-A due to reduced electrical generation of the main engines (for supplying both electrical and thermal loads), decreased Jet-A due to fuel pre-heating, and water production by the fuel cell system. A reduction in mass due to smaller required engine generators is also calculated.

The figure reveals that, except for cases 1a and 1b, all the systems have very little difference in the hardware portion (the fuel cell (blue), hydrogen storage (red), hydrogen (green), piping and accessories (light purple), heat exchangers, pumps, and blowers (orange), and electrical (pink)). The largest

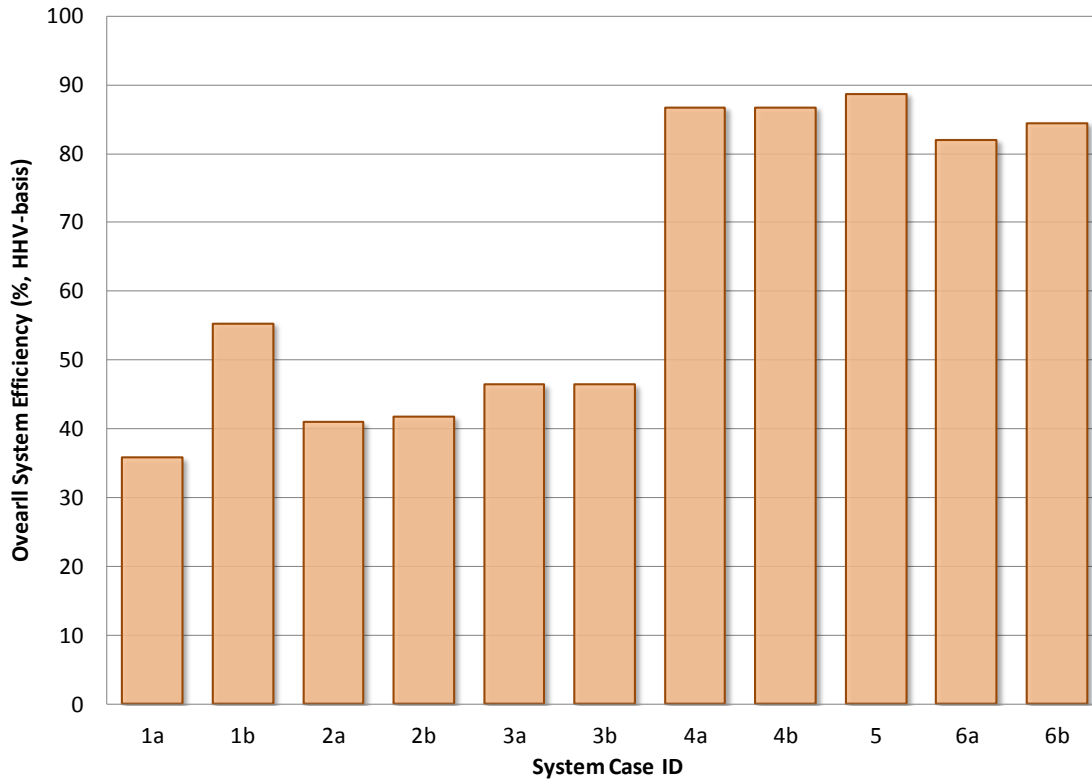


Figure 40: Overall system efficiency of the eleven system case options for the 20 kW in-flight entertainment load. The cases with the most waste heat recovery (cases 4-6) have the highest overall system efficiencies.

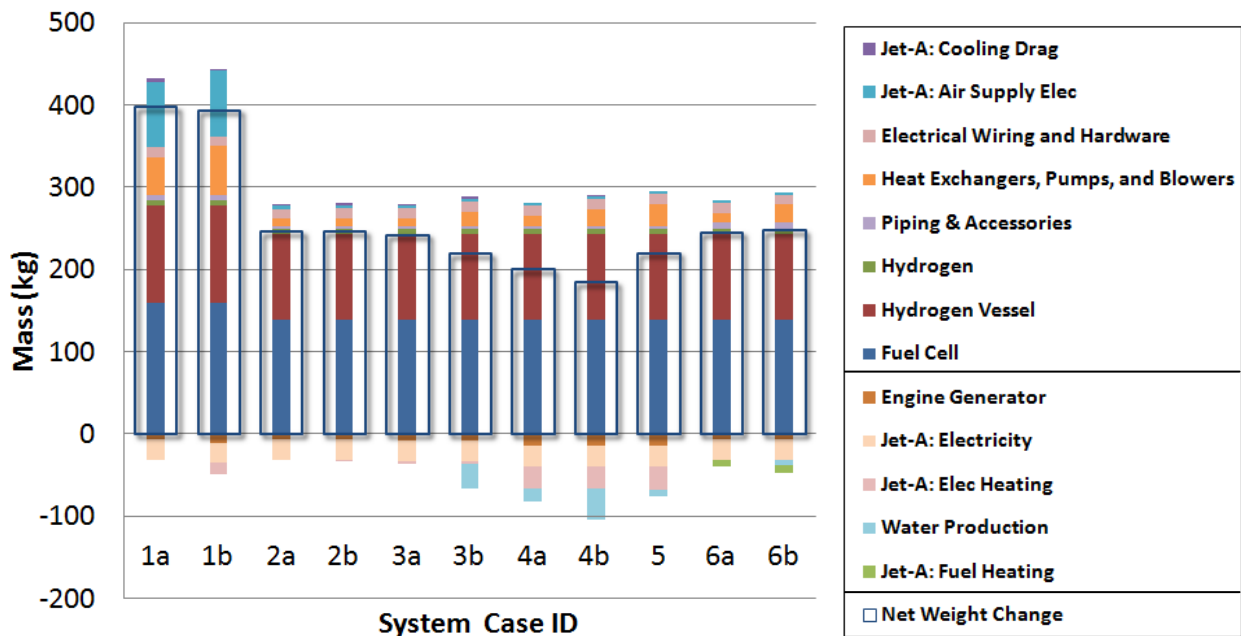


Figure 41: Summary of the mass analysis for each case. The different colors in the narrow bars represent different components. Quantities above the zero-line are for mass added to the system, and quantities below the zero-line are for mass credits. The net change (the sum of the added mass and mass credits) is shown by the wide hollow bar. For comparison, the “standard passenger” has a mass of 104 kg (230 lb) including luggage.



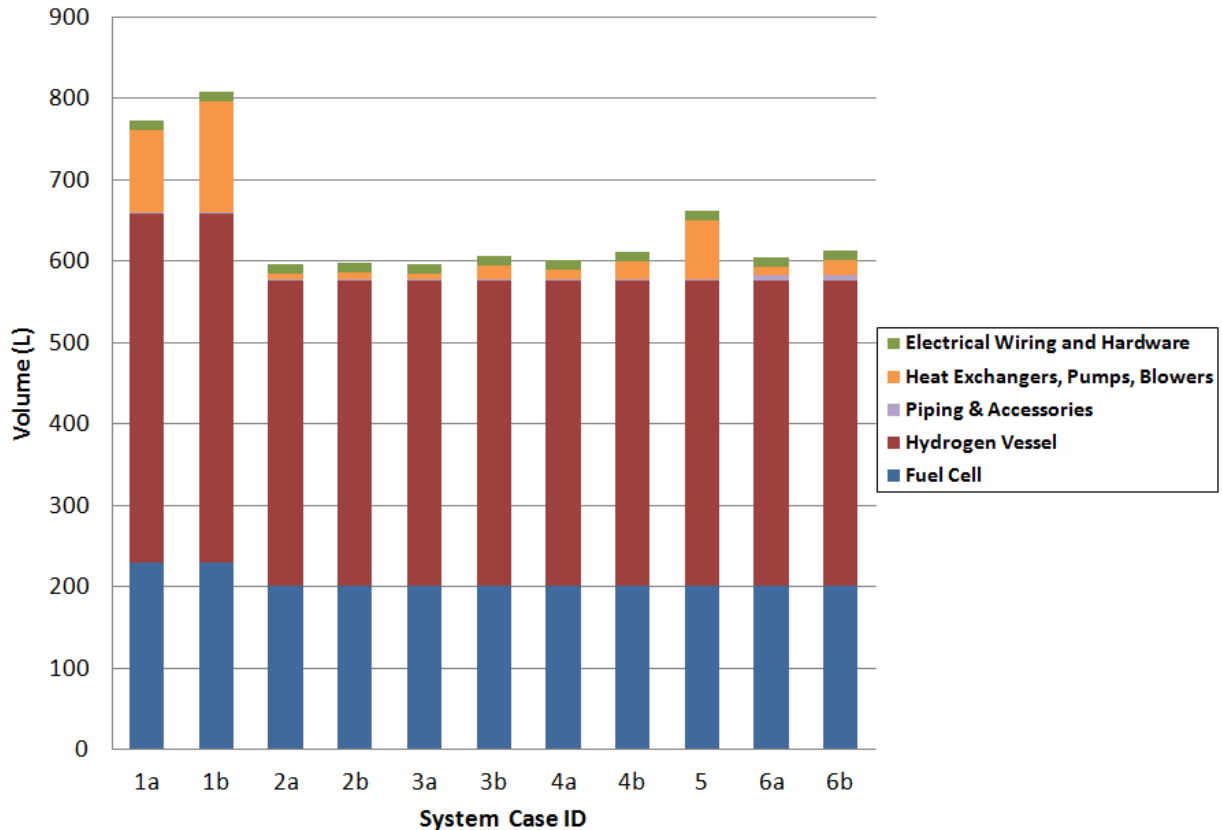
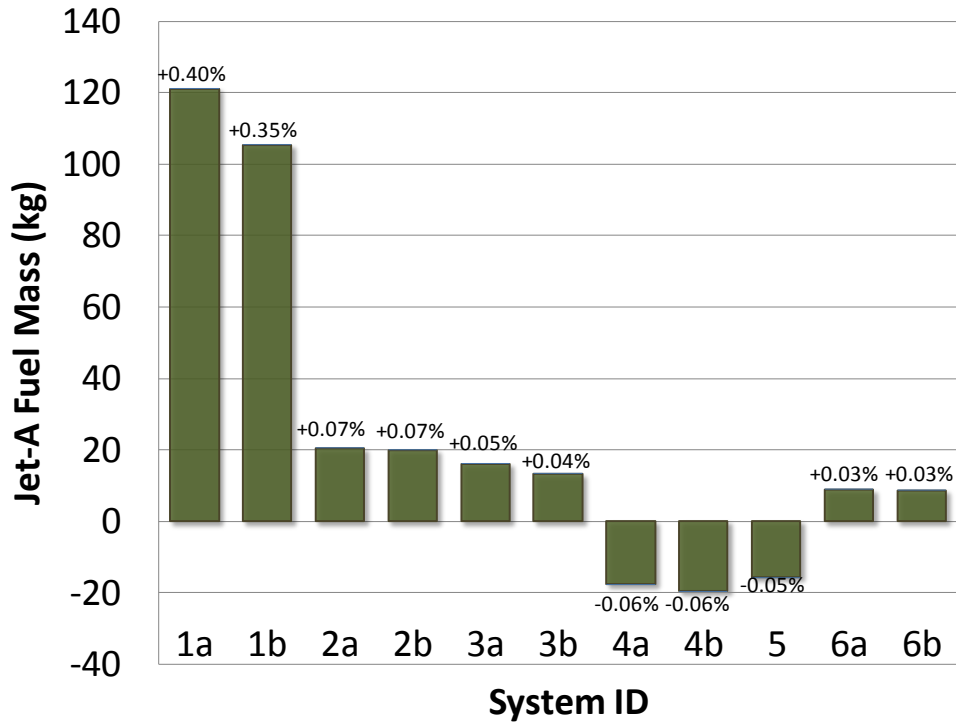


Figure 42: Summary of the volume analysis for each case. The volume of each component is shown by a different color. The larger volumes of the air-cooled cases (1a and 1b) are due to the larger heat exchangers required in addition to the increased fuel cell and hydrogen requirements. Because volume is most influenced by the size of the fuel cell and hydrogen tanks, the differences between the other cases are relatively small. For comparison, a typical galley beverage cart has a volume of 240 L (8.5 ft<sup>3</sup>).

differences come from the additional Jet-A requirements and savings, and water recovery savings. For this reason, a system that can reject little or no heat to the airplane’s cooling system and recover potable water, such as case 4b, has a net mass advantage compared to others.

Figure 42 summarizes the volume analysis. For comparison, a typical galley beverage cart has a volume of 240 L (8.5 ft<sup>3</sup>), with the available volume in the tail cone area estimated to be over 2,800 L (100 ft<sup>3</sup>), and possibly more in the fairing area. This analysis only considers the physical hardware required for the system, as it is assumed that the volume of the fuel or water tanks will not be changed and any more or less Jet-A or water carried will have no effect on the volume. From this figure it is apparent that all cases except for cases 1a and 1b have similar system volumes. The reason for Case 5’s difference in volume is the hydrogen combustor/furnace, which has a large volume.

Figure 43 combines all of the effects of the fuel cell system to find the impact on Jet-A requirements for each case. In this figure, the number in parenthesis represents the amount of additional Jet-A as a percentage of total mission fuel. It can be seen that only cases 4a, 4b, and 5 resulted in a performance



**Figure 43: The overall effect of the fuel cell system on airplane performance, as measured by the amount of additional Jet-A the fuel cell-equipped airplane needs to accomplish the same mission as the base airplane. The numbers in parenthesis express this amount as a percentage of total mission fuel. Only Cases 4a, 4b, and 5 results in a performance benefit.**

benefit to the airplane. All other non-air cooled cases led to similar results, and the air cooled cases (1a and 1b) are considerably worse.

Recommended cases are chosen according to the following criteria:

- Feasibility
- Ease of implementation (low complexity)
- Overall impact on airplane performance as measured by the change in Jet-A requirements

Based on the results, Cases 2a, 3b, and 6a were determined to be the most feasible options for implementation and selected for further analysis. The following sub-sections describe the details of each case’s analysis.

#### 6.1.4 Cases 1a and 1b: Air Cooled

Cases 1a and 1b are both air cooled. This requires 836 SCFM of cooling air, nearly 20-times the amount of air needed for fuel cell operation. Because we assume the fuel cell provides the power needed by the fan to move this amount of air, it places a parasitic load on the fuel cell module of 2.87 kW, more than 10% of the fuel cell’s gross power output. In turn, this requires a larger fuel cell and more hydrogen storage. While the fuel cell operates at the same efficiency as all other cases (40.9%), the increased parasitic load decreased the system efficiency to 35.76% for Case 1a.

Case 1b was able to extract heat from the cooling air to heat water at 6.8 L/min (1.5 gpm), increasing its system efficiency to 55.3%. However, this amount of water is 5- to 10-times that which is estimated to be reasonably used on board the airplane (see Section 0).

Both of these cases placed large demands on the airplane because of the extra cooling air required, which is equivalent to that needed for 70 passengers or 120% of the current maximum capacity. The environmental control system must increase its design flow to handle this, adding electrical power requirements to the compression system and cooling requirements to the air conditioning packs. The added mass and volume of increasing the size of the ECS is not considered in this analysis but will further contribute to the undesirability of these two cases.

These two cases were not selected for further analysis.

### **6.1.5 Cases 2a and 2b: Simple Water Cooled**

Cases 2a and 2b reject heat from the fuel cell's cooling system to the airplane's power electronics cooling system (PECS); no heat is recovered from the cooling water. However, Case 2b uses the heat of the fuel cell's warm, oxygen depleted exhaust air to heat water. The amount of heat that can be extracted from this air is small, less than 400 W, so the thermal efficiencies are nearly the same at 40.9% and 41.7% (Cases 2a and 2b, respectively). The extra heat exchanger required for Case 2b adds to the system size so the overall difference between the two cases is negligible. This means that the added heat recovery system has no real benefit to offset the added complexity and Case 2b should be discarded.

Although Case 2a does not favorably benefit airplane performance, it is selected for further analysis because of its simplicity and thus high ease of implementation.

### **6.1.6 Cases 3a and 3b: Water Cooled with Limited Heat Recovery**

Cases 3a and 3b utilize the fuel cell's rejected heat to make hot water, but hot water production is limited to a maximum of 0.85 LPM (0.225 gpm). This was chosen as a reasonable amount based on estimated actual hot water usage for both consumption and washing. However, the fuel cell generates more heat than can be rejected to this limited amount of water, so the remainder is rejected to the PECS. Case 3b additionally uses the PECS to cool the fuel cell's exhaust stream and recover 30.8 L of liquid water. Because the amount of waste heat recovered is the same for either case, the overall efficiencies are the same at 46.4%.

Case 3b requires additional heat exchanger equipment, and has a slightly increased amount of Jet-A required to provide the extra cooling to condense the water. However, the water credit more than makes up for these penalties, indicating that water recovery adds an overall performance benefit to the airplane. Both of these systems' feature a reasonable amount of heat recovery leading to a performance improvement over the case without any heat recovery (Case 2a). Case 3b is slightly better performing than Case 3a and was selected for further analysis.

### **6.1.7 Cases 4a and 4b: Water Cooled with Maximum Heat Recovery**

Cases 4a and 4b are nearly identical to 3a and 3b except the amount of hot water generated is not constrained. This also enables cases 4a and 4b to utilize the fuel cell's exhaust heat to further heat the water. Like 3b, case 4b further cools the fuel cell's exhaust (rejecting heat to the PECS) to capture 37.9 L of water. Both cases have the same overall efficiency of 86.6%.

Compared to Case 4a, the water capture of Case 4b requires extra equipment and Jet-A to overcome the cooling load. As in Case 3b, the water recovered more than makes up for this extra burden.

In spite of being among the best performing systems, these two cases were rejected for further analysis because of the impracticality of generating so much hot water on board the airplane. However, because they are so similar to cases 3a and 3b except for the amount of hot water generated, it is useful to compare the sets of cases to reveal the large benefit associated with fully utilizing the waste heat and displacing electrical heating loads.

These cases also illustrate the potential of a heat sink that could be cooled or regenerated while the airplane is on the ground. If all the heat from the fuel cell could be captured by a sink during flight, the benefit to the airplane could outweigh the size of the sink.

### **6.1.8 Case 5: Water Cooled with High Grade Waste Heat Recovery**

One problem with attempting to recover heat from a PEM fuel cell system is that the low operating temperature produces low temperature waste heat. This reduces the effectiveness of heat exchangers which limits the amount of heat that can be captured in a reasonably-sized heat exchanger. A potential solution to this problem is to heat the exhaust stream by burning the small amount of hydrogen that is wasted by the fuel cell. Case 5 examines this arrangement.

In Case 5, the hydrogen and oxygen-depleted air exhaust are kept separate when they exit the fuel cell. The hydrogen is combusted with a portion of the air in a hydrogen furnace and the products are mixed with the remaining air. This stream exits the furnace at 882 °C (1,620 °F) and is sent directly to the galley ovens. The ovens are heated to 450 °F (232 °C), utilizing 1.7 kW of the heat energy from this stream.

The oven exhaust stream is used to heat water at an unconstrained rate of 11.4 LPM (2.5 gpm). Prior to being heated by the oven exhaust stream, the water is heated by the fuel cell's heat.

Case 5 exhibits the highest system efficiency (88.62%) and its performance is only behind Cases 4a and 4b. However, it suffers the same drawback as them in that it produces an unreasonable amount of hot water. Additionally, the overall performance is worse than Cases 4 and 4b because of the added equipment (hydrogen furnace) and less water recovery.

One way to make Case 5 more practical in terms of hot water generation is to limit the amount of hot water, similarly to Cases 3a and 3b. The effect of this will be nearly equivalent to the difference between Cases 3a and 4a. That is, the performance will be close to but higher than Case 3a. The added complexity compared to Case 3a combined with the worse performance makes this an option not worth pursuing.

### **6.1.9 Cases 6a and 6b: Fuel Cooled**

Cases 6a and 6b reject all of the fuel cell's heat to the airplane's fuel (Jet-A). This arrangement does not require any cooling from the airplane's environmental systems (and thus does not add any cooling drag) and has the added benefit of increasing the enthalpy of the fuel so that less fuel needs to be burned to generate the same amount of thrust.

Case 6b additionally utilizes the fuel to cool the fuel cell exhaust stream and extract water. The efficiency (84.4%) is slightly higher than Case 6a (81.9%) because of the extra heat recovered in this process. However, the amount of water recovered is small (6.9 L) and the added equipment results in a system with nearly the same overall performance benefit as Case 6a. In addition, there are potential hazards associated with a leak developing in the heat exchangers and the mixing of fuel, air, and/or water in either the fuel system or the potable water system.

These cases are the best performing "practical" cases (excluding 4a, 4b, and 5) and led to Case 6a being selected for further analysis. Case 6b was rejected because of the increased complexity and hazard potential without any performance benefit.

### **6.1.10 Summary**

The following general observations can be made regarding system configurations:

- Air cooled systems are not preferred: they require large increase in current air handling units' capacities, have large weight and volumes, and have large performance penalties.
- The uses of low-grade waste heat within the cabin are limited. The amount of hot water that could be generated by the fuel cell's exhaust heat is approximately 5- to 10-times of what could be reasonably used on the airplane.
- Adding a heat exchanger to cool the fuel cell's exhaust and recovering the water results in an overall benefit despite the added equipment and cooling drag.
- The most weight-impactful non-hardware factors on the airplane's performance are the amounts of water and waste heat that can be recovered. However, waste heat recovery is limited by available on-board uses while water recovery depends on the effectiveness of the heat exchanger cooling the exhaust stream.
- The fuel cell and hydrogen are the most important (heaviest) hardware components.

Table 11 summarizes the three cases selected for further analysis. The results described above show that any of these systems are technically feasible for on-board implementation.

## **6.2 System Performance with Current Technology**

The three system configurations selected from the screening analysis (Cases 2a, 3b, and 6a) were simulated using the thermodynamic model to meet each of the nine load scenarios summarized in Table 4 (repeated here as Table 12 for convenience). The goal of this part of the study is to see how different loads impact the overall performance of the systems, thus enabling recommendations of not only the best-performing system configuration but also the on-board load(s) to be powered by the system.

**Table 11: Summary of the three cases selected from the screening analysis. Each system is designed to meet a constant 20 kW IFE electrical load operating for all phases of flight.**

Case ID	2a	3b	6a
<b>Description</b>	Simple water cooled	Water cooled, limited hot water, water recovery	Fuel cooled
<b>Overall System Efficiency (HHV)</b>	40.9%	46.4%	81.9%
<b>Waste Heat Use</b>	None	Hot water: 0.225 gpm @ 60 °C.	Fuel pre-heating
<b>Water Recovery</b>	None	0.027 gpm (0.1 LPM); 30.8 L	None
<b>Cooling Load on Airplane</b>	20 kW heat rejected to PECS	17.4 kW heat rejected to PECS	None
<b>Total System Weight (kg)</b>	274	282	281
<b>Total System Volume (L)</b>	597	606	605
<b>Net Change in Jet-A required (kg)</b>	+20.3	+13.1	+8.8
<b>Net Change in Jet-A required (% of total mission fuel)</b>	+0.07%	+0.04%	+0.03%

**Table 12: The nine different load scenarios considered in this study (Table 4 repeated for convenience).**

ID	Load Description	Maximum Electrical Demand	Phases of Flight
1	In-flight entertainment (IFE)	20 kW	All
2	Mid-galley	20 kW	Initial taxi, takeoff/climb, and cruise
3	Forward galley	40 kW	Initial taxi, takeoff/climb, and cruise
4	Aft galley	60 kW	Initial taxi, takeoff/climb, and cruise
5	All galleys combined	120 kW	Initial taxi, takeoff/climb, and cruise
6	Single peaker	75 kW	Descent and landing
7	Both peakers	150 kW	Descent and landing
8	All galleys (5) and both peakers (7)	150 kW	120 kW during initial taxi, takeoff/climb, and cruise; 150 kW during descent and landing
9	All loads (1, 5, and 7)	170 kW	140 kW during initial taxi, takeoff/climb, and cruise; 170 kW during descent and landing, 20 kW during final taxi

“Current Technology” refers to a PEM fuel cell with a specific power of 149 W/kg (67.6 W/lb) and the power density is 103 W/L (2,920 W/ft<sup>3</sup>) as described in Section 3.1.2 and a hydrogen vessel with approximately 6.1% gravimetric density and 17.0 gH<sub>2</sub>/L (1.06 lb/ft<sup>3</sup>) volumetric density as described in Section 3.2.3.

### **6.2.1 Mass**

Because the mass of the system affects overall airplane performance, the mass is analyzed first. The mass analysis for each of the load scenarios for Cases 2a, 3b, and 6a are shown in Figure 44, Figure 45, and Figure 46, respectively. These figures assume current technology for the fuel cell and hydrogen storage.

For all cases, the overall trends are the same, and the dominant trend is that the fuel cell and hydrogen storage vessel are responsible for a large fraction of the overall system mass. The next largest component is the electrical hardware, primarily the DC-DC converter. It can also be seen that the mass savings due to collecting the generated water reducing the amount of jet fuel required by the engines to generate electricity can add up to a large amount, nearly the size of the hydrogen vessel.

Another feature is that, in general, the system mass increases with the size of the load. However, an exception to this can be seen when comparing the “All Galleys” load scenario, which is 120 kW, to the “Both Peakers” scenario, which is 150 kW. The reason the higher-power Both Peakers has a lower net mass is because the peakers only operate for the descent and landing phases of flight (25 minutes total) compared to the All Galleys which operate for initial taxi, takeoff and climb, and cruise (4 hours and 28 minutes). Thus, the hydrogen and hydrogen storage system required for the Peakers case is much smaller.

Another feature of the different load scenarios that becomes evident through this analysis is the complementary nature of the galley loads with the peaker load. For Case 2a, the All Galleys scenario has a net mass of 1,506 kg (3,320 lb) and the Both Peakers has a net mass of 1,244 kg (2,743 lb). However, combining these two loads in the Both Peakers and All Galleys scenario has a net mass of 1,858 kg (4,096), or just 68% of the mass if these two systems were considered separately. The reason for this is that the two systems operate at different phases of flight so they can share the same fuel cell.

### **6.2.2 Volume**

A major assumption of this study is that the airplane shape will not change because of the fuel cell system, but that the fuel cell system will be installed in areas with extra space. This means that the volume of the system will not directly affect overall performance. However, the volume analysis is still presented for completeness.

The volume analysis of the load scenarios for Cases 2a, 3b, and 6a are shown in Figure 47, Figure 48, and Figure 49, respectively. These figures assume current technology for the fuel cell and hydrogen storage. Differences in Jet-A and water savings or consumption is not considered because it is assumed that the volume of the fuel or water tanks will not be changed and any more or less Jet-A or water carried will

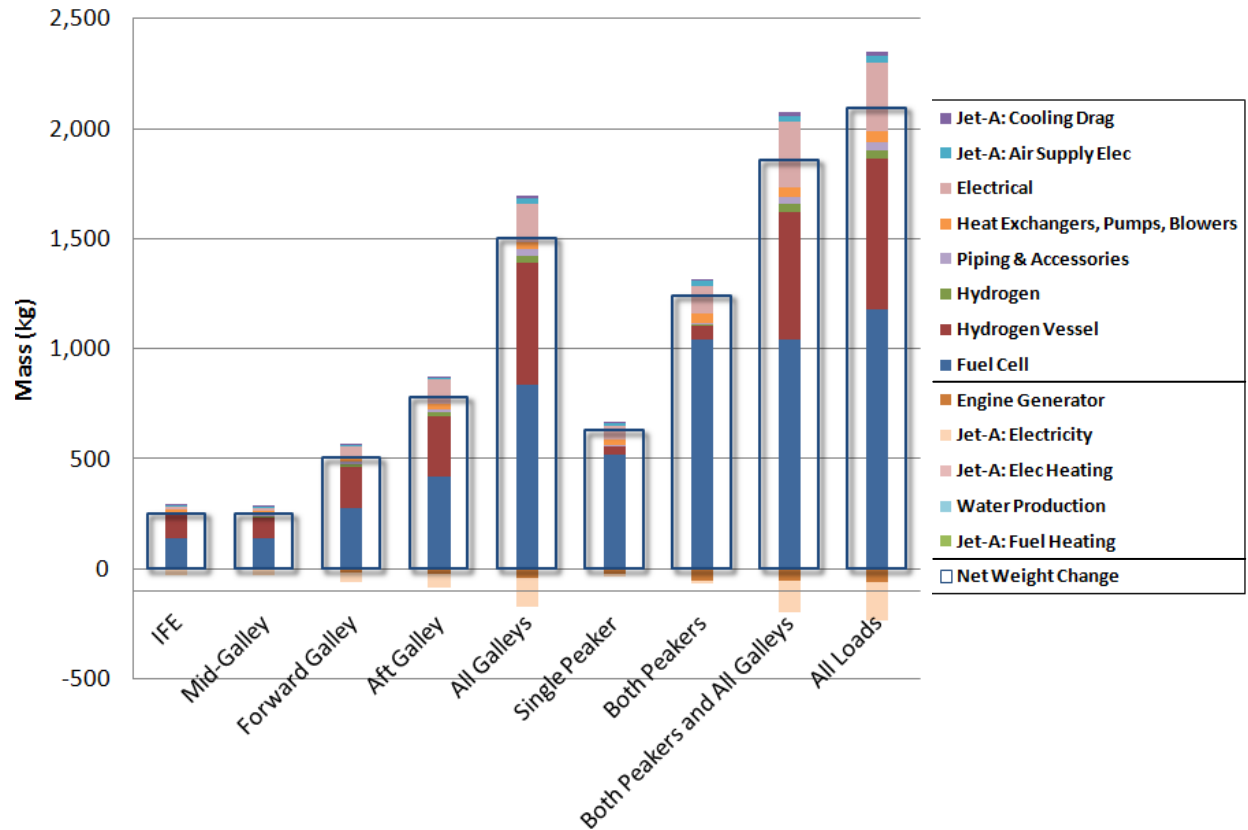


**Figure 44: Mass distribution for Case 2a (water cooled, no heat recovery) for the different loads, using current technology for the fuel cell and hydrogen storage. The different colors in the narrow bars represent different components. Quantities above the zero-line are for mass added to the system, and quantities below the zero-line are for mass credits. The net change (the sum of the added mass and mass credits) is shown by the wide hollow bar. For comparison, the “standard passenger” has a mass of 104 kg (230 lb) including luggage.**

have no effect on the volume. The engine generator may decrease its size but its volume is already so small compared to the overall system volume that any changes are negligible and are not presented.

The trends in volume are similar to those in mass. However, the large volumes of the hydrogen storage vessels become more apparent, accentuating the difference between the systems that require more hydrogen but have a lower power (e.g., All Galleys at 120 kW) and the systems that require less hydrogen but have a higher power (e.g, Both Peakers at 150 kW) due to differences in operating times. All but the largest systems should be able to fit within the tail cone area (volume estimated to be over 2,800 L (100 ft<sup>3</sup>)), and the fairing volume is estimated to be even larger.



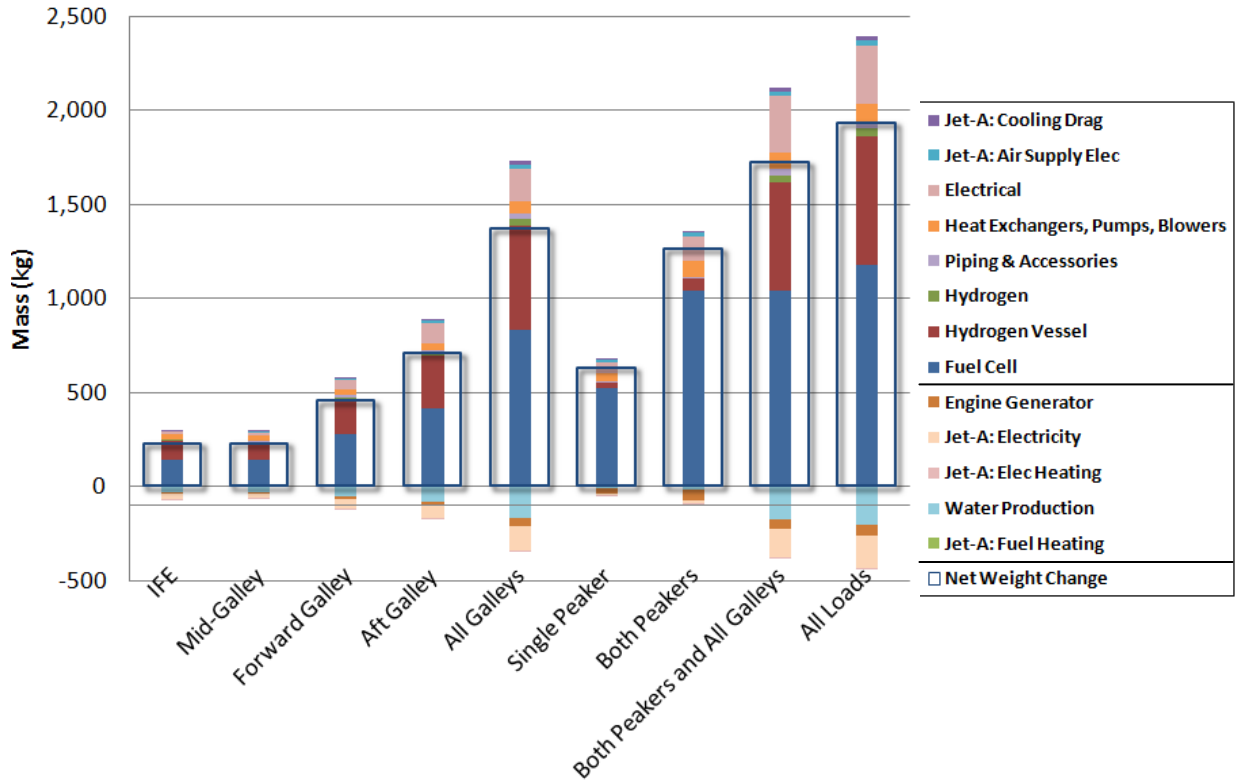


Figure 45: Mass distribution for Case 3b (water cooled, water recovery, limited hot water) for the different loads, using current technology for the fuel cell and hydrogen storage. The different colors in the narrow bars represent different components. Quantities above the zero-line are for mass added to the system, and quantities below the zero-line are for mass credits. The net change (the sum of the added mass and mass credits) is shown by the wide hollow bar. For comparison, the “standard passenger” has a mass of 104 kg (230 lb) including luggage.

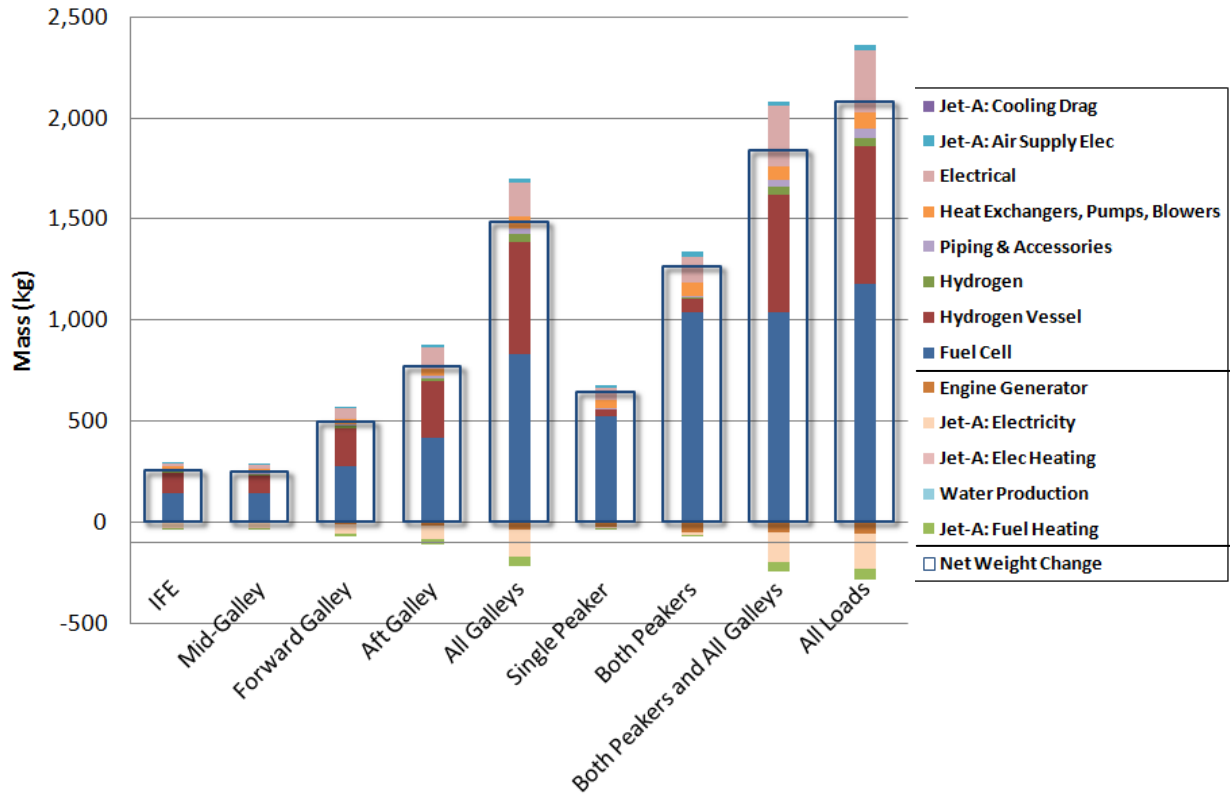


Figure 46: Mass distribution for Case 6a (fuel cooled) for the different loads, using current technology for the fuel cell and hydrogen storage. The different colors in the narrow bars represent different components. Quantities above the zero-line are for mass added to the system, and quantities below the zero-line are for mass credits. The net change (the sum of the added mass and mass credits) is shown by the wide hollow bar. For comparison, the “standard passenger” has a mass of 104 kg (230 lb) including luggage.

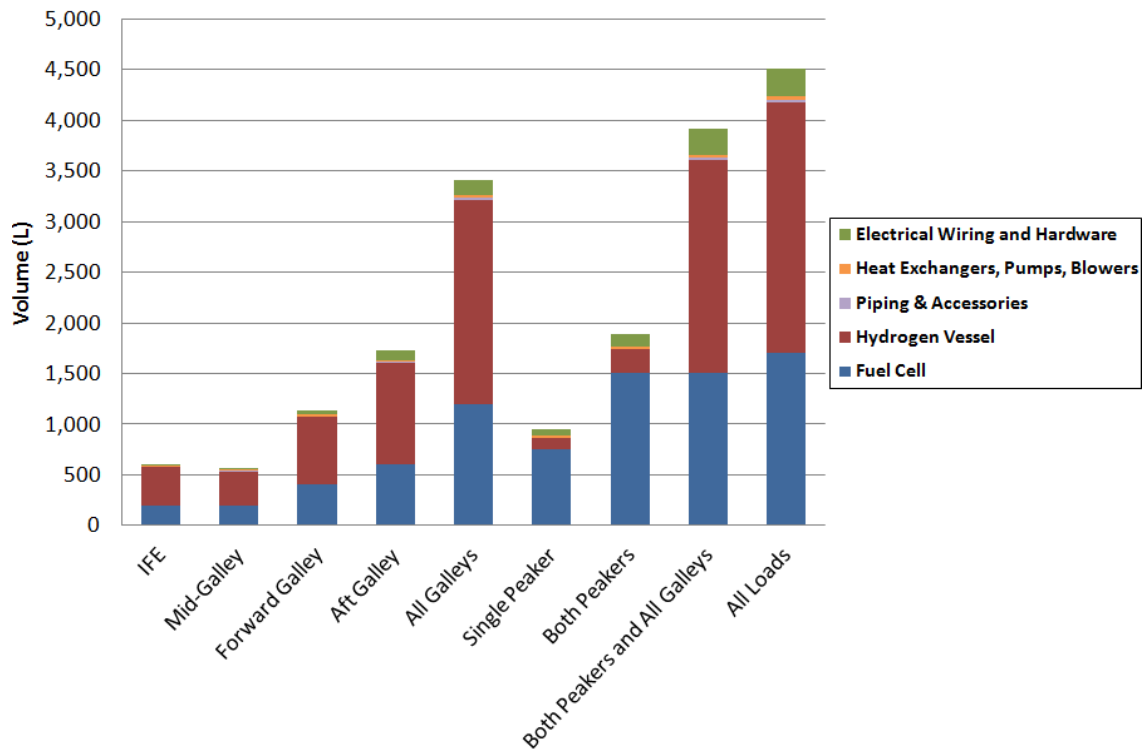


Figure 47: Summary of the volume analysis for Case 2a (water cooled, no heat recovery). The volume of each component is shown by a different color. For comparison, a typical galley beverage cart has a volume of 240 L (8.5 ft<sup>3</sup>).

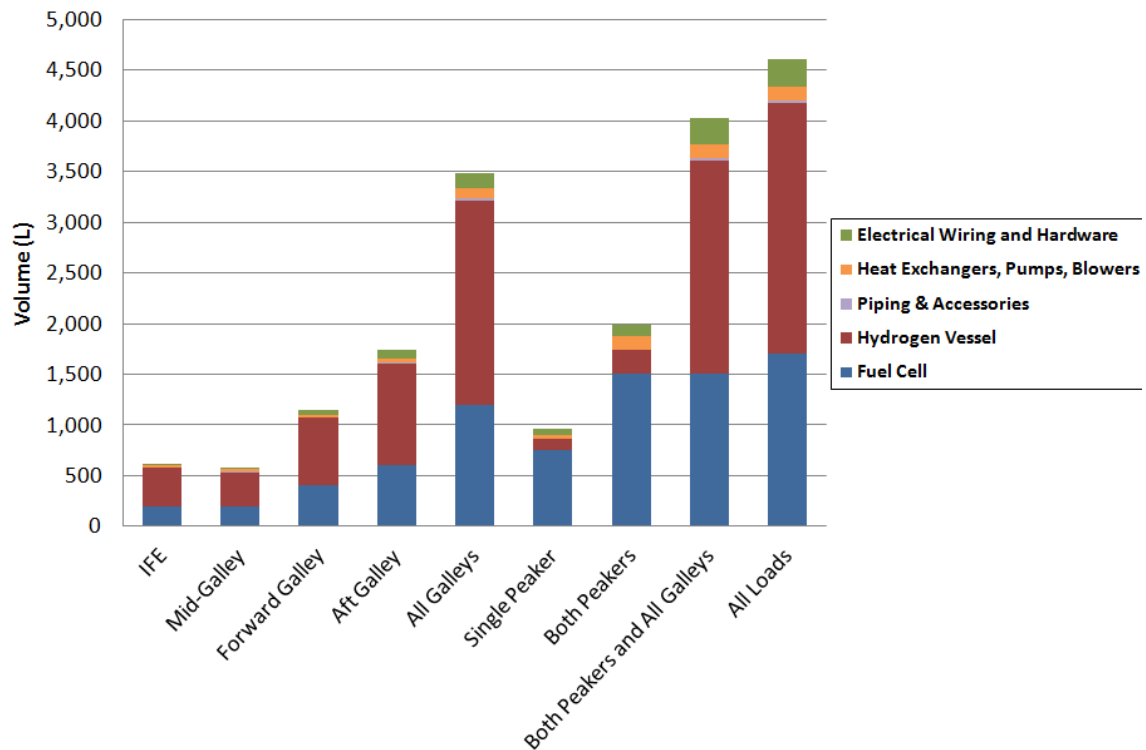


Figure 48: Summary of the volume analysis for Case 3b (water cooled, water recovery, limited hot water). The volume of each component is shown by a different color. For comparison, a typical galley beverage cart has a volume of 240 L (8.5 ft<sup>3</sup>).

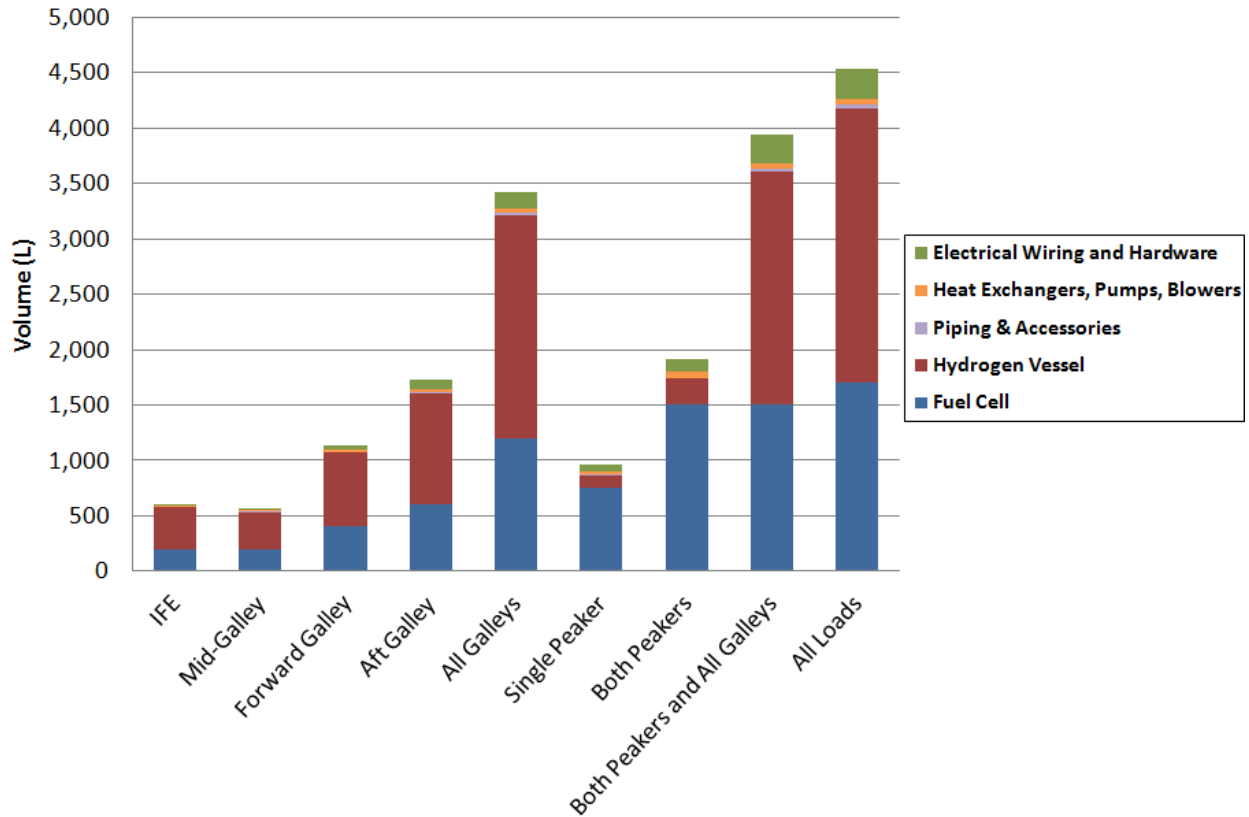


Figure 49: Summary of the volume analysis for Case 6a (fuel cooled). The volume of each component is shown by a different color. For comparison, a typical galley beverage cart has a volume of 240 L (8.5 ft<sup>3</sup>).

### 6.2.3 Performance

All of the effects of the fuel cell system can be consolidated find the overall impact on Jet-A requirements for the airplane, using the method described in Section 2.7. Figure 50 shows the change in jet fuel that results from each of the three system configurations (Cases 2a, 3b, and 6a) and all of the possible load scenarios. It is evident that, when considering current technology for the fuel cell and hydrogen storage system, every possibility will require the airplane with the fuel cell to use more jet fuel than the airplane without.

Other, more subtle effects are also discernable from this figure. While Figure 44, Figure 45, and Figure 46 showed that the Both Peakers scenario has a lower net mass than the All Galleys scenario, from this figure it can be seen that the All Galleys scenario performs better. In fact, the Both Peakers scenario (150 kW) has a worse performance than the All Loads scenario (170 kW), which includes the peakers! The reason for this goes back to the fact that the peakers only operate for a short duration of the flight. While this saves hydrogen storage mass, it does not allow the system to get any significant amount of “credits” for generating electricity, water, or heat. In essence, the airplane has to spend fuel to carry the peaker system without getting much benefit. On the other hand, the systems that operate for longer periods generate large amounts of usable water and/or heat, offsetting the extra fuel that must be carried to transport these systems. This observation can be generalized by saying that if a fuel cell system is going to be carried on-board, the best overall performance will result from operating it as

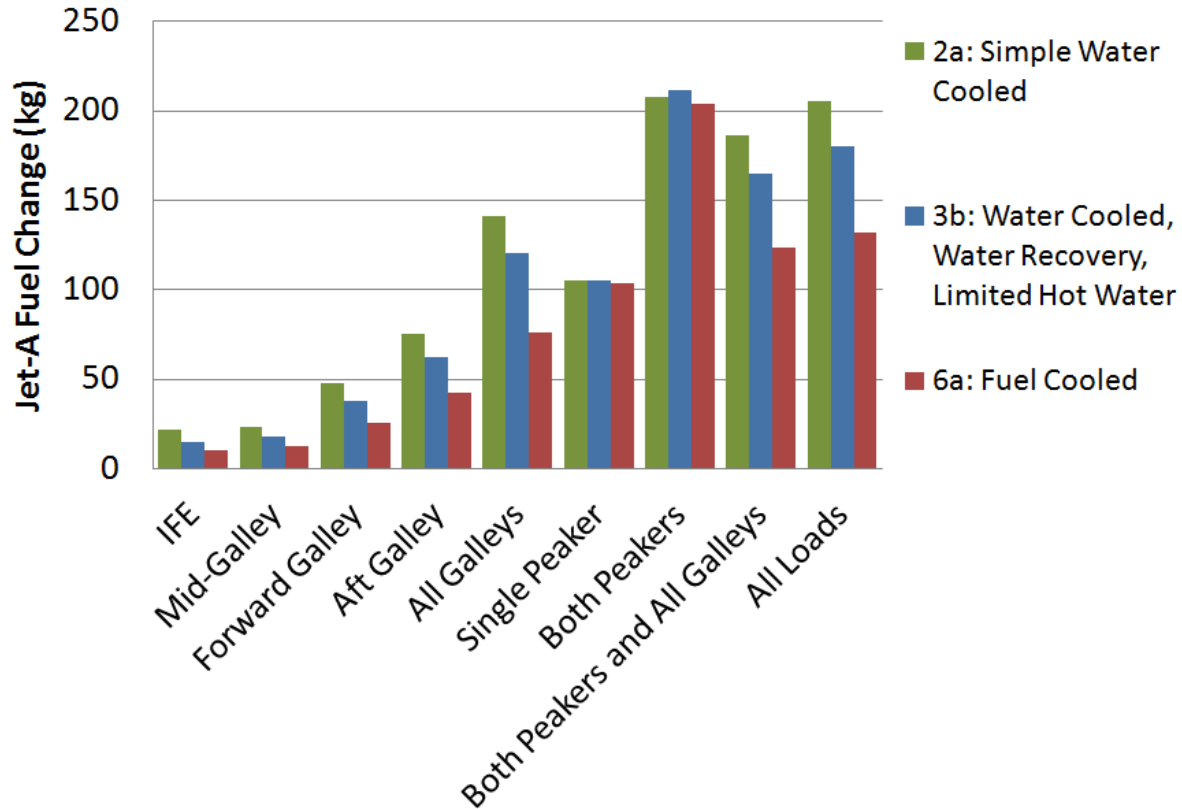


Figure 50: The overall effect of the fuel cell system on airplane performance, as measured by the amount of additional Jet-A the fuel cell-equipped airplane needs to accomplish the same mission as the base airplane. The chart assumes current technology for the fuel cell and hydrogen storage systems. As a comparison, the base airplane on the base mission is estimated to carry 22,680 kg (50,000 lb) of Jet-A at takeoff.

much as possible. The same observation was made by Mackay et al. [22]. However, there may be other reasons to operate a fuel cell sparingly, such as in a peaker application, that outweigh the performance penalty. For a fuel cell used all the time, fuel cell degradation would force the user to replace the fuel cell more often, or to oversize it to achieve a length of service comparable to a gas turbine (Roth and Giffin [58] estimate that fuel cell degradation would require over-sizing the fuel cell by about 4% to achieve the same length-of-service (20,000 hr) typical for a gas turbine). Both options would add cost to the system and the latter would also increase the mass penalty.

Another effect that can be partially found by examining this figure is the difference between saving mass through water recovery and heat recovery to the potable water system, versus saving fuel through heat recovery to the jet fuel. This can be seen by comparing Case 3b with Case 6a for any of the load scenarios, looking at this figure and both Figure 45 and Figure 46. As an example, the All Loads scenario is considered, and the relevant information is summarized in Table 13. While Case 3a has a 203 kg larger mass savings compared to Case 6a, Case 6a has a 17 kg overall jet fuel savings. The reason for this apparent discrepancy is that the type of savings matters. One kilogram of jet fuel saved through fuel heating is a direct savings. But one kilogram of mass saved only saves about 0.16 kg of fuel because of the relationship between mass and fuel requirement through the Breguet equation (see Eq. (12) and

**Table 13: Savings data for Cases 3b and 6a, illustrating the more beneficial effect of saving Jet-A directly vs. saving mass.**

Data (All Loads scenario)	Case 3b	Case 6a
<b>Direct Jet Fuel Savings</b>	<b>176 kg</b>	<b>225 kg</b>
Engine-generated Electricity	176 kg	173 kg
Jet Fuel Heating	0 kg	52 kg
<b>Jet Fuel Savings Due to Mass Savings<sup>1</sup></b>	<b>41 kg</b>	<b>9 kg</b>
Total Mass Savings	262 kg	59 kg
Water Recovery	202 kg	0 kg
Engine Generator	60 kg	59 kg
<b>Total Jet Fuel Savings</b>	<b>217 kg</b>	<b>234 kg</b>

<sup>1</sup>Using the Breguet equation method to find the change in fuel due to a change in airplane mass equal to “Total Mass Savings”. See Eq. (12) and Section 2.7.2.1 for more details on the method.

Section 2.7.2.1). To put it another way, it requires saving about 6 kg of mass to equal the savings of 1 kg of jet fuel. Although Case 6a doesn’t save as much mass as Case 3b, it saves more jet fuel (through fuel heating) and that is a more “valuable” savings than mass. The message is that a system that saves jet fuel directly, such as through reducing the engine electrical load or fuel pre-heating, is more likely to have a better overall performance than a system that only saves mass.

This also illustrates the importance of factoring in the mass of the system on overall airplane fuel burn. As an example, Case 2a has a mass of 255 kg and an added Jet-A requirement of 47 kg for the IFE load scenario. Of this 47 kg, 41 kg is due to the system mass and the Breguet relationship. Without taking this into account, the performance of these systems would seem much better than they would have in actuality.

#### 6.2.4 Summary

The current technology analysis revealed the following:

- The fuel cell and hydrogen vessel are responsible for the majority of the system mass and volume.
- In terms of jet fuel required to accomplish the mission, a system that will provide a performance benefit to the airplane has not been found.
- A complementary effect between the peaker and galleys was discovered, allowing the same fuel cell to be used for both applications.
- From a performance point of view, a system that operates at full load throughout the flight will have a better benefit than one that does not.
- Saving jet fuel directly, through fuel heating or by reducing engine fuel consumption, provides a more “valuable” benefit than saving an equal amount of mass by the ratio of approximately 6:1.

### 6.3 System Performance with DOE Target Technology

The analysis done in the previous section was repeated with the only change being the sizes of the fuel cell and hydrogen storage vessel, in order to see what the effect of future technology might have on the feasibility and performance of an on-board fuel cell system.

“DOE Target Technology” refers to a PEM fuel cell with a specific power of 650 W/kg (295 W/lb) and power density of 650 W/L (18,400 W/ft<sup>3</sup>) as described in Section 3.1.2, and a hydrogen vessel with 7.5% gravimetric density and 70 gH<sub>2</sub>/L (4.37 lb/ft<sup>3</sup>) volumetric density as described in Section 3.2.3.

### 6.3.1 Mass and Volume

Mass and volume distributions are shown for completeness in Figure 51 through Figure 56. The trends are nearly identical to those in the results for the current technology. The only exception is that the fraction of total mass due to the fuel cell and hydrogen storage has decreased, as expected. In fact, the electrical equipment surpasses the fuel cell in terms of mass in mass and nearly in volume.

Upon comparison to the analogous current technology graphs, it can be seen that the total mass has decreased by nearly a factor of two, and the total volume by nearly a factor of four. Thus, achieving the DOE targets for vehicles will result in drastically smaller systems for fuel cell electricity generation on board an airplane. All systems should be able to easily fit within the confines of either the tail cone area (volume estimated to be over 2,800 L (100 ft<sup>3</sup>)), and the even-larger fairing area.

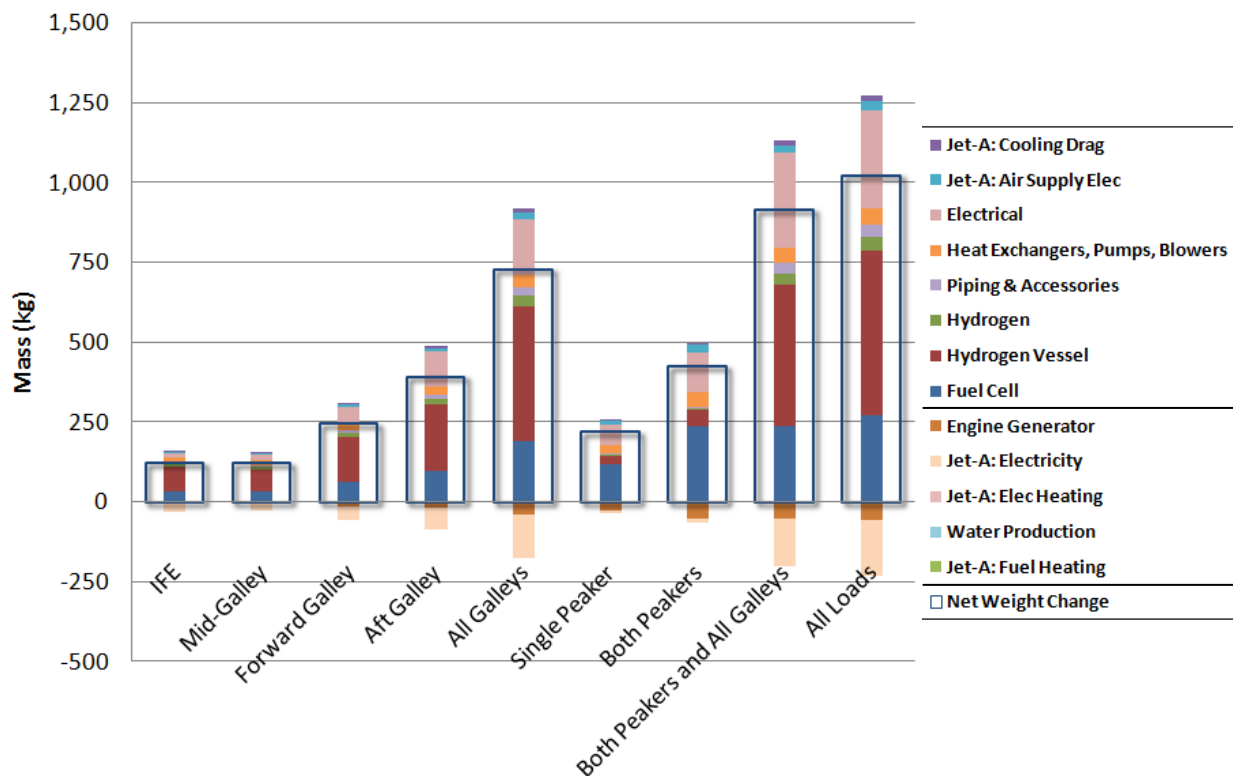


Figure 51: Mass distribution for Case 2a (water cooled, no heat recovery) for the different loads, using DOE target technology for the fuel cell and hydrogen storage. The different colors in the narrow bars represent different components. Quantities above the zero-line are for mass added to the system, and quantities below the zero-line are for mass credits. The net change (the sum of the added mass and mass credits) is shown by the wide hollow bar. For comparison, the “standard passenger” has a mass of 104 kg (230 lb) including luggage.

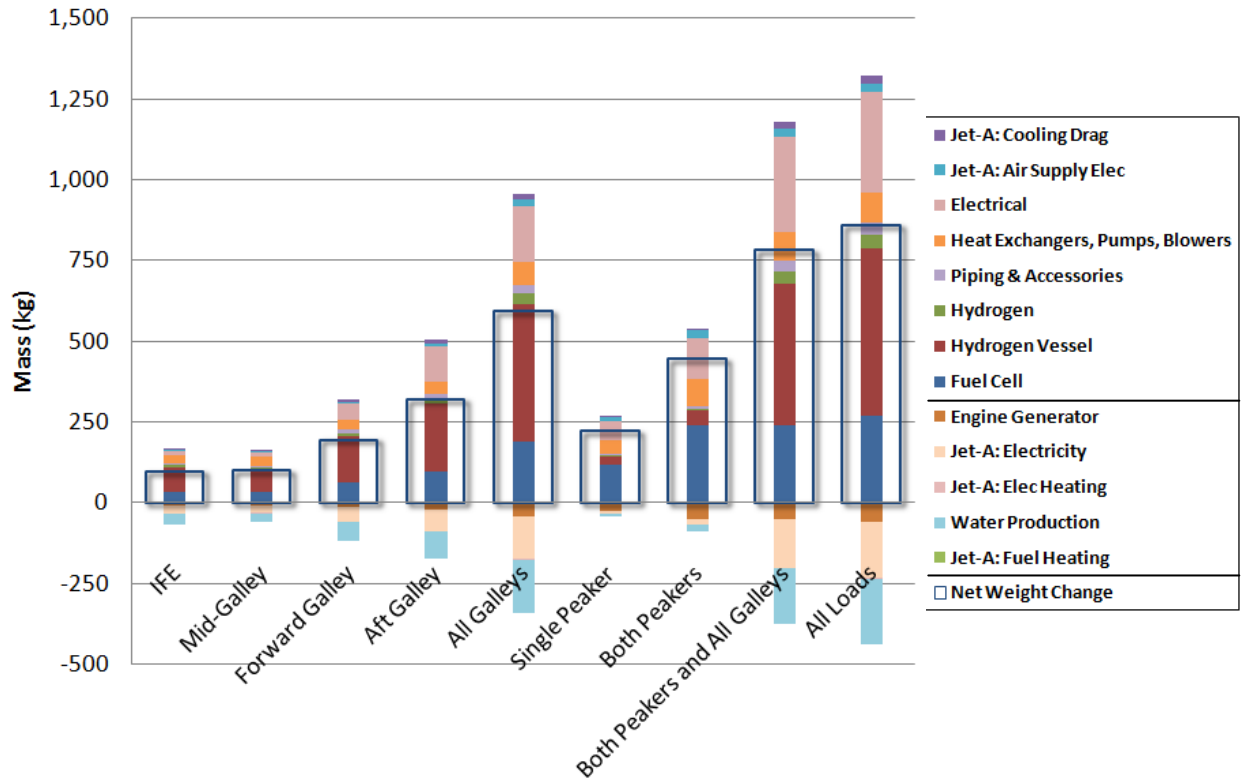


Figure 52: Mass distribution for Case 3b (water cooled, water recovery, limited hot water) for the different loads, using DOE target technology for the fuel cell and hydrogen storage. The different colors in the narrow bars represent different components. Quantities above the zero-line are for mass added to the system, and quantities below the zero-line are for mass credits. The net change (the sum of the added mass and mass credits) is shown by the wide hollow bar. For comparison, the “standard passenger” has a mass of 104 kg (230 lb) including luggage.

### 6.3.2 Performance

Like the current technology analysis, the impact of the system on overall airplane performance, as defined by the amount of jet fuel (Jet-A) added or subtracted from the base airplane to the airplane with the fuel cell, was determined. Figure 57 is the result for all load scenarios and the three system configurations, assuming DOE target technology for the fuel cell and hydrogen storage vessel.

From here it is evident that the fuel cell system is able to provide a performance benefit to the airplane when the fuel cooled system (Case 6a) is implemented, and to a lesser degree when the water cooled / water recovery / limited hot water system (Case 3b) is chosen. The simple water cooled system without any heat or water recovery (Case 2a) still does not provide a benefit.

The amount of the benefit is also shown to depend on the load scenario. The trends are a little different than the current technology analysis, and not so straightforward. For example, the benefit of Case 3b increases with decreased system size, similar to the current technology results, but the All Galleys scenario shows the opposite trend – a better benefit with a larger system. And comparing the IFE and Mid-Galley scenarios shows a difference in the benefit in spite of the fact that both systems are 20 kW. The reason for this is that the effects of load location become more important, as piping and wiring



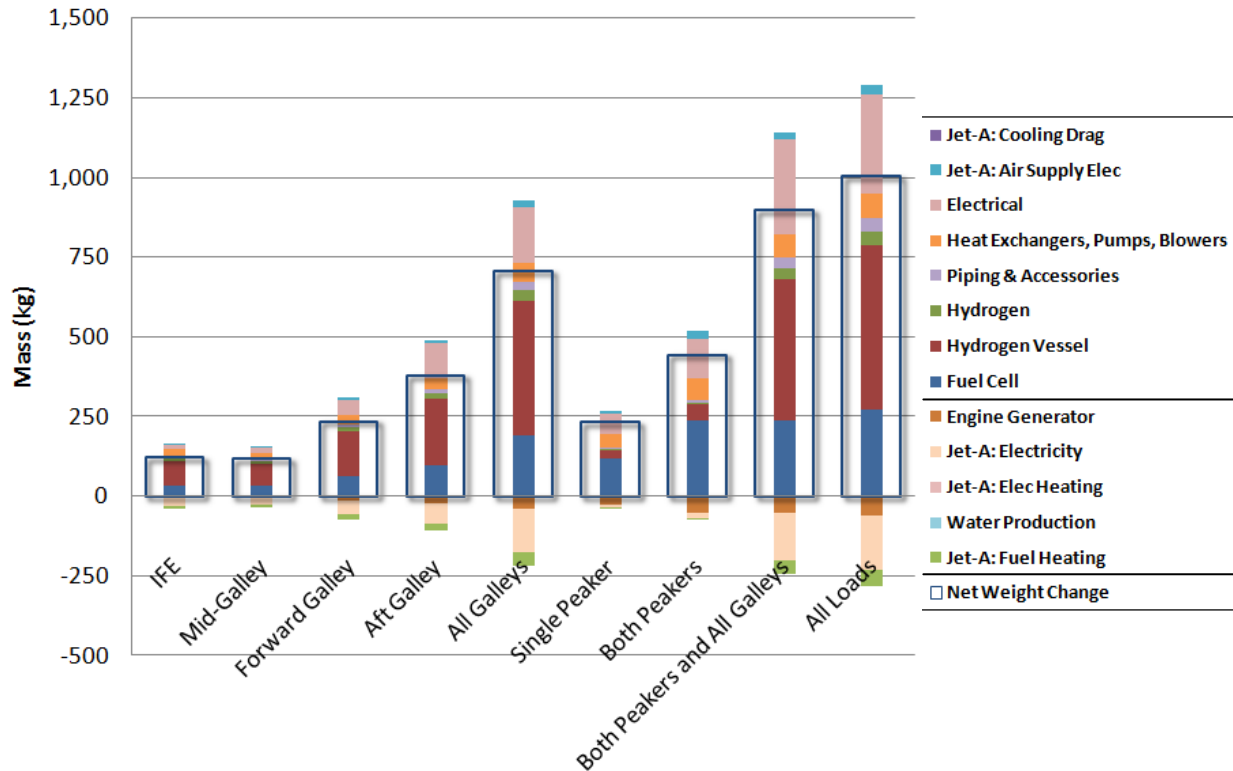


Figure 53: Mass distribution for Case 6a (fuel cooled) for the different loads, using DOE target technology for the fuel cell and hydrogen storage. The different colors in the narrow bars represent different components. Quantities above the zero-line are for mass added to the system, and quantities below the zero-line are for mass credits. The net change (the sum of the added mass and mass credits) is shown by the wide hollow bar. For comparison, the “standard passenger” has a mass of 104 kg (230 lb) including luggage.

masses become a larger fraction of the total mass (because the fuel cell and hydrogen mass has decreased so much).

There are two ways to illustrate the benefit (or penalty) a fuel cell system provides to the airplane. One way is to compare the total fuel required by the base airplane to the total fuel required by the airplane with a fuel cell to accomplish the mission. In some ways this method is appropriate because this is what may be most useful to an airplane customer as it reflects a “bottom line” effect. For example, looking at the fuel cooled system configuration supplying electricity to all galleys, the fuel savings is 46 kg. That means that while the base airplane requires 22,680 kg of fuel, the airplane with the fuel cell requires 22,634 kg, a decrease of about 0.2%. A customer could project a 0.2% fuel savings over their expected usage and decide if it makes economic sense considering all the factors that affect their business.

Another way to illustrate the benefit (or penalty) is to compare the fuel cell system impact not to the entire airplane, but just to the portion of the airplane that is directly impacted by the fuel cell system. This can be done by comparing only the portion of jet fuel it takes the base airplane to supply the electrical and heat loads to the amount of jet fuel required by the fuel cell system to do the same. (Note that while the fuel cell system does not directly consume any jet fuel, it will increase the jet fuel required by the airplane because of things like added weight, drag, and the electricity required by the

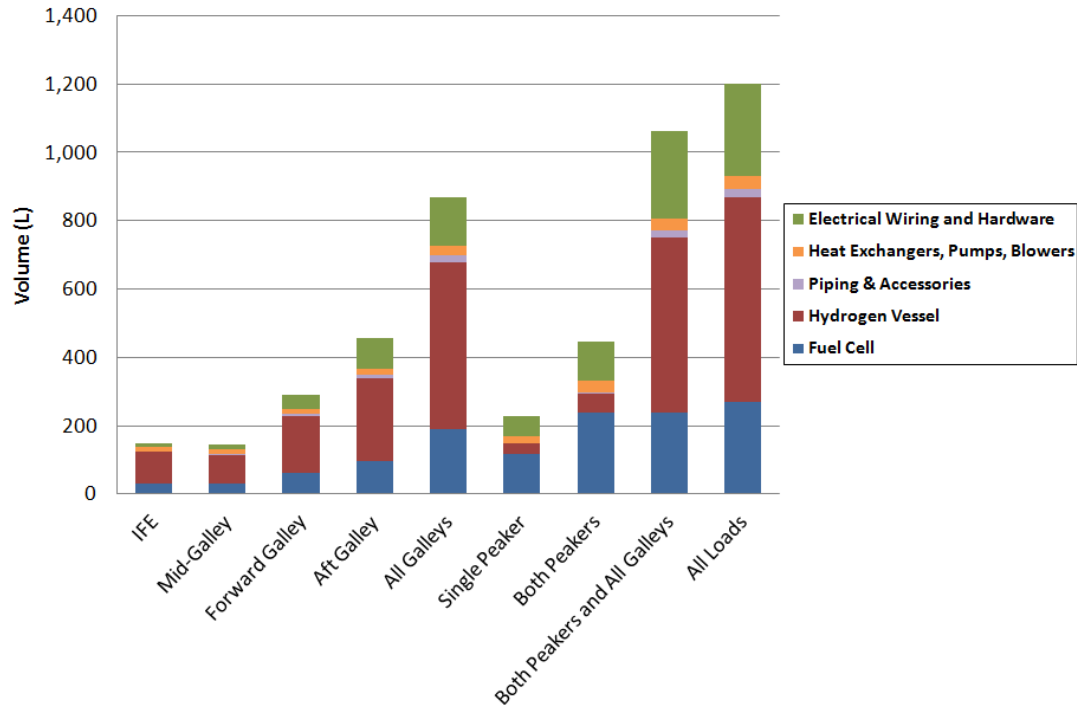


Figure 54: Summary of the volume analysis for Case 2a (water cooled, no heat recovery) with DOE target technology. The volume of each component is shown by a different color. For comparison, a typical galley beverage cart has a volume of 240 L (8.5 ft<sup>3</sup>).

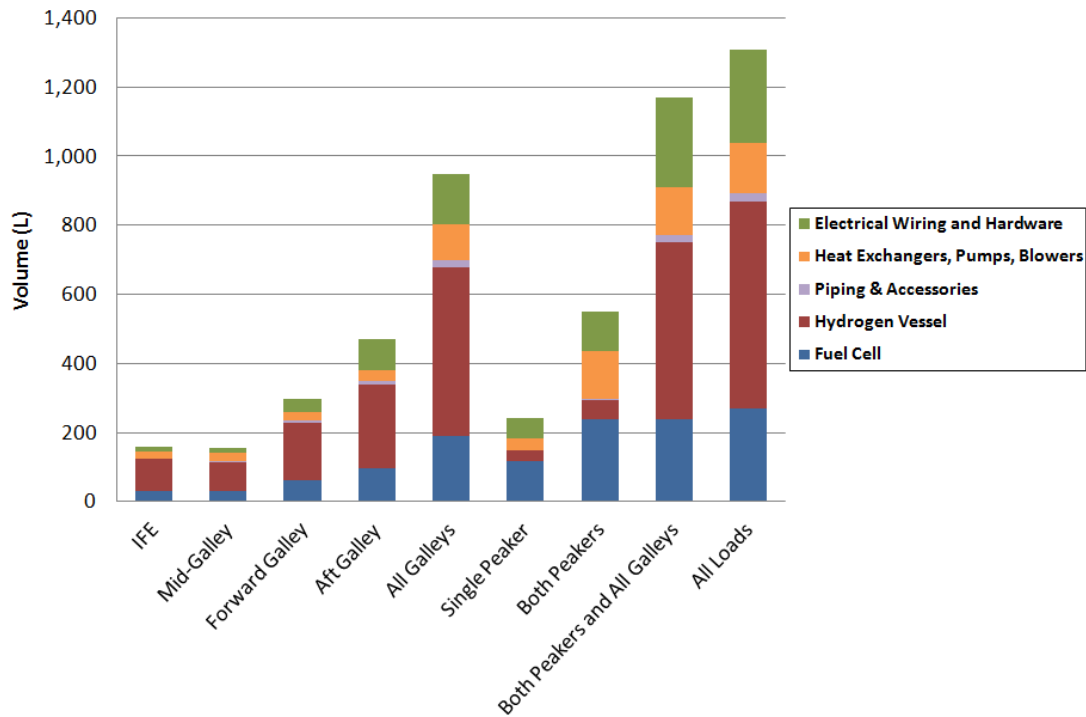


Figure 55: Summary of the volume analysis for Case 3b (water cooled, water recovery, limited hot water) with DOE target technology. The volume of each component is shown by a different color. For comparison, a typical galley beverage cart has a volume of 240 L (8.5 ft<sup>3</sup>).

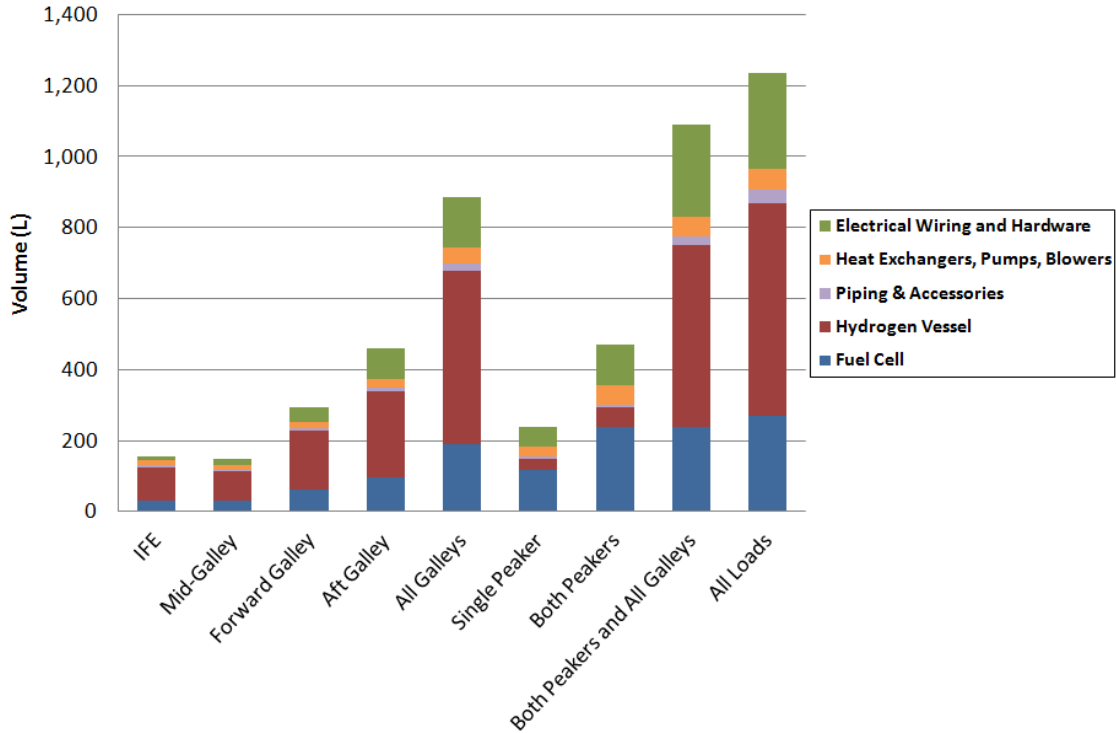


Figure 56: Summary of the volume analysis for Case 6a (fuel cooled) with DOE target technology. The volume of each component is shown by a different color. For comparison, a typical galley beverage cart has a volume of 240 L (8.5 ft<sup>3</sup>).

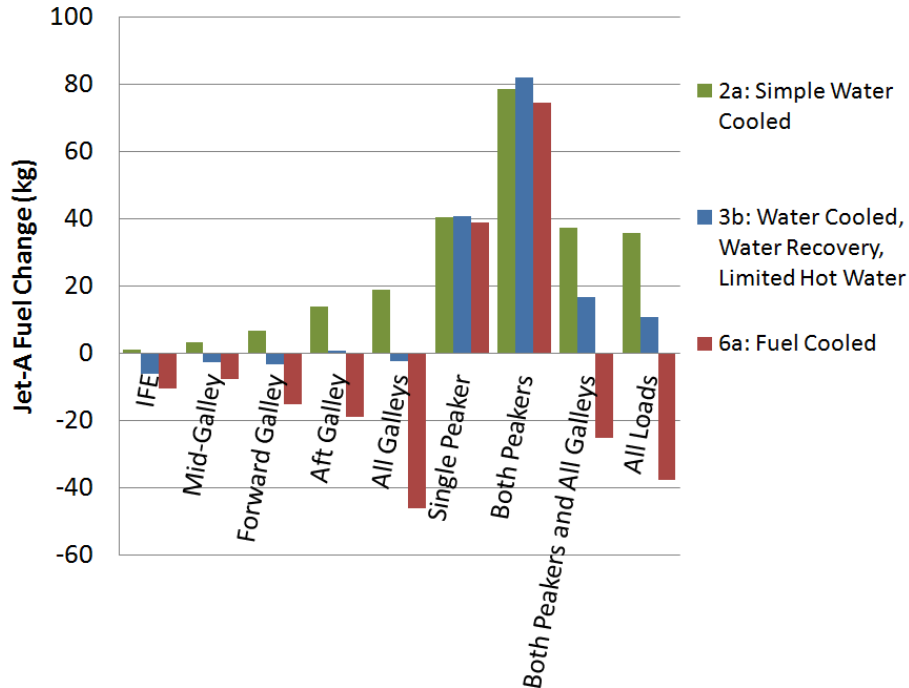


Figure 57: The overall effect of the fuel cell system on airplane performance, as measured by the amount of additional Jet-A the fuel cell-equipped airplane needs to accomplish the same mission as the base airplane. The chart assumes DOE target technology for the fuel cell and hydrogen storage systems. As a comparison, the base airplane on the base mission is estimated to carry 22,680 kg (50,000 lb) of Jet-A at takeoff.

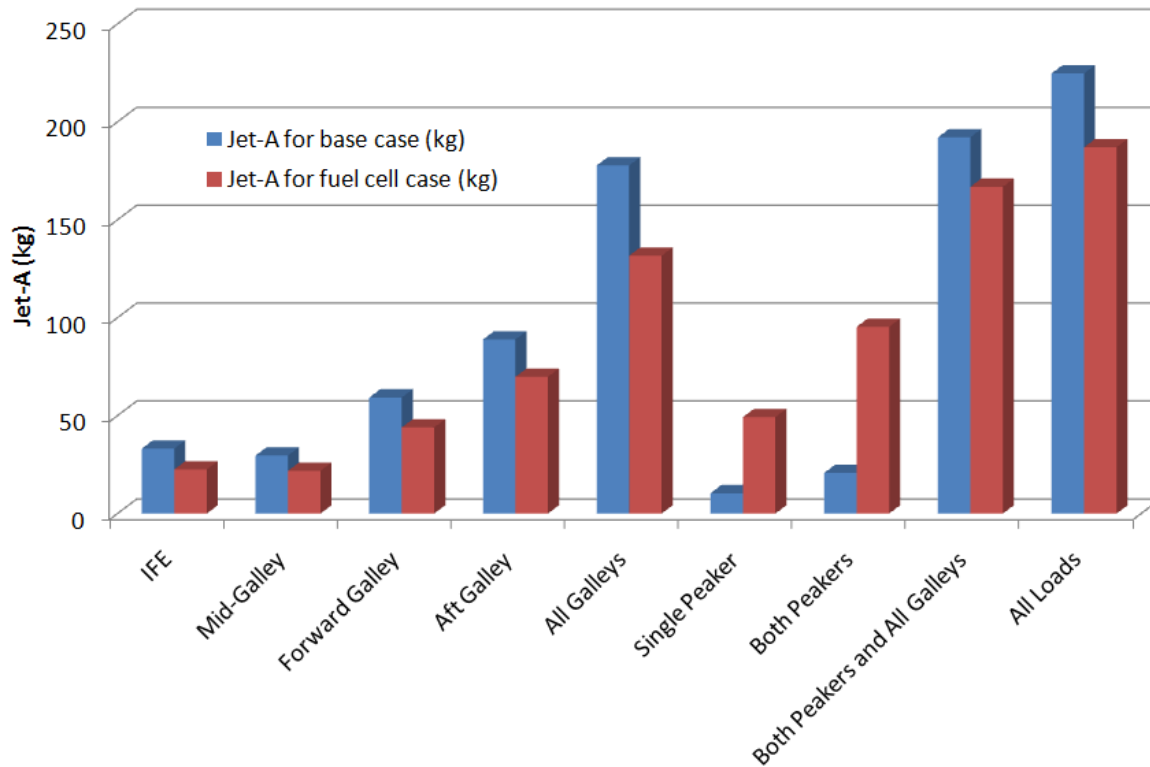


Figure 58: The amount of fuel required by the base airplane and the airplane with the fuel cell to generate electricity and heat for the different load scenarios. The base airplane uses the main engine generator with a fuel-to-electricity efficiency of 34%, while the fuel cell assumes the fuel cooled configuration with DOE target technology. The numbers are presented below in Table 14.

Table 14: A summary of the numbers plotted above in Figure 58, and the calculated percentages, comparing the fuel needed by the base airplane and the fuel cell airplane to generate the required electricity. The percentage shows the amount of fuel required by the fuel cell airplane relative to that required by the base airplane. Percentages below 100% show a fuel savings of the fuel cell airplane, over 100% show a fuel penalty.

Load Scenario	Fuel Required by Base Airplane (main engine generator, 34% efficiency) (kg)	Fuel Required by Fuel Cell Airplane (fuel cooled system with DOE target technology) (kg)	Percentage (fuel cell airplane / base airplane)
IFE	33.2	22.5	67.9%
Mid-Galley	29.6	21.8	73.7%
Forward Galley	59.3	44.0	74.2%
Aft Galley	88.9	69.8	78.6%
All Galleys	177	132	74.1%
Single Peaker	10.4	49.3	475%
Both Peakers	20.7	95.3	460%
Both Peakers and All Galleys	192	167	86.8%
All Loads	225	187	83.2%

pressurization system to supply the fuel cell's air.) This method is appropriate because it is a direct comparison of the two competing technologies as opposed to comparing the effect of a fuel cell system to the entire airplane. It has already been noted that the base airplane weighs 173,998 kg at takeoff and carries 22,680 kg of fuel, while the fuel cell system weighs (worst case: largest system with current technology) about 2,000 kg and adds about 150 kg of fuel, or only about 0.1% of the respective totals. So while the "bottom line" method as described is appropriate in some cases, changes to the fuel cell system become nearly lost in the small overall numbers, whereas comparing the fuel cell system to the current electrical system allows for more insight into the effectiveness of the systems themselves.

To that end, Figure 58 compares the amount of fuel required by the base airplane to generate electricity to the amount required by the fuel cell to do the same. This chart is for the fuel cooled system using DOE target technology. The efficiency of the airplane to generate electricity from the main engines is taken as 34%. This is possibly lower in practice, down to 25% depending on the electrical system. And if the auxiliary power unit is used, the efficiency will be about half that of the main engines. Using lower efficiency numbers would have the effect of increasing the amount of fuel needed by the base airplane to generate electricity (the blue bars) while not affecting the fuel cell's requirements (the red bars). Table 14 summarizes the numbers and also shows the differences in terms of percentages. In the case of galleys, the fuel cell system saves around 25% of the jet fuel compared to the base airplane. For the peakers, the fuel cell system results in a large penalty (nearly 5-times the fuel required).

The results can be cast in another way, and that is by putting the fuel savings in terms of CO<sub>2</sub> emissions. This is shown in Figure 59, where "avoided CO<sub>2</sub>" refers to the CO<sub>2</sub> emissions saved by comparing the fuel cell airplane to the base airplane, using the fuel requirements given in Table 14. Here, it is shown for yearly emissions of a fleet of 1,000 airplanes each flying 150 base missions, and assuming there is no contribution from hydrogen production to CO<sub>2</sub> emissions (i.e., renewable energy is used to generate the hydrogen used in the fuel cells). Boeing currently has over 800 orders for the 787 [59], and predicts that the market for 787-class airplanes ("small twin aisle") will be 4,430 by 2029 [60], so 1,000 787-type airplanes is reasonable. 150 base missions is equivalent to 750 hrs of flight time per year, which is what was used in Ref. [25]. CO<sub>2</sub> is calculated by assuming complete combustion of C<sub>12</sub>H<sub>23</sub>, used to represent the average hydrocarbon content of jet fuel, yielding 3.16 kg of CO<sub>2</sub> generated for every 1 kg of jet fuel burned. The figure does not include either of the peaker load scenarios since those do not provide any avoided emissions.

### 6.3.3 Summary

The DOE target technology analysis showed:

- Overall airplane performance benefits can result from improved fuel cell and hydrogen technologies in accordance with DOE targets.
- While the performance as measured by fuel savings is small when compared to the entire airplane's fuel consumption, the fuel cell system can save over 30% of the fuel that is devoted to electricity generation (Case 6a with the IFE load).

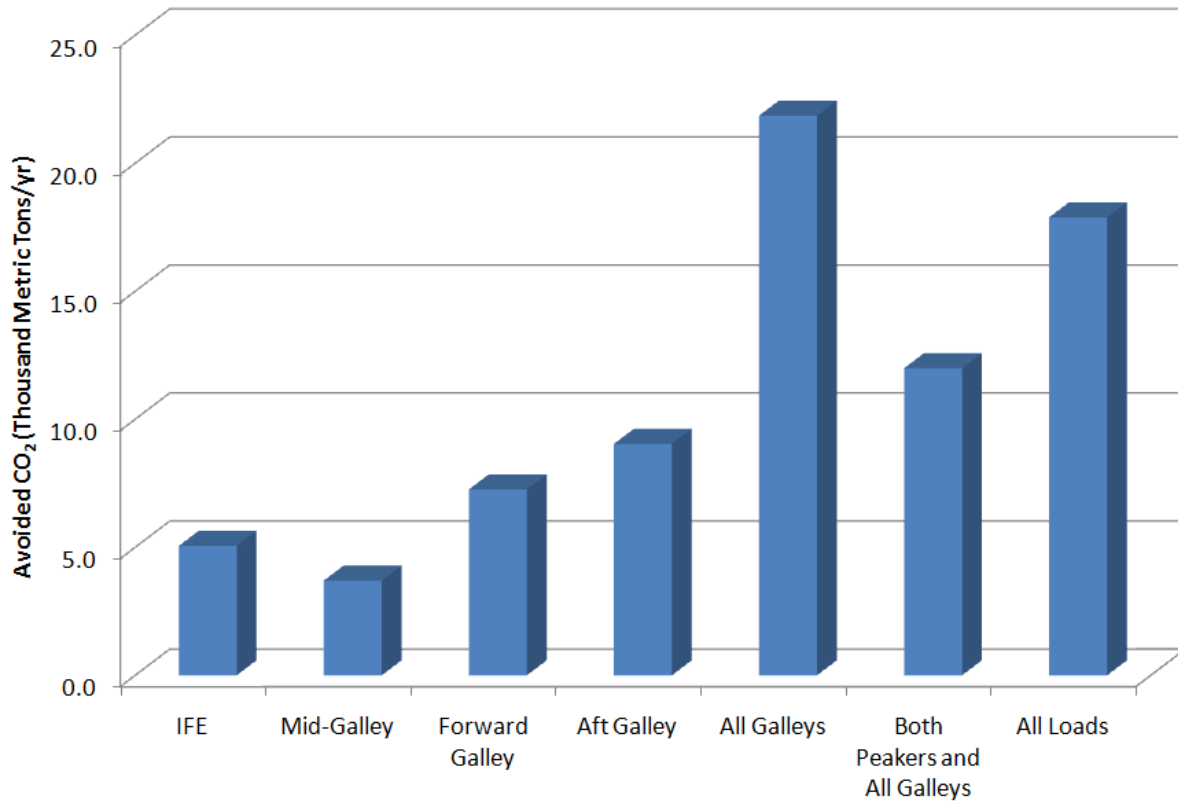


Figure 59: Yearly avoided CO<sub>2</sub> emissions for a fleet of 1,000 fuel cell-equipped airplanes operating 750 hrs/yr, using a fuel cooled fuel cell system (Case 6a) and renewable hydrogen, and comparing to the base airplane generating electricity via the main engines at 34% efficiency.

## 6.4 Electrical System Behavior

The electrical system models described in Chapter 5 were used to determine if the fuel cell could satisfactorily perform the desired functions. The electrical stability and transient characteristics of the on-board fuel cell system were determined. Stability was measured by the ability of the system to provide the power needed by the load in real-time as well as the ability to not cause un-necessary transients or voltage fluctuations.

Acceptable transient behavior of airplane electrical systems is often dictated by the ability of the system to meet the requirements of the Department of Defense Interface Standard – Aircraft Electric Power Characteristics, referred to by MIL-STD-704F [61]. Although this is a Department of Defense standard, this is used by commercial airplane equipment suppliers and integrators (such as Boeing) in the design of their electrical system and components as well. The MIL-STD-704F transient requirements for 28 VDC and 270 VDC systems are shown in Figure 60 and Figure 61, respectively. These black solid lines in these figures show the maximum and minimum allowable voltages following a transient event.

Due to the complexity of the models and of the components within them, the models were only run for 10 seconds or less (simulated time) in order to obtain results within a reasonable amount of time. Ten seconds is sufficient to capture the transients that are of interest.

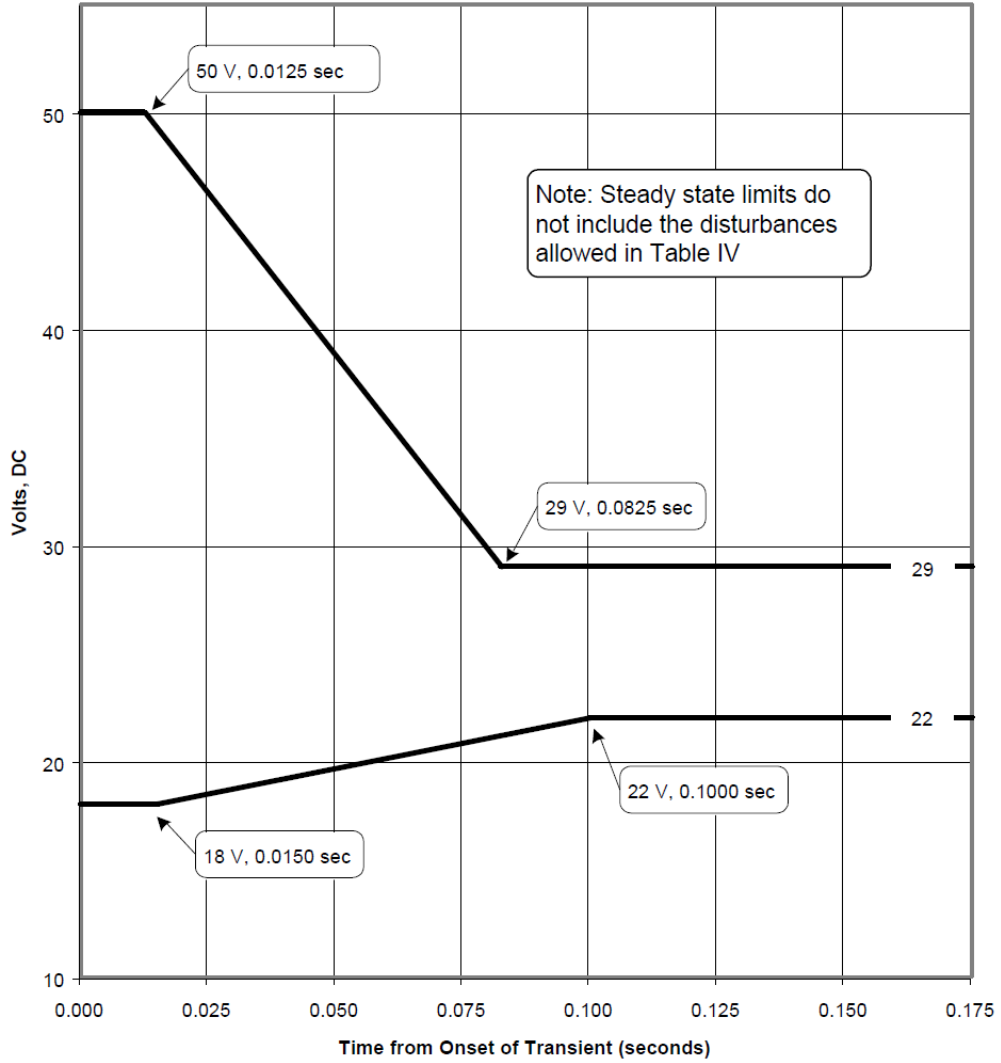
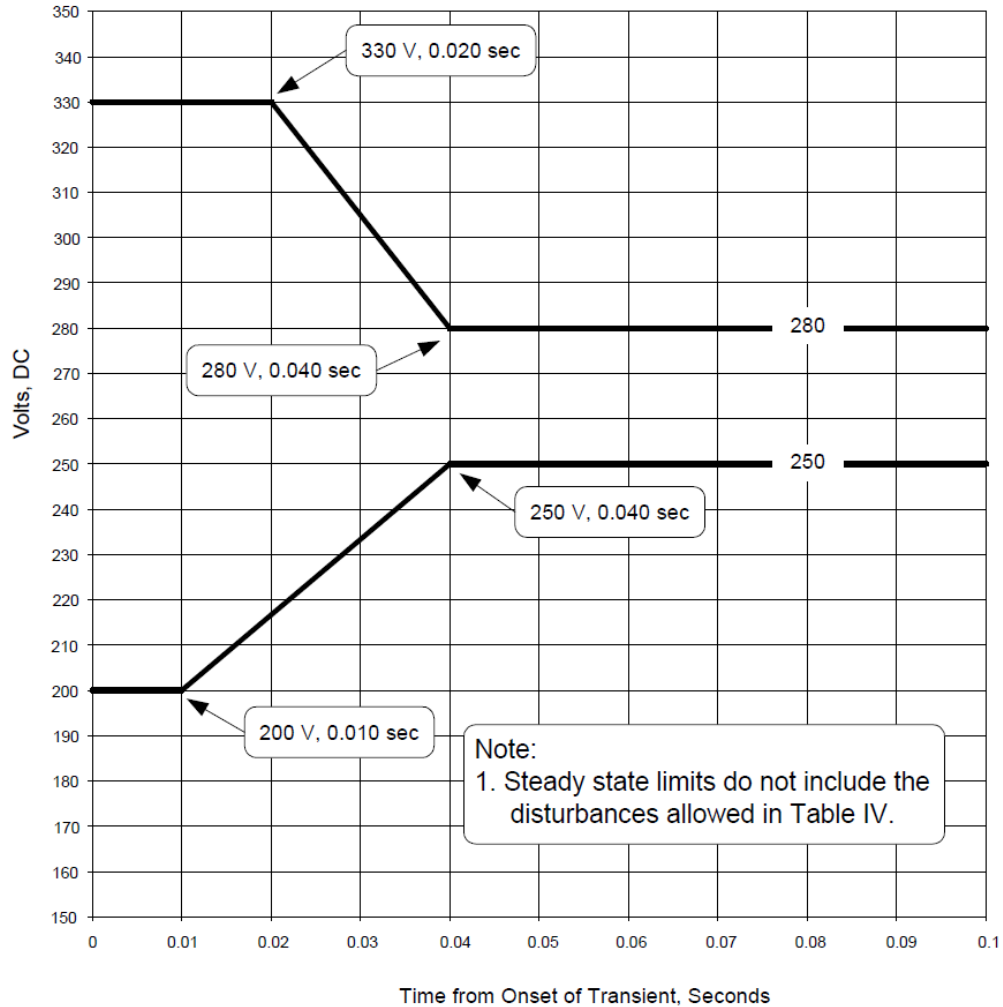


Figure 60: Allowed voltage transient for 28 VDC systems. During transients, the system voltage must not go higher than the top solid line or lower than the bottom solid line. (Figure 13 in MIL-STD-704F [61].)



**Figure 61: Allowed voltage transient for 270 VDC systems. During transients, the system voltage must not go higher than the top solid line or lower than the bottom solid line. (Figure 16 in MIL-STD-704F [61].)**

### 6.4.1 Stand-alone Galley Model Simulation Results

As stated before, for the stand-alone galley scenario, no more than two loads were allowed to turn on at once. The simulation starts off with the fuel cell serving a load of 12 kW. At 5 seconds a water boiler is turned on, adding 4,240 Watts to the load. Several other loads are turned on at different times during the simulation. Table 15 lists the loads that turn on during the simulation and the times at which they turn on.

Although the galley was modeled as a stand-alone system and therefore is not required to meet the MIL-STD-704F standards, these standards were used as a means to measure power quality of the system. Figure 62 shows the voltage at the load during the simulation. The voltage transients at 5, 6, 7 and 8 seconds can be attributed to the increase in power demand from the load (see Table 15). It can be seen from this figure that the system is stable with no unintended fluctuations or transients.



**Table 15: Load increases during stand-alone galley simulation.**

Simulation Time (seconds)	Load(s) Turned On	Additional Power Demand	Total Power Demand
0	Initial Load	12,000 Watts	12,000 Watts
5	(1) Water Boiler	4,240 Watts	16,240 Watts
6	(2) Ovens	7,600 Watts	23,840 Watts
7	(1) Thermoelectric Refrigerator	1,620 Watts	25,460 Watts
8	(2) Beverage Makers	5,520 Watts	30,980 Watts

To meet MIL-STD-704F standards, the voltage for a 28 VDC system must remain between 18 and 50 volts at all times. It is clearly seen from Figure 62 that the voltage does not go below 18 Volts or above 50 Volts during any of the transients. At 6 seconds, when the load increase was 7,600 W, the voltage only drops down to 19 Volts.

MIL-STD-704F standards also require that during a transient the voltage levels return to the steady state values (22-29 Volts) within a certain amount of time: Figure 60 shows that if the voltage drops below 22 Volts (lower steady-state limit) it must return to at least 22 Volts within 0.085 seconds, and if the voltage goes above 29 Volts it must return to at least 29 Volts within 0.07 seconds. Figure 63 shows the detail of voltage at 6 seconds, and it can be seen that the voltage returns to 22 Volts in about 0.0001 seconds, easily satisfying the MIL-STD-704F requirements.

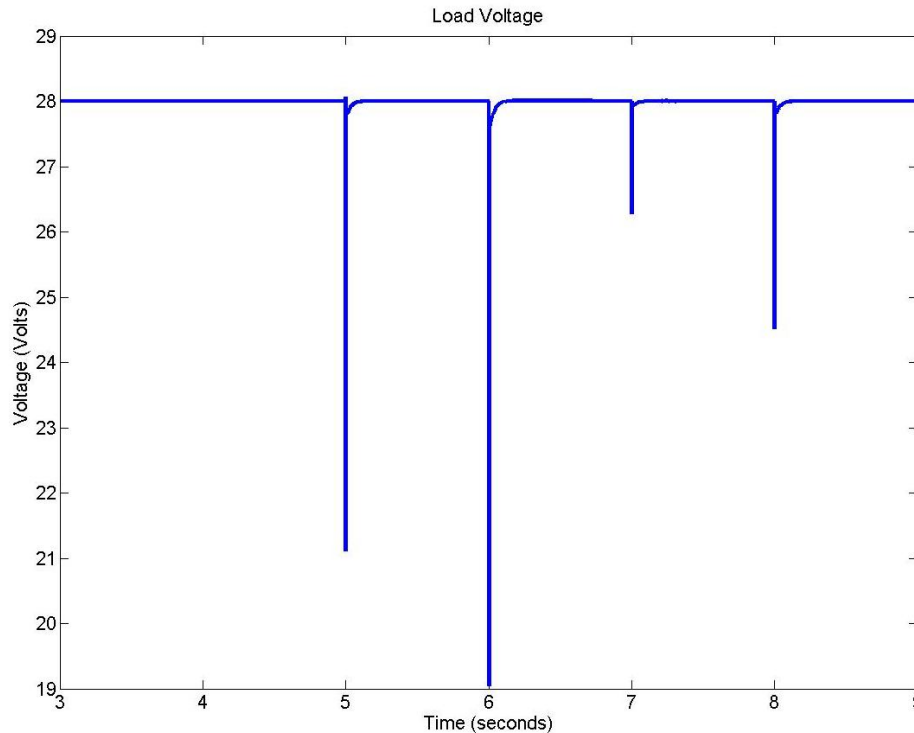


**Figure 62: Stand-alone galley system simulation: voltage as measured at the load.**

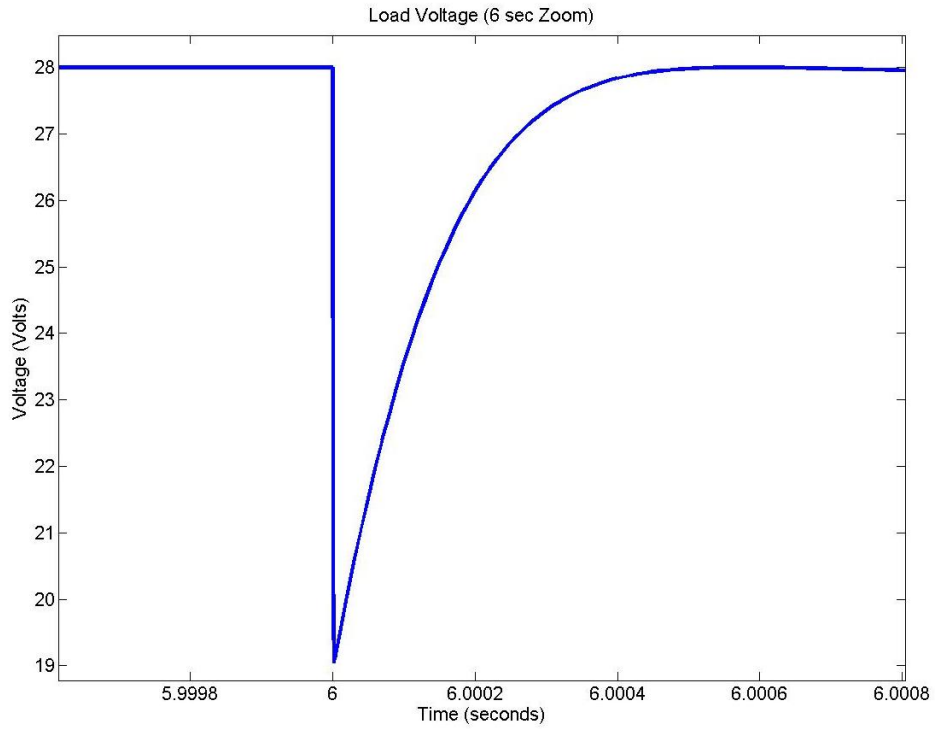


**Figure 63: Stand-alone galley system simulation: Detail of the voltage transient at 6 seconds, showing that voltage recovers to more than 22 V within about 0.0001 seconds, easily satisfying the MIL-STD-704F requirements.**

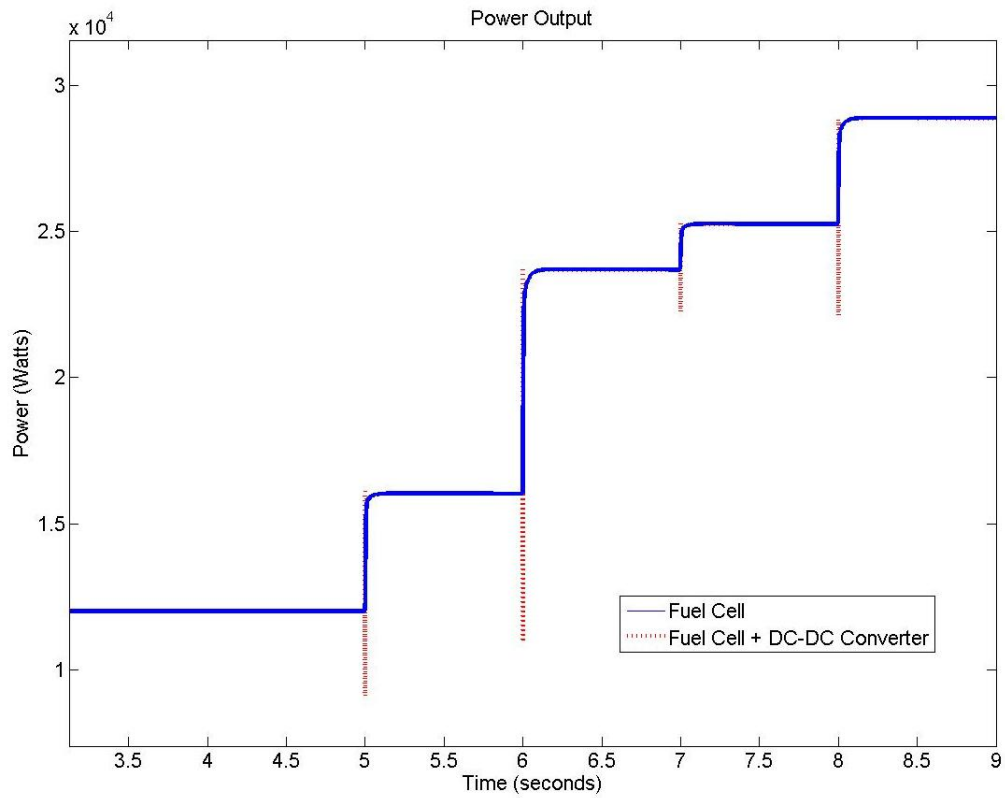


**Figure 64: Stand-alone galley system simulation: Power response from the fuel cell and the fuel cell + DC-DC converter**

The previous figures show that the fuel cell system for the stand-alone galley is capable of meeting the transient response requirements in less than one millisecond, even though the fuel cell itself has a 5-second transient time. To investigate this phenomenon, the power response from the DC-DC converter was examined; this is shown in Figure 64. From this figure it becomes evident that the capacitor within the DC-DC converter is used to aid the fuel cell in meeting the power demand as fast as possible.

### 6.4.2 Peaker System Model Simulation Results

Figure 65 shows the power demand and supply for the peaker system simulation. The figure shows the power demand from the load (blue line, hidden behind black dashed line), the total power supplied (black dashed line), as well as the power outputs from the engine generator (pink line), fuel cell (green line), and DC-DC converter (red line).

The simulation starts off with the 200 KVA main-engine generator serving a base load of 150 kW ( $1.5 \times 10^5$  Watts in the figure). At 1, 1.5, and 2 seconds there are load increases of 15 kW, 15 kW, and 20 kW respectively, bringing the total load to 200 kW. All three of these load increases are fully met by the engine generator. At 4 seconds there is another increase in load of 50 kW. The generator can no longer meet the power demand so the fuel cell supplies the power through the DC-DC converter, as evidenced by the jump in the green and red lines. At 5 seconds a second load increase, this time 20 kW, is also handled by the fuel cell and DC-DC converter.

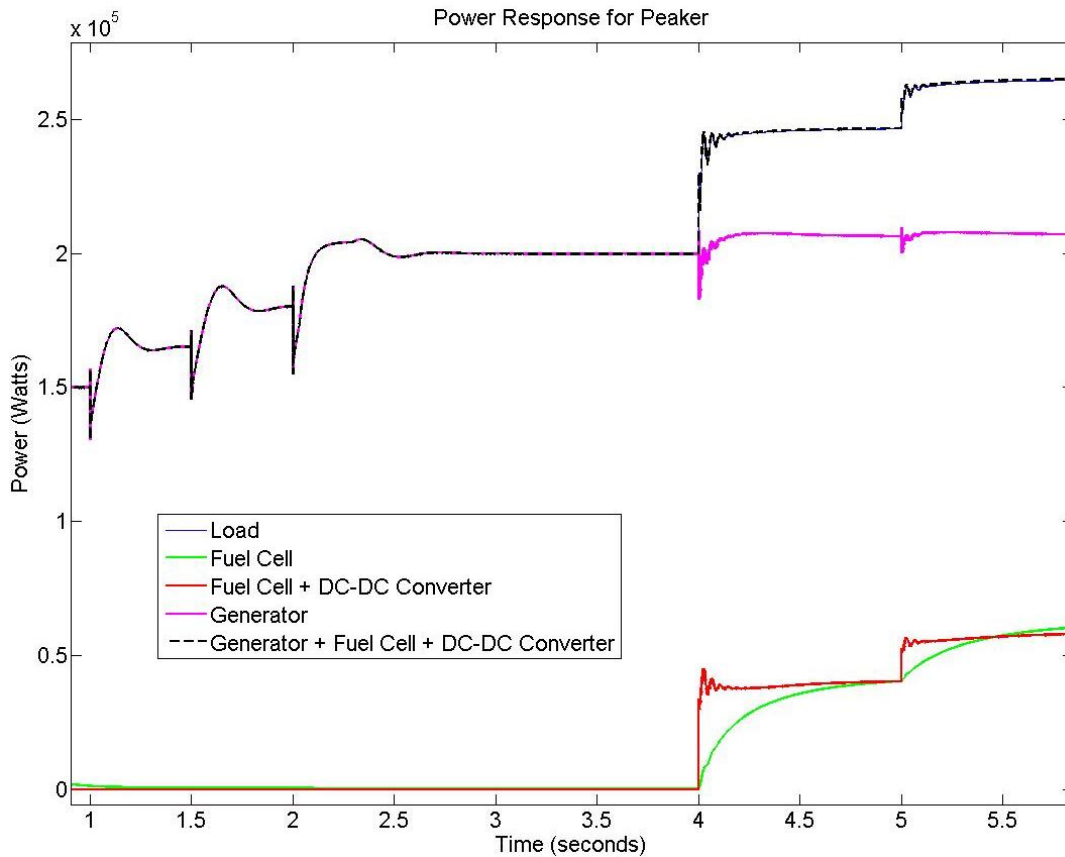
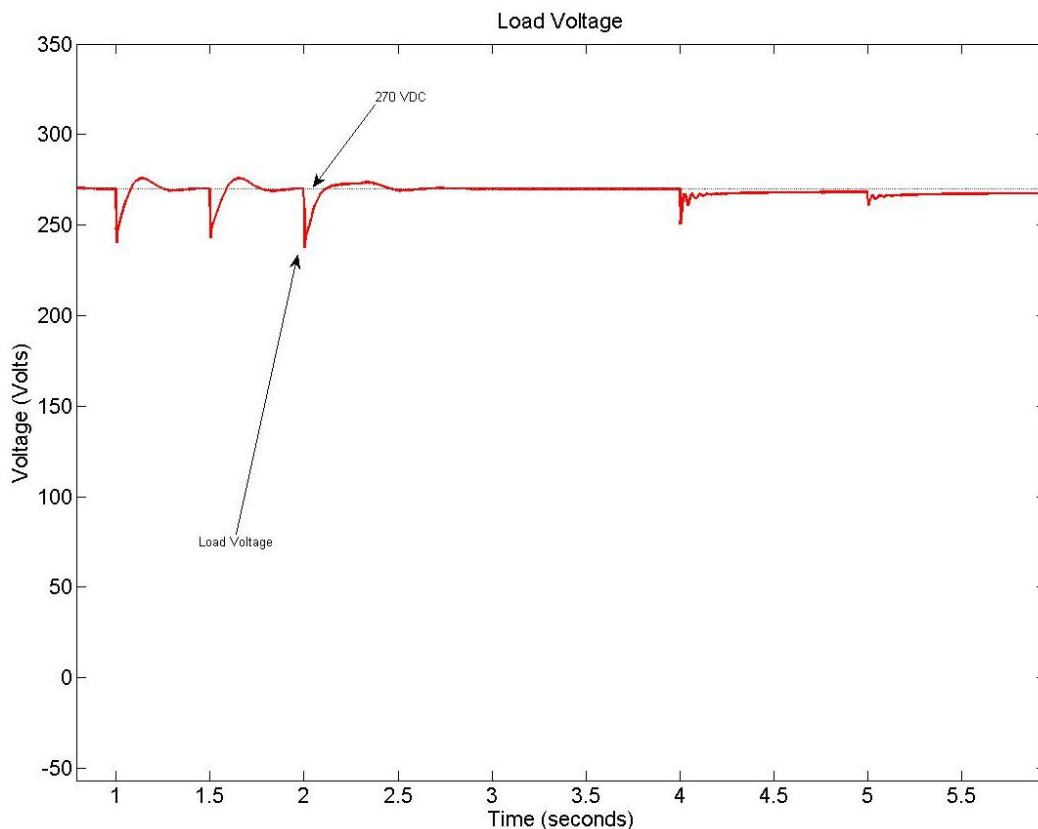


Figure 65: Peaker system simulation: Power responses.

It can be seen from these results that the power stabilizes after the transients and the addition of the fuel cell system to the existing electrical system does not cause any adverse effects. The fluctuations in power following the transients at 4 and 5 seconds are due to the PI (Proportional-Integral) controller inside the DC-DC converter may be able to be minimized with proper tuning. Comparison of the initial load increases that are handled completely by the engine generator to the load increases handled by the fuel cell and DC-DC converter reveals that the fuel cell along with the DC-DC converter responds much faster than the generator. This is due to the capacitor within the DC-DC converter and the instantaneous power that it is able to supply. The addition of the fuel cell system in this case actually improves the overall performance of the airplane's electrical system.

Figure 66 shows the voltage at the load during the simulation. Although there are voltage dips during a load increase, the voltage still remains within the limits specified by MIL-STD-704F (see Figure 67). The largest voltage sags are during the simulation period when the generator picks up the load. It is important to note that the ATRU was modeled as a simple transformer-rectifier and it was not based on the specification of a real system. Therefore, the voltage sags may not be an accurate representation of a real system. As can be seen by comparing Figure 67 and Figure 68 (which both use the same scales),



**Figure 66: Peaker system simulation: Voltage at the load. Detail of the transient at 2 seconds (where only the engine generator is supplying power) is shown in Figure 67. Detail of the transient at 4 seconds (where the fuel cell is supplying the additional power) is shown in Figure 68. The system is stable and the transients are all within the MIL-STD-704F specifications.**

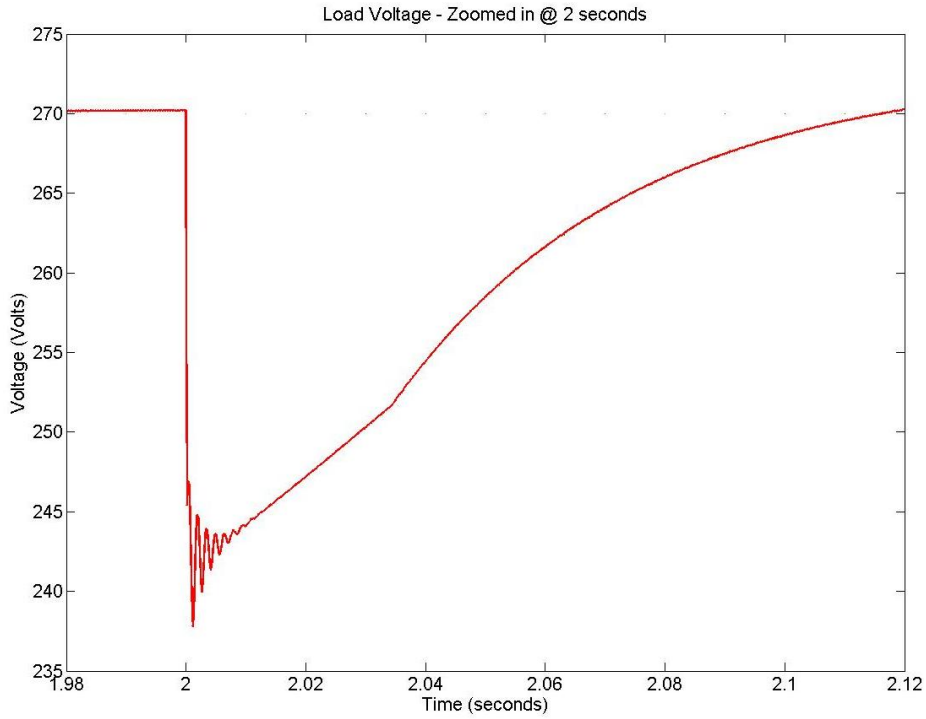


**Figure 67: Peaker system simulation: Detail of the voltage transient at 2 seconds as shown in Figure 66. This load change is fully met by the engine generators. The transient recovers within the time specified by MIL-STD-704F.**

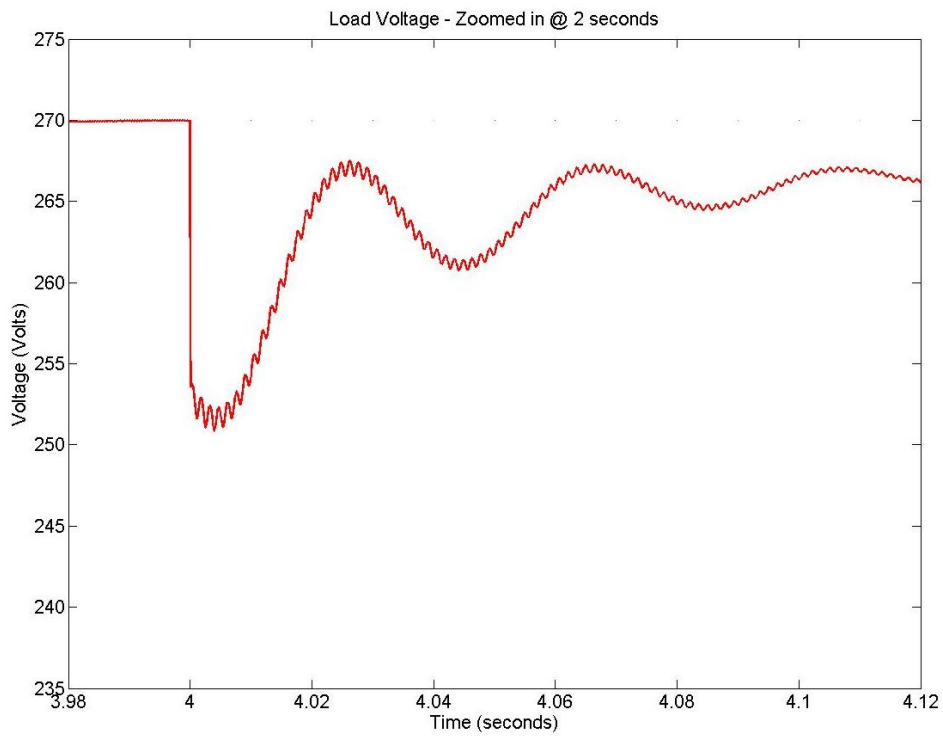


**Figure 68: Peaker system simulation: Details of the voltage transient at 4 seconds as shown in Figure 66. This load change is fully met by the fuel cell system. The transient recovers within the time specified by MIL-STD-704F, and has a much faster recovery than that of the engine generator alone (Figure 67).**

the voltage sags of the fuel cell are far less significant than those of the generator and easily meet the MIL-STD-704F standards. In Figure 68, the higher frequency small amplitude oscillations are an artifact of the DC-DC converter switching, while the longer, higher amplitude result from the PI (Proportional-Integral) controller in the DC-DC converter and may be able to be minimized with proper tuning.

### **6.4.3 Summary**

The fuel cell system can perform the required electrical functions for galley, IFE, and peaker power. It does not adversely affect system stability and meets the requirement for transients as put forth by MIL-STD-704F. Transient behavior is possibly better than the existing engine generator-based system, largely due to the capacitors inherent in the DC-DC converters.



## 7 Conclusions, Recommendations, and Future Work

This chapter presents the overall conclusions, recommended implementation strategies, and suggestions for future work aimed at furthering the use of on-board PEM fuel cells to enable higher energy efficiency for airplanes.

### 7.1 Conclusions and Recommendations

**Implementation of an on-board PEM fuel cell system is feasible using today's technology, and can be done without disrupting the current airplane design or functionality.**

- There is ample space on-board the airplane to install a fuel cell system. And in areas like the fairing and tail, the fuel cell system could occupy space that is currently empty.
- Overall, the weight of the fuel cell system (at most 2,500 kg) is very small compared to the weight of the airplane (173,998 kg at takeoff for the base mission).
- However, a system made with today's fuel cell and hydrogen storage technology will most likely not be able to provide an overall performance benefit to the airplane.

**It is necessary to consider the effect of the fuel cell system on the airplane to obtain the most realistic evaluation.**

- Any amount of weight or heat (and corresponding cooling drag) added to the airplane will require more fuel to achieve the same mission (per the Breguet equation).
- Any additional air needed by the fuel cell will require more engine electricity, and corresponding fuel use, to power the environmental control (pressurization) system if cabin air is used.
- Because a fuel cell system is nearly always more efficient than the main engines, not taking into account the above penalties will give the appearance that fuel cell systems will nearly always provide a benefit to the airplane, which is not the case.

**The fuel cell and hydrogen storage should be located together in either the fairing area or the tail cone area.**

- Locating the fuel cell near the hydrogen supply saves hydrogen supply tubing, and locating the fuel cell near the electrical load saves wiring. Doing both can save 50 to 100 kg in system mass. However, the fuel cell systems are not small, so locating them near the load may cause existing equipment to be displaced or require the use of cargo space.

**Maximizing the use of waste heat increases the attractiveness of the fuel cell system.**

- The main engines are required to produce less electricity, thus saving fuel.
- This is true even though waste heat recovery requires additional tubing and equipment.
- Rejecting the fuel cell's heat to the atmosphere imposes a drag penalty on the airplane and adds a corresponding fuel penalty.

**Maximizing the recovery of water from the fuel cell exhaust also provides a benefit.**

- This is true even though water recovery requires additional tubing and equipment.
- The gain is not as significant as for waste heat recovery.



**Recovering the fuel cell's waste heat using the airplane's fuel results in the best overall performance.**

- No other currently available on-board use of waste heat can practically absorb all the heat that the fuel cell produces.
- Not only will the jet fuel absorb all of the fuel cell's waste heat, eliminating the drag penalty, but also the increased jet fuel temperature provides an efficiency benefit to the main engines.

**For maximum performance benefit, the fuel cell should be used at full load for the entire flight; loads such as the in-flight entertainment and galley are attractive because of this.**

- For partially operating systems, the benefit of heat and water recovery is limited to only the portion of flight that it is operating, but the mass penalty takes effect for the entire flight.
- Installing a fuel cell for the peaker application only, which operates for less than 10% of the flight time, leads to the worst overall performance of any load.
- Because they operate during different phases of flight, a complementary effect between the peaker and galleys was discovered, allowing the same fuel cell to be used for both applications and increasing the overall airplane's performance.

**A high voltage DC electrical distribution system results in the lowest system weight and volume and should be considered.**

- The system could be conveniently tied into the existing  $\pm 270$  Volt DC bus.
- A high voltage DC distribution system saves mass and volume over the analogous AC system, primarily because the DC distribution system does not require a DC-AC inverter.
- Low voltage distribution systems, although attractive from a maintenance and safety perspective, require large currents and wires, making them unsuitable for even modest (e.g., 20 kW) load combinations.

**It is feasible for the fuel cell to feed the existing 230 Volt AC distribution bus.**

- Dynamic simulations showed no adverse effect on the airplane's electrical system.
- The fuel cell system provides the potential benefit of a faster transient response than the existing system.
- While heavier and larger than the  $\pm 270$  Volt DC system, the differences are small (approximately 60 kg maximum) and the be

**A future fuel cell system, comprised of DOE-target technology for the fuel cell and hydrogen storage, will provide an overall performance benefit to the airplane.**

- The fuel cell and hydrogen vessel are responsible for the majority of the system mass and volume, so reducing the sizes of these has a large impact on the overall system.

**A future fuel cell system would provide an electrical generation efficiency gain of over 30% in some cases, even when considering the added mass and drag effects on the airplane. This could result in a savings of over 20,000 metric tons of CO<sub>2</sub> emissions per year if implemented on a fleet of 1,000 airplanes such as the 787.**

## 7.2 Future Work

The following aspects were not part of the scope of this study but may warrant further investigation.

### Analysis, Engineering, and Simulation

- Mechanical System
  - Feasibility of on-board reforming of Jet-A, biofuel, or mixtures so that hydrogen is not needed on-board.
  - Feasibility of other possible, but not currently used, on-board heat recovery technologies such as absorption chillers and heat sinks.
- Electrical System
  - More exact modeling and simulation using accurate load profiles during entire flight envelope, existing generator parameters, actual fuel cell and power conditioning unit parameters.
- Transient and part-load analysis of the entire system, both mechanically and electrically.

### Hardware Testing

- Mechanical system (fuel cell, hydrogen, and heat recovery)
- Electrical integration (utilizing the various sources and sinks at Sandia's Distributed Energy Technology Laboratory)
- Combined mechanical-electrical system
- Combined system on an airplane or mock-up

### Optimization

- Hardware
- System Design

Sandia National Laboratories has the facilities and expertise to pursue these and other related pathways to assist in enabling or discovering the various aspects of energy efficient airplanes.



## References

- [1] Sinnett, M. (2007). "787 No-Bleed Systems: Saving Fuel and Enhancing Operational Efficiencies." *Aero Quarterly*, 6-11.
- [2] Airbus (2008). "Emission free power for civil aircraft: Airbus successfully demonstrates fuel cells in flight."
- [3] "Emission-free airports – DLR develops a fuel cell-powered electric nose wheel for commercial aircraft." (2011). German Aerospace Center (DLR), available online at: [http://www.dlr.de/en/desktopdefault.aspx/tabid-1/86\\_read-28858/](http://www.dlr.de/en/desktopdefault.aspx/tabid-1/86_read-28858/) (accessed Feb. 18, 2011).
- [4] Karimi, K. J. (2007). "Future Aircraft Power Systems - Integration Challenges." The Boeing Company.
- [5] Breit, J. S., Szydlo-Moore, J. A., and Lorhammer, K. (2009). "Vehicular Power Distribution System and Method." US patent 7,550,866 B2, The Boeing Company.
- [6] Spenser, J. (2004). "Fuel cells in the air." *Boeing Frontiers Online*.
- [7] The Boeing Company (2001). "Boeing to Explore Electric Airplane." available online at: [http://www.boeing.com/news/releases/2001/q4/nr\\_011127a.html](http://www.boeing.com/news/releases/2001/q4/nr_011127a.html) (accessed Feb 23 2011).
- [8] Klebanoff, L. E., and Cornelius, C. J. (2007). "Analysis of hydrogen storage for a fuel cell emergency power system (FCEPS) for commercial aircraft." Report SAND2007-4542P, Sandia National Laboratories.
- [9] Breit, J. (2010). "Finding an Optimum Path to Fuel Cell Technology for Airplanes." *8th International Energy Conversion Engineering Conference*, Nashville, TN.
- [10] Mazur, A. M. (2011). "Fuel Cell System Integration for Combined Heat and Auxiliary Power Generation on Commercial Aircraft." MS Thesis, University of Iceland, Akureyri, Iceland.
- [11] "787 Airplane Characteristics for Airport Planning." (2009). Boeing Commercial Airplanes, Seattle, WA.
- [12] Hunt, E. H., Reid, D. H., Space, D. R., and Tilton, F. E. (2009). "Commercial Airliner Environmental Control System, Engineering Aspects of Cabin Air Quality." The Boeing Company.
- [13] Nelson, T. (2005). "787 Systems and Performance." The Boeing Company.
- [14] United States Committee on Extension to the Standard Atmosphere (COESA) (1976). *U.S. Standard Atmosphere, 1976*, U.S. Government Printing Office, Washington, D.C.
- [15] "Airworthiness Standards: Transport Category Airplanes; Subpart D: Design and Construction - Ventilation." (1997). *Code of Federal Regulations*, Title 14, Pt. 25.831(D).
- [16] Norris, G. (2010). "Big Weekend for 787." 4/9/2010 In: Things With Wings: The Commercial Aviation Blog. Aviation Week, available online at: [http://www.aviationweek.com/aw/blogs/commercial\\_aviation/ThingsWithWings/](http://www.aviationweek.com/aw/blogs/commercial_aviation/ThingsWithWings/) (accessed 2/18/2011).
- [17] Dornheim, M. A. (2005). "Massive 787 Electrical System Pressurizes Cabin." *Aviation Week & Space Technology*.
- [18] Fossen, J. (2008). "Preparing Ramp Operations for the 787-8." *Aero Quarterly*, The Boeing Company, 4-13.
- [19] Freeh, J. E., Pratt, J. W., and Brouwer, J. "Development of a solid-oxide fuel cell / gas turbine hybrid system model for aerospace applications." *Proc., Proceedings of ASME Turbo Expo 2004: Power for Land, Sea, and Air*, ASME.
- [20] Daggett, D. (2003). "Fuel Cell APU Overview." *SECA Annual Meeting*, Seattle, WA.
- [21] Rajashekara, K., Grieve, J., and Daggett, D. "Solid Oxide Fuel Cell/Gas Turbine Hybrid APU System for Aerospace Applications." *Proc., IEEE Industry Applications Conference, 2006. 41st IAS Annual Meeting.*, 2185-2192.
- [22] Mackay, A., Hill, J., and Rajashekara, K. "Modelling of Fuel Cell APU Utilisation for Aircraft Applications." *Proc., 8th International Energy Conversion Engineering Conference*, AIAA.

- [23] Roskam, J., and Lan, C.-T. E. (1997). *Airplane Aerodynamics and Performance*, DARcorporation, Lawrence, KS.
- [24] "Boeing's New Airplane - Design Highlights - Lower Fuel Consumption." (date unknown). Boeing, available online at: [http://www.newairplane.com/787/design\\_highlights/](http://www.newairplane.com/787/design_highlights/) (accessed Feb. 18 2011).
- [25] "Fuel Consumption Analysis of the Boeing 767-200ER and Airbus 330-200 in Commercial Service when operated at High Take-off Gross Weight with Oil at \$100 and \$125 per Barrel." (2008). Conklin & de Decker Aviation Information, Arlington, TX.
- [26] Hilkevitch, J., and Johnsson, J. (2010). "Cost-cutting measure fuels debate at American Airlines." *Chicago Tribune* available online at: [http://articles.chicagotribune.com/2010-06-27/travel/ct-biz-0627-pilots-fuel-20100626\\_1\\_american-airlines-fuel-pilots-and-dispatchers](http://articles.chicagotribune.com/2010-06-27/travel/ct-biz-0627-pilots-fuel-20100626_1_american-airlines-fuel-pilots-and-dispatchers) (accessed Feb. 18, 2011).
- [27] Filippone, A. (2006). "Flight Performance of Fixed and Rotary Wing Aircraft." Butterworth-Heinemann, Online at Books24x7.
- [28] "Boeing's New Airplane - Visionary Design." (date unknown). Boeing, available online at: [http://www.newairplane.com/787/design\\_highlights/](http://www.newairplane.com/787/design_highlights/) (accessed Feb. 18 2011).
- [29] Larminie, J., and Dicks, A. (2003). *Fuel cell systems explained*, John Wiley & Sons, Inc., Hoboken, NJ.
- [30] Lutz, A. E., Larson, R. S., and Keller, J. O. (2002). "Thermodynamic comparison of fuel cells to the Carnot cycle." *International Journal of Hydrogen Energy*, 27(10), 1103-1111.
- [31] Wright, S. E. (2004). "Comparison of the theoretical performance potential of fuel cells and heat engines." *Renewable Energy*, 29(2), 179-195.
- [32] "HYPM-Power Modules: 03-2010." (2010). Hydrogenics Corporation, Mississauga, Ontario.
- [33] "Technical Plan - Fuel Cells." (2007). *Hydrogen, Fuel Cells & Infrastructure Technologies Program Multi-Year Research Development and Demonstration Plan*, U.S. Department of Energy.
- [34] Aceves, S. M., Espinosa-Loza, F., Ledesma-Orozco, E., Ross, T. O., Weisberg, A. H., Brunner, T. C., and Kircher, O. (2010). "High-density automotive hydrogen storage with cryogenic capable pressure vessels." *International Journal of Hydrogen Energy*, 35(3), 1219-1226.
- [35] Ahluwalia, R. K., Hua, T. Q., Peng, J. K., Lasher, S., McKenney, K., Sinha, J., and Gardiner, M. (2010). "Technical assessment of cryo-compressed hydrogen storage tank systems for automotive applications." *International Journal of Hydrogen Energy*, 35(9), 4171-4184.
- [36] Chao, B. S., Young, R. C., Myasnikov, V., Li, Y., Huang, B., Gingl, F., Ferro, P. D., Sobolev, V., and Ovshinsky, S. R. (2004). "Recent Advances in Solid Hydrogen Storage Systems." *Materials Research Society Symposium Proceedings*, 801, BB1.4.1-BB1.4.13.
- [37] "Tuffshell® H2 Fuel Tanks." (date unknown). Lincoln Composites, Lincoln, NE.
- [38] "High Pressure Lightweight Type IV H2 Cylinders – 34L/ 40L." (date unknown). Quantum Fuel Systems Technologies Worldwide Inc., Lake Forest, CA.
- [39] "High Pressure Lightweight Type IV H2 Cylinders – 38L." (date unknown). Quantum Fuel Systems Technologies Worldwide Inc., Lake Forest, CA.
- [40] "High Pressure Lightweight Type IV H2 Cylinders – 129L." (date unknown). Quantum Fuel Systems Technologies Worldwide Inc., Lake Forest, CA.
- [41] "Development of Innovative Hydrogen Storage Technologies." (2010). Magna Steyr, available online at: [http://www.magna.com/xchg/SID-0A200004-DF65BCBE/complete\\_vehicle/XSL/standard.xsl/-/content/9\\_1418.htm](http://www.magna.com/xchg/SID-0A200004-DF65BCBE/complete_vehicle/XSL/standard.xsl/-/content/9_1418.htm) (accessed Oct. 13 2010).
- [42] "Storing Hydrogen." (2010). Air Liquide, available online at: <http://www.dta.airliquide.com/en/our-offer/decentralized-energies/hydrogen-energy-5/storing-hydrogen.html> (accessed Nov. 17 2010).
- [43] Grochala, W., and Edwards, P. P. (2004). "Thermal Decomposition of the Non-Interstitial Hydrides for the Storage and Production of Hydrogen." *Chemical Reviews*, 104(3), 1283-1316.

- [44] Bogdanovic, B., and Schwickardi, M. (1997). "Ti-doped alkali metal aluminium hydrides as potential novel reversible hydrogen storage materials." *Journal of Alloys and Compounds*, 253-254, 1-9.
- [45] Johnson, T. A., and Kanouff, M. P. (2010). "Parameter Study of a Vehicle-scale Hydrogen Storage System." Report SAND2010-2140, Sandia National Laboratories.
- [46] "Technical Plan - Storage." (2009). *Hydrogen, Fuel Cells & Infrastructure Technologies Program Multi-Year Research Development and Demonstration Plan*, U.S. Department of Energy.
- [47] "Engineering Services: Fuel Cell DC-DC Converter." (date unknown). AeroVironment, Inc., available online at: [http://www.avinc.com/engineering/dc-dc\\_converter](http://www.avinc.com/engineering/dc-dc_converter) (accessed February 22 2011).
- [48] "Three-Phase DC-AC Converter DA02 (Export Power)." (2010). US Hybrid, Torrance, CA.
- [49] "World Jet Fuel Specifications with Avgas Supplement." (2005). ExxonMobil Aviation, Leatherhead, UK.
- [50] EG&G Technical Services Inc (2004). *Fuel Cell Handbook*, U.S. Department of Energy.
- [51] Le Canut, J.-M., Abouatallah, R. M., and Harrington, D. A. (2006). "Detection of Membrane Drying, Fuel Cell Flooding, and Anode Catalyst Poisoning on PEMFC Stacks by Electrochemical Impedance Spectroscopy." *Journal of The Electrochemical Society*, 153(5), A857-A864.
- [52] "DF3000 Convection Oven." (date unknown). B/E Aerospace, The Netherlands.
- [53] "Thermoelectric Refrigerator Model 1026 Series." (date unknown). TIA Galley Products, Sterling, VA.
- [54] "Endura® Beverage Maker." (date unknown). B/E Aerospace, Lenexa, KS.
- [55] "Espresso/Cappuccino Maker." (date unknown). B/E Aerospace, Lenexa, KS.
- [56] "DS3000 Steam Oven." (date unknown). B/E Aerospace, The Netherlands.
- [57] "Endura® Water Boiler." (date unknown). B/E Aerospace, Lenexa, KS.
- [58] Roth, B., and III, R. G. "Fuel Cell Hybrid Propulsion Challenges and Opportunities for Commercial Aviation." *Proc., 8th International Energy Conversion Engineering Conference*, AIAA.
- [59] "Orders and Deliveries." (date unknown). Boeing, available online at: <http://active.boeing.com/commercial/orders/index.cfm> (accessed March 30 2011).
- [60] "Long-Term Market, Current Market Outlook 2010-2029." (date unknown). Boeing, available online at: [http://active.boeing.com/commercial/forecast\\_data/index.cfm](http://active.boeing.com/commercial/forecast_data/index.cfm) (accessed March 30 2011).
- [61] Department of Defense (2004). "Department of Defense Interface Standard - Aircraft Electric Power Characteristics." *MIL-STD-704F*.

## Distribution

2 U.S. Department of Energy  
Attn: Peter Devlin (1)  
Attn: Nancy Garland (1)  
1000 Independence Ave., SW  
Washington, D.C. 20585-0121

4	MS1108	Karina Munoz-Ramos	06111
1	MS1108	Juan Torres	06111
4	MS1108	Benjamin Schenkman	06113
4	MS1108	Abbas Akhil	06113
1	MS1108	Ross Guttromson	06113
1	MS9052	Jay Keller	08360
1	MS9052	Daniel Dedrick	08367
1	MS9054	Bob Carling	08300
1	MS9054	Art Pontau	08360
4	MS9161	Lennie Klebanoff	08367
4	MS9409	Joseph W. Pratt	08365
4	MS9409	Dita Curgus	08365
1	MS9409	Neal Fornaciari	08365
1	MS0899	Technical Library	9536 (electronic copy)





